

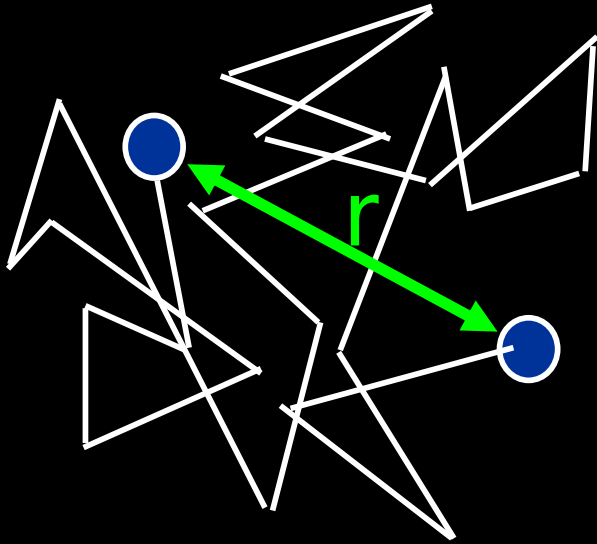
NIH summer MRI course

# What we can and can not do with Diffusion MRI

Carlo Pierpaoli

NIBIB

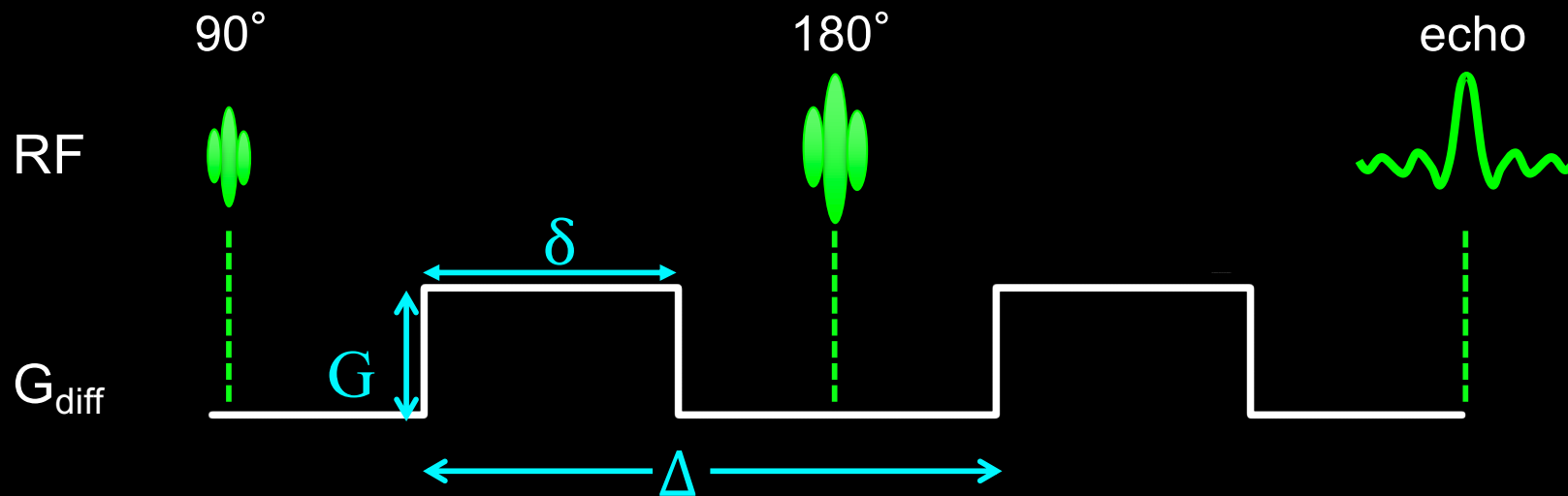
Diffusion is a transport process in which molecules change their position by random thermal collisions.



$$\langle r^2 \rangle = 6 D t$$

$\langle r^2 \rangle$  : mean-square displacement.  
t : diffusion time.

# Spin-echo Diffusion Preparation



$$b = (\gamma G \delta)^2 \left( \Delta - \frac{\delta}{3} \right)$$

# DWI

$$S = S_0 e^{-bD}$$

Non-diffusion-weighted  
signal intensity

B-value  
sec/mm<sup>2</sup>

Diffusion  
Coefficient  
mm<sup>2</sup>/sec

# Spin Diffusion Measurements: Spin Echoes in the Presence of a Time-Dependent Field Gradient\*

E. O. STEJSKAL† AND J. E. TANNER

*Department of Chemistry, University of Wisconsin, Madison, Wisconsin*

(Received 20 July 1964)

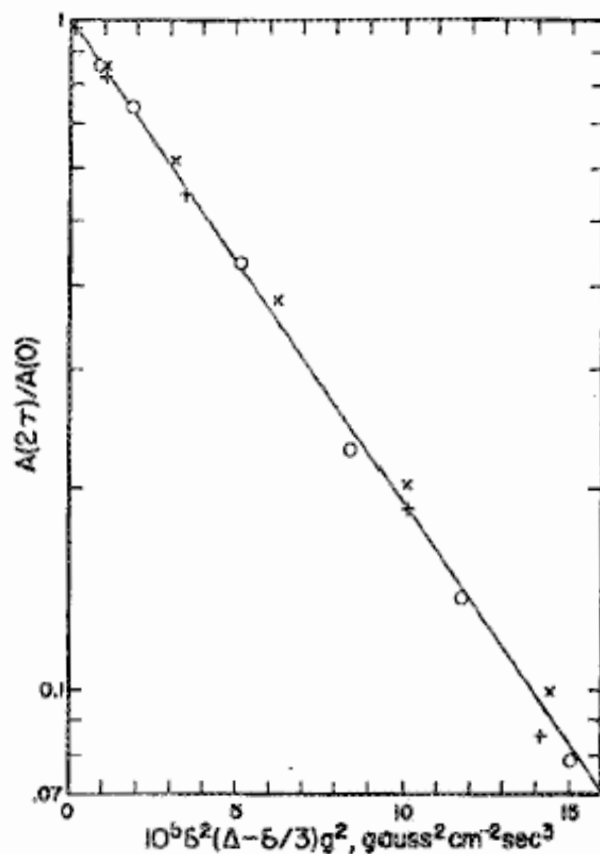


FIG. 1. Effect of the pulsed gradient on the echo amplitude, as observed in several aqueous  $\text{CuSO}_4$  solutions at  $25.5^\circ \pm 0.5^\circ \text{C}$ . (See Table I for an identification of the symbols used.)

# Diffusion MRI

IVIM (Intravoxel Incoherent Motion)

DTI (Diffusion Tensor Imaging)

HARDI (High Angular Resolution  
Diffusion Imaging)

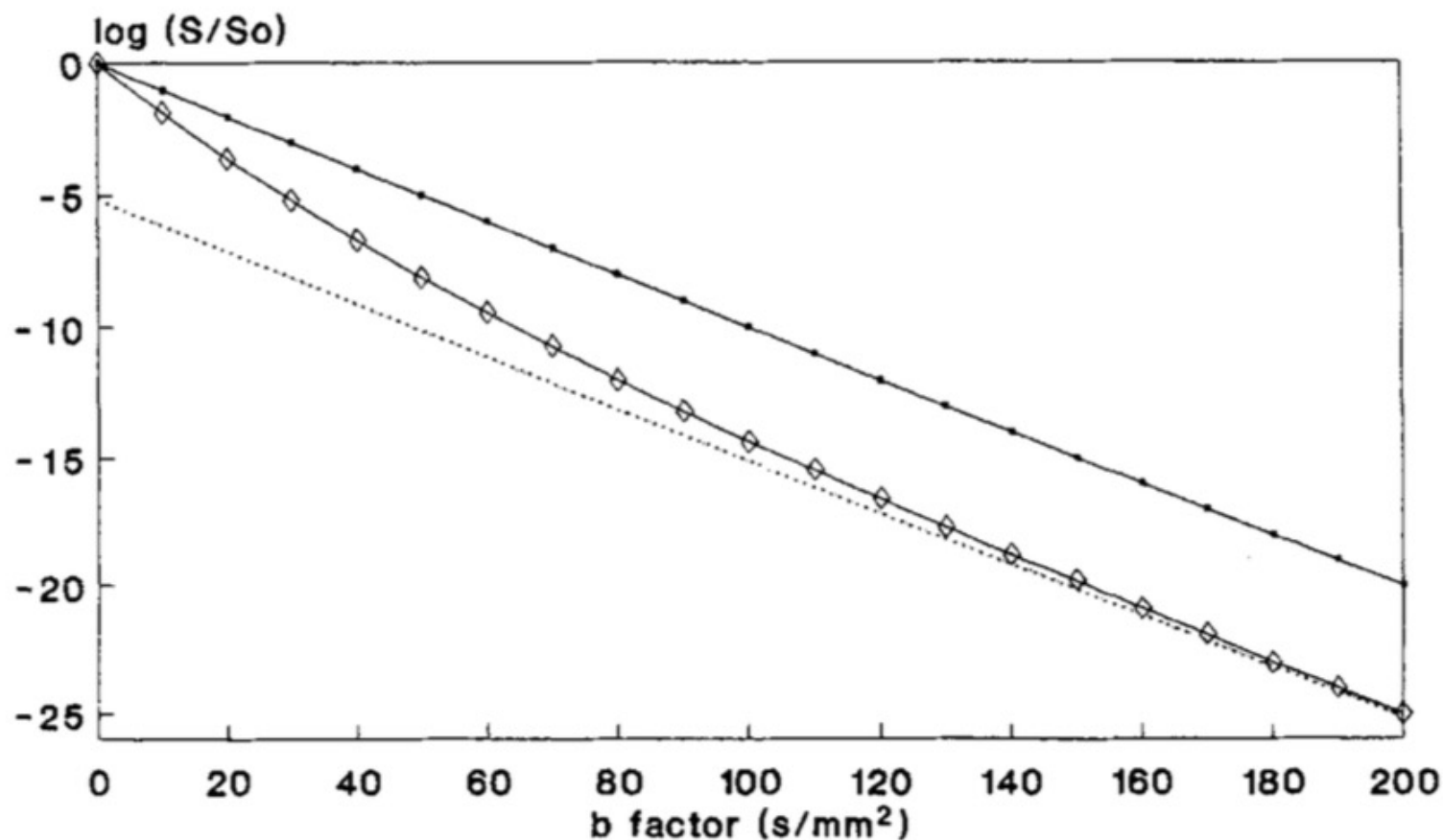
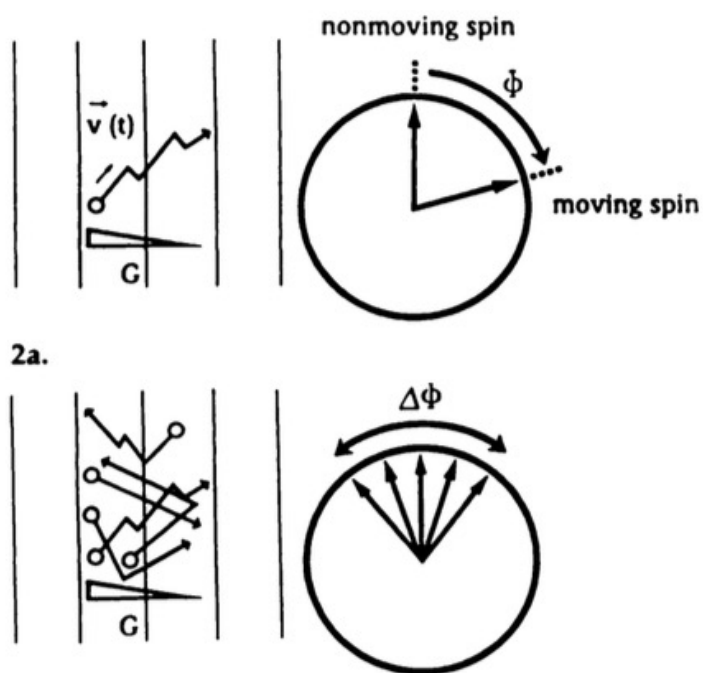


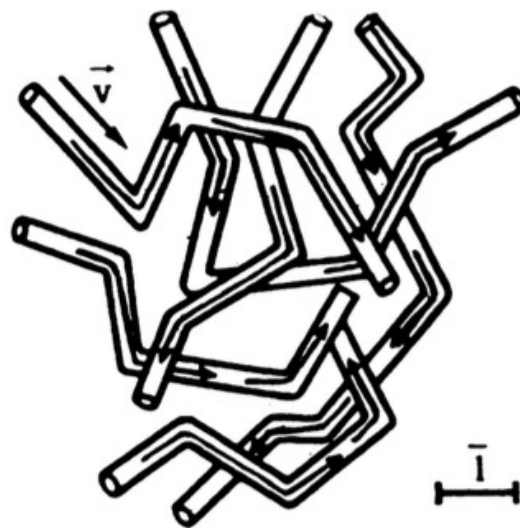
FIG. 2. Model of voxel. In a voxel, effects of both the flowing component and the static component must be taken into account. The first perfusion model was used ( $D^* = 20 \times 10^{-3} \text{ mm}^2/\text{s}$ ) in this simulation. The capillary volume is typically 5 ml/100 mg of tissue. The logarithm of the signal attenuation is plotted against the  $b$  factor. The overall effect of perfusion is to shift the attenuation curve by a quantity  $\log(1 - f)$ , so that the intercept gives the perfusion factor  $f$ . The slope of the attenuation curve, as measured with large  $b$  values ( $b > 100 \text{ s/mm}^2$ ) gives the diffusion coefficient  $D$ . Perfusion and diffusion effects may be integrated in the "apparent diffusion coefficient," which is the slope of the attenuation curve obtained for smaller  $b$  values (typically between 0 and  $100 \text{ s/mm}^2$ ). (■) Diffusion only; (◇) diffusion + perfusion; (···) asymptote to diffusion.



2a.

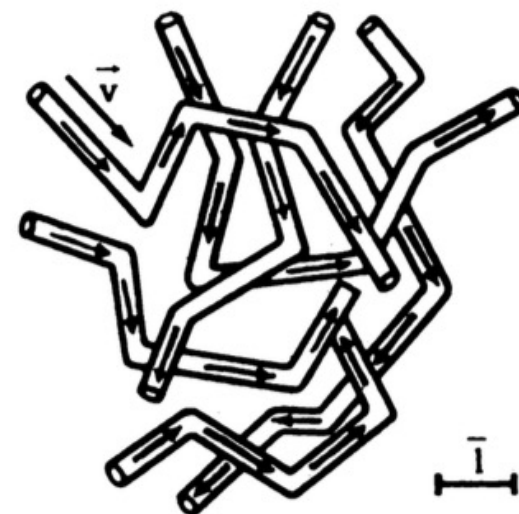
2b.

### FIRST MODEL



3a.

### SECOND MODEL



3b.

**Figures 2, 3.** (2) Effect of IVIM on the MR spin-echo signal. (a) Spin movements in the direction of a magnetic field gradient  $G$  produce phase shifts  $\Phi$  of the transverse magnetization, as compared with nonmoving spins, due to changes in their precession frequency. (b) If spins present different movements in a given voxel, a distribution of phase shifts  $\Delta\Phi$  results. This loss of coherence in transverse magnetization decreases the echo signal amplitude, as a function of the differences in spin motions and of the field gradients used. In the case of molecular diffusion, for instance, the echo attenuation is an exponential function of the diffusion coefficient  $D$ . (3) For capillary flow, the spin-echo amplitude attenuation  $F$  is a function of blood velocity  $\bar{v}$  and capillary geometry. Assuming that the capillary network can be described by a succession of straight capillary segments, the mean length of which is  $\bar{l}$ , two situations can be considered to determine  $F$ . (a) If blood flow changes segments several times during the spin-echo sequence, movement of water in capillaries looks like a diffusion process—that is, a random walk—but at a more complex level. A pseudodiffusion coefficient  $D^*$  can be defined, the value of which would be determined by  $\bar{l}$  and  $\bar{v}$ . (b) If blood flow does not change segment during the spin-echo sequence, the echo attenuation law becomes different. This situation occurs when the capillary segments are longer, the blood velocity is slower, or the spin-echo delay is shorter. Nevertheless, the echo attenuation  $F$  can be calculated by assuming a random orientation of the capillary segments at the voxel level. In both these cases, the echo attenuation due to perfusion is always greater than that due to diffusion, potentially allowing them to be separated on a quantitative basis.

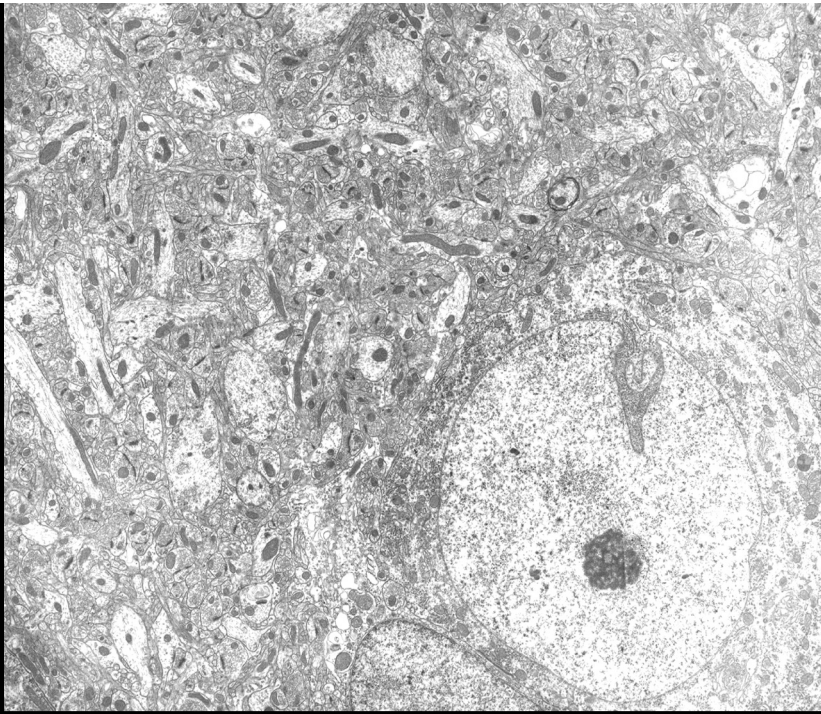


## MR Diffusion *Tensor* Spectroscopy and Imaging

Peter J. Basser,\* James Mattiello,\* and Denis LeBihan<sup>‡</sup>

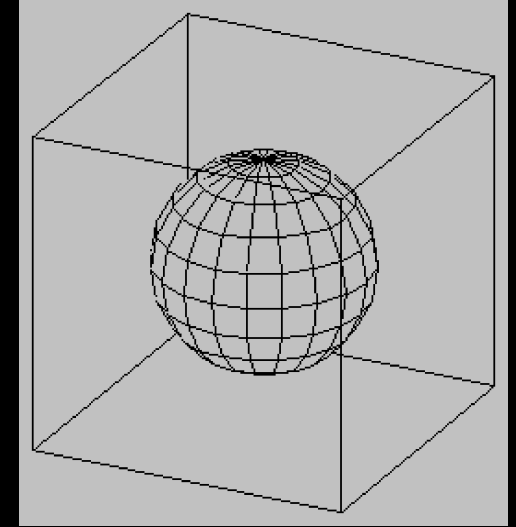
\*Biomedical Engineering and Instrumentation Program, National Center for Research Resources, and <sup>‡</sup>Diagnostic Radiology Department, The Warren G. Magnuson Clinical Center, National Institutes of Health, Bethesda, Maryland 20892 USA

**ABSTRACT** This paper describes a new NMR imaging modality—MR diffusion *tensor* imaging. It consists of estimating an effective diffusion tensor,  $\mathbf{D}_{\text{eff}}$ , within a voxel, and then displaying useful quantities derived from it. We show how the phenomenon of anisotropic diffusion of water (or metabolites) in anisotropic tissues, measured noninvasively by these NMR methods, is exploited to determine fiber tract orientation and mean particle displacements. Once  $\mathbf{D}_{\text{eff}}$  is estimated from a series of NMR pulsed-gradient, spin-echo experiments, a tissue's three orthotropic axes can be determined. They coincide with the eigenvectors of  $\mathbf{D}_{\text{eff}}$ , while the effective diffusivities along these orthotropic directions are the eigenvalues of  $\mathbf{D}_{\text{eff}}$ . Diffusion ellipsoids, constructed in each voxel from  $\mathbf{D}_{\text{eff}}$ , depict both these orthotropic axes and the mean diffusion distances in these directions. Moreover, the three scalar invariants of  $\mathbf{D}_{\text{eff}}$ , which are independent of the tissue's orientation in the laboratory frame of reference, reveal useful information about molecular mobility reflective of local microstructure and anatomy. Inherently, tensors (like  $\mathbf{D}_{\text{eff}}$ ) describing transport processes in anisotropic media contain new information *within a macroscopic voxel* that scalars (such as the apparent diffusivity, proton density,  $T_1$ , and  $T_2$ ) do not.

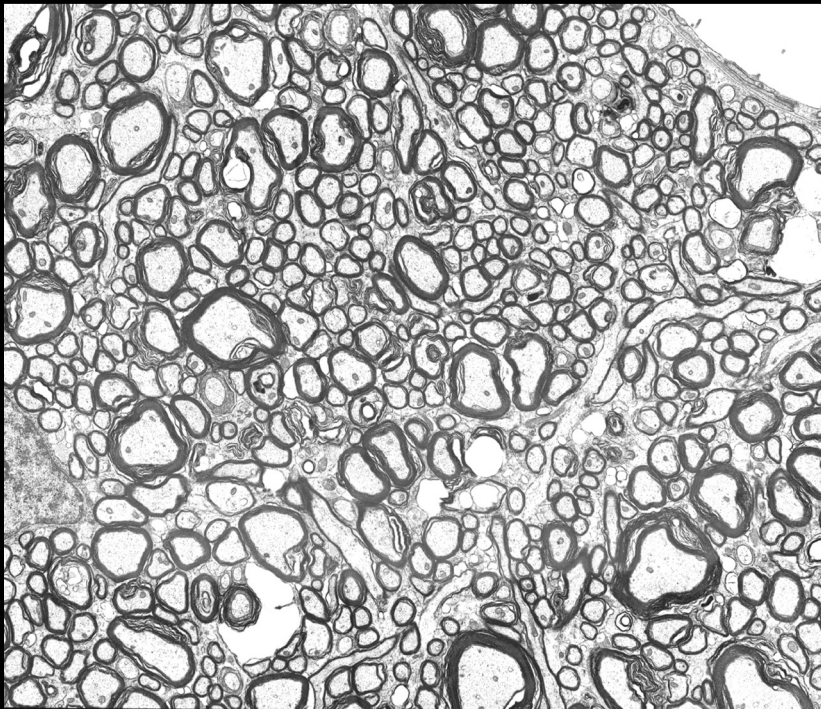


Gray matter  
(Cortex)

isotropic  
diffusion

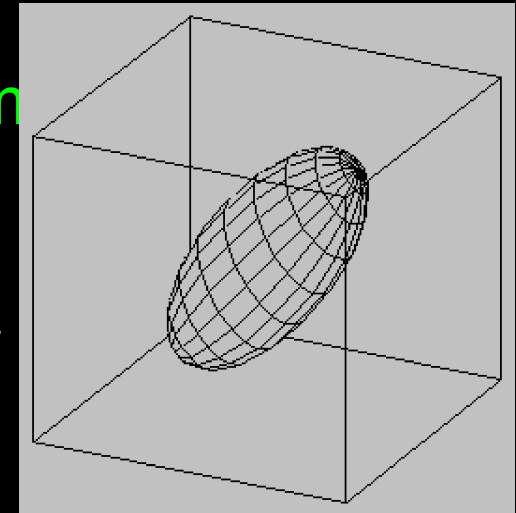


← ~ microns →

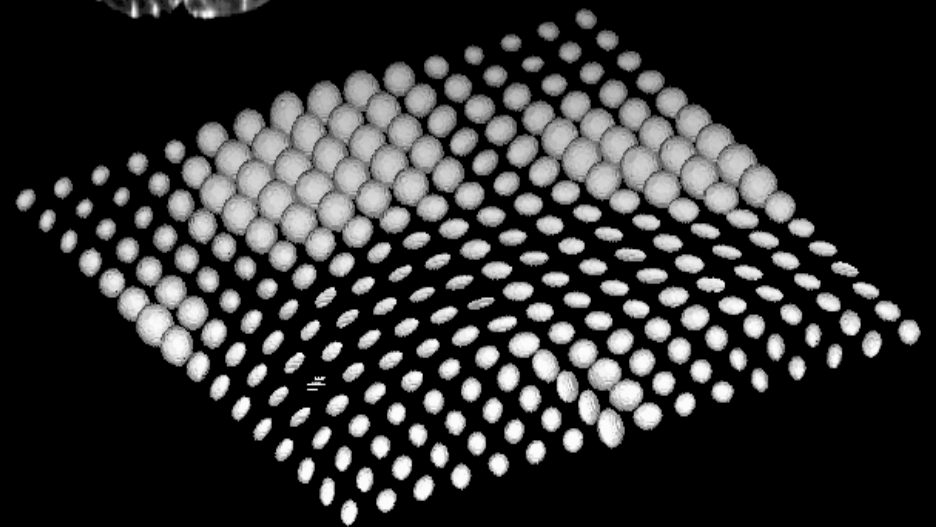
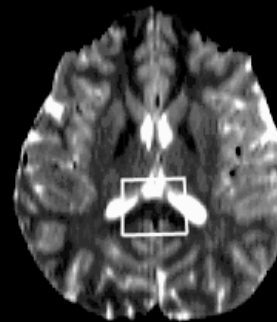
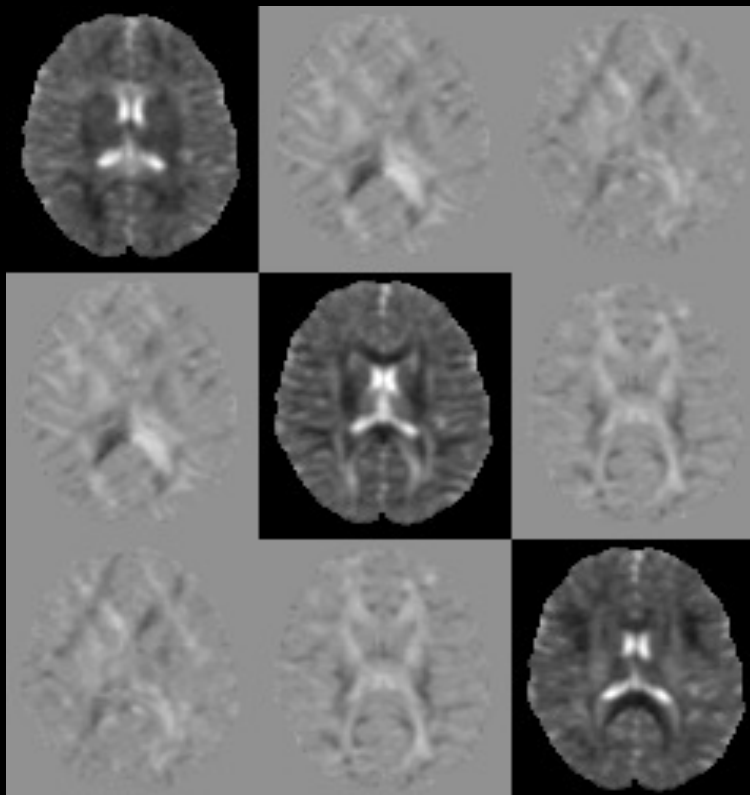
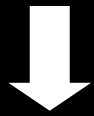
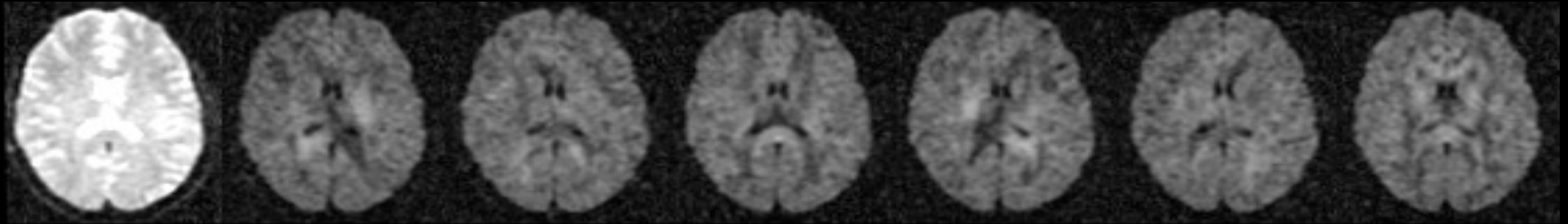


White matter  
(Corpus callosum)

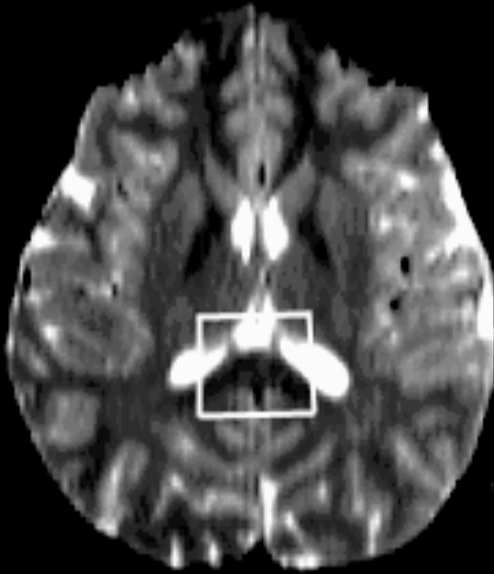
*anisotropic*  
diffusion



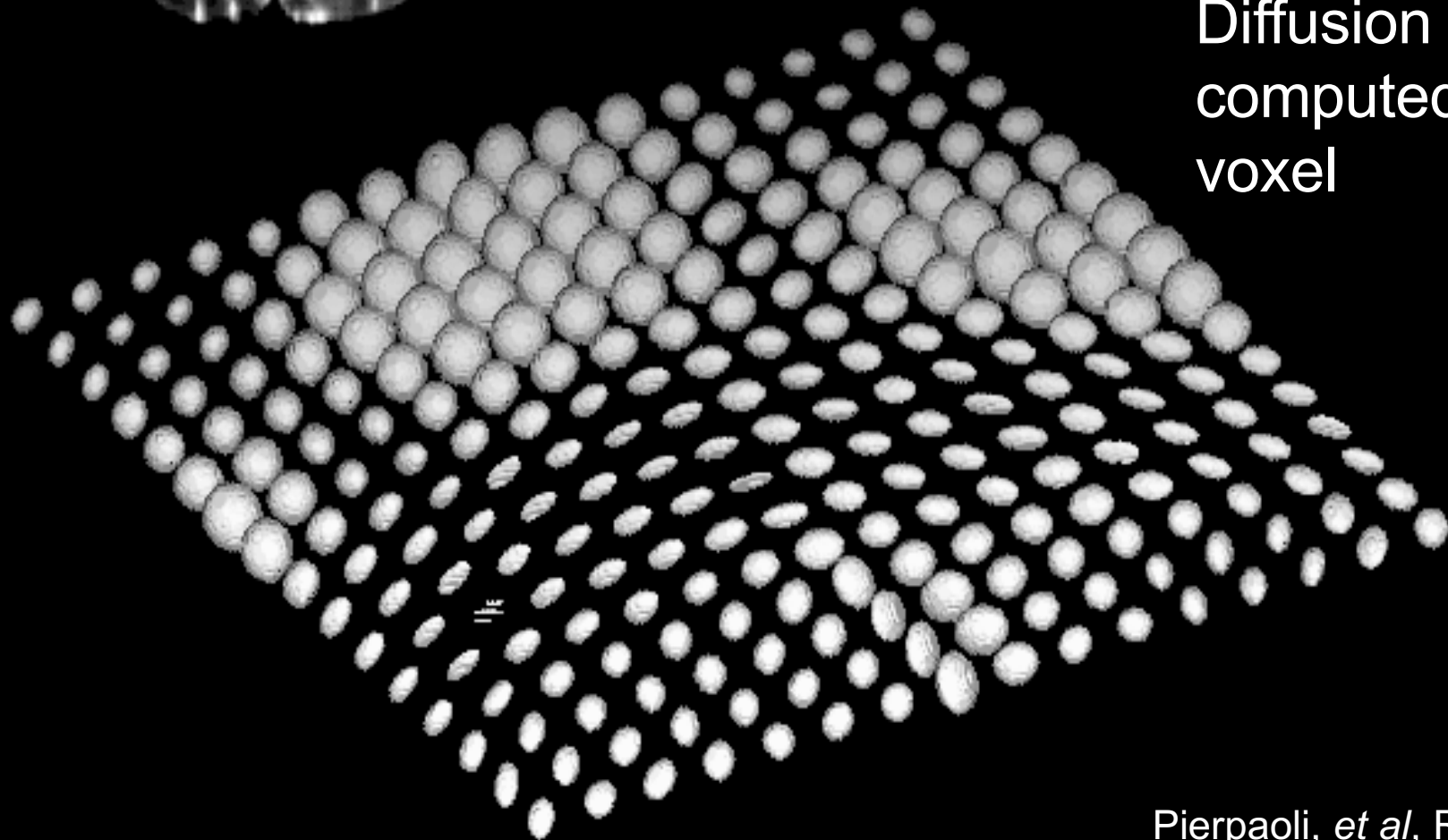
# Diffusion Tensor MRI Flowchart



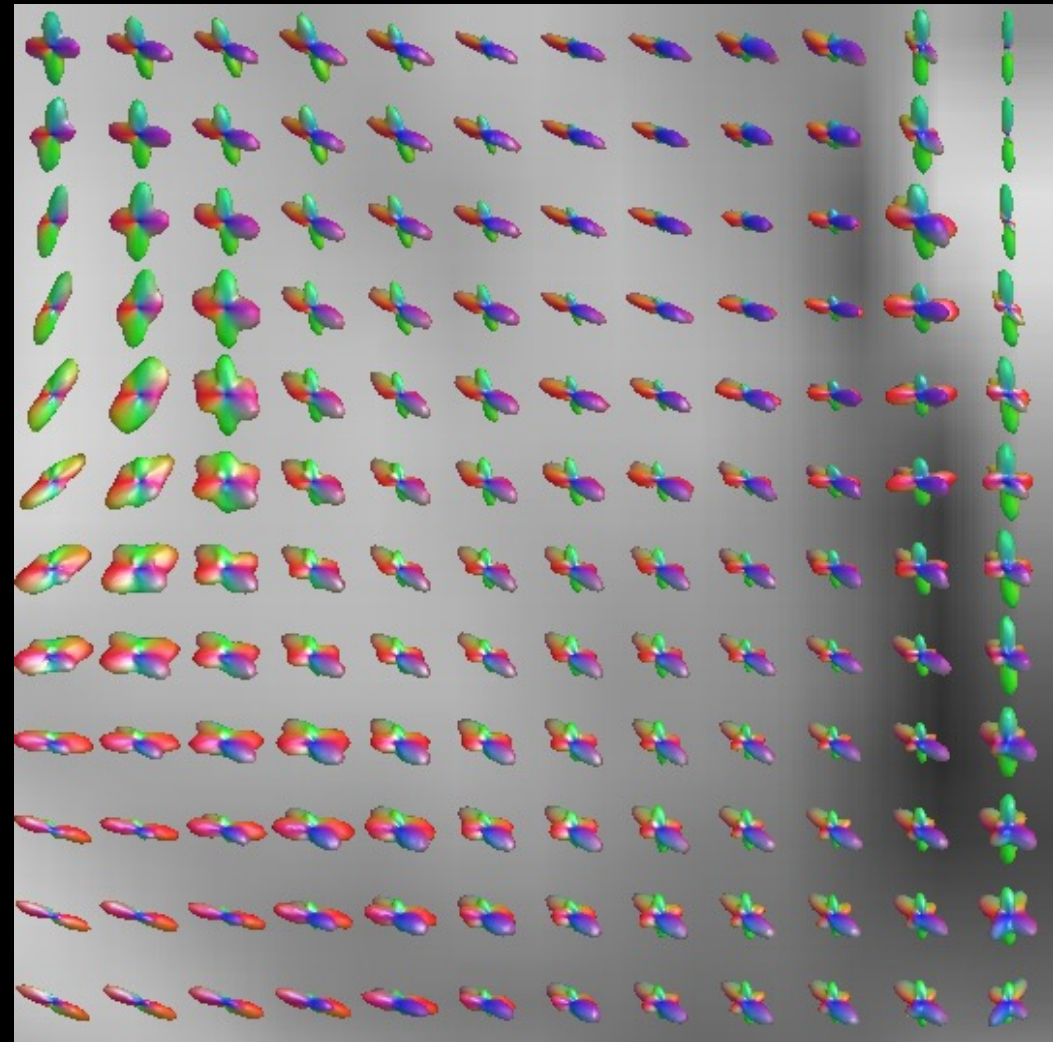
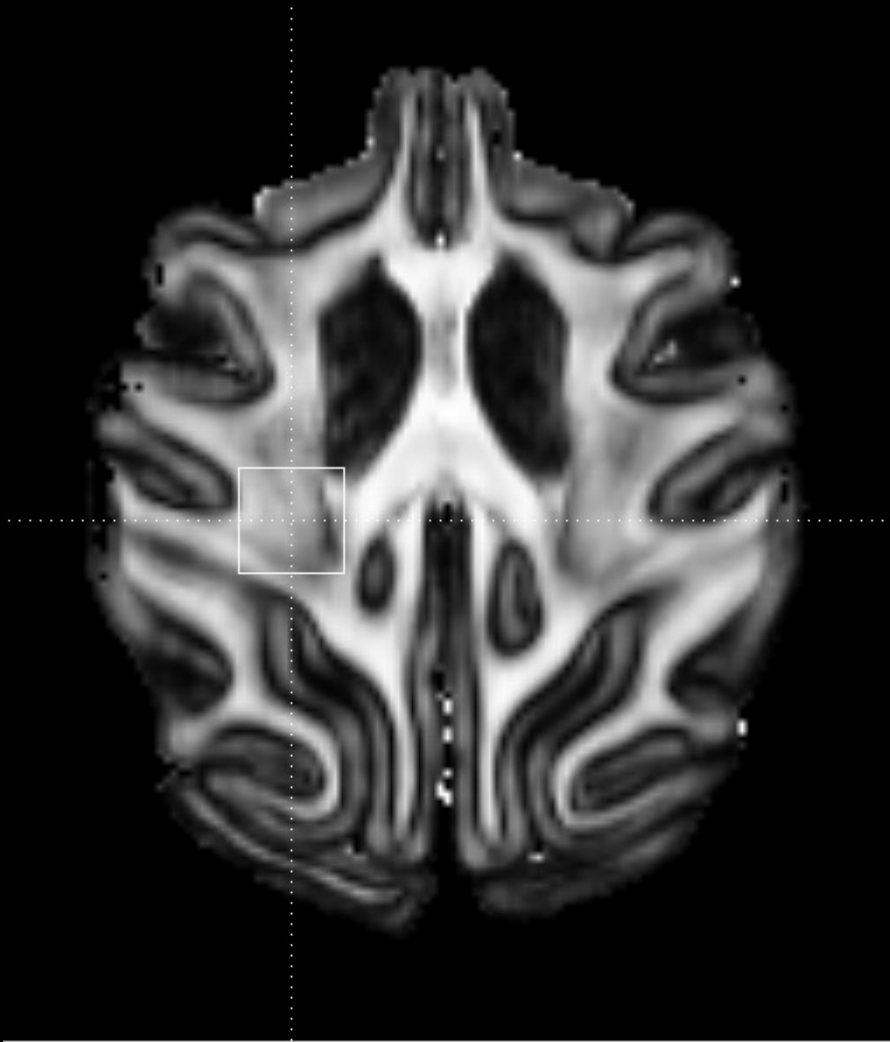
# Diffusion Tensor MRI of the Human Brain.



Diffusion ellipsoids  
computed in each  
voxel



# High Angular Resolution Diffusion Imaging (HARDI)

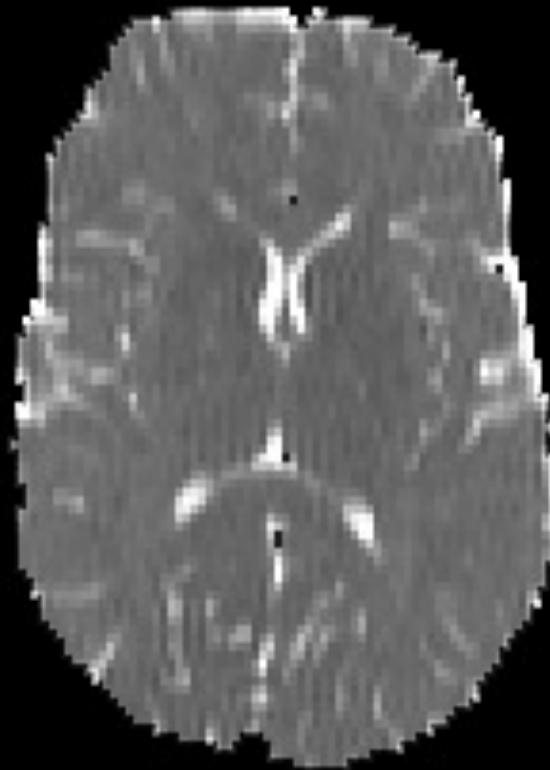


3D SHORE Courtesy of Evren Ozarslan

# Trace(D) (averaged mean-squared displacement)



T2 weighted image

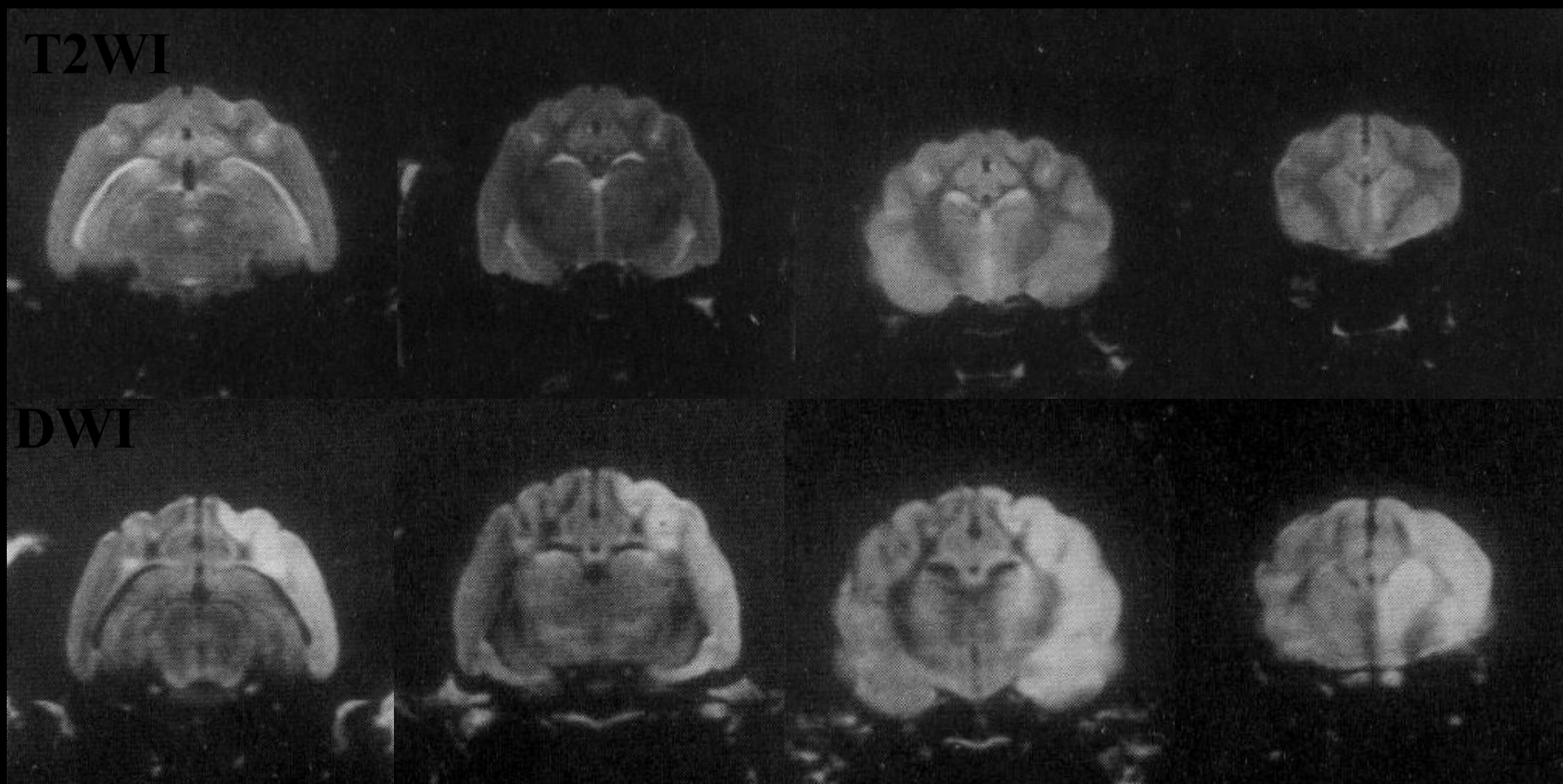


Trace(D) map (also called ADC or MD)

- Trace(D) is homogeneous in normal brain parenchyma
- Low inter-subject variability

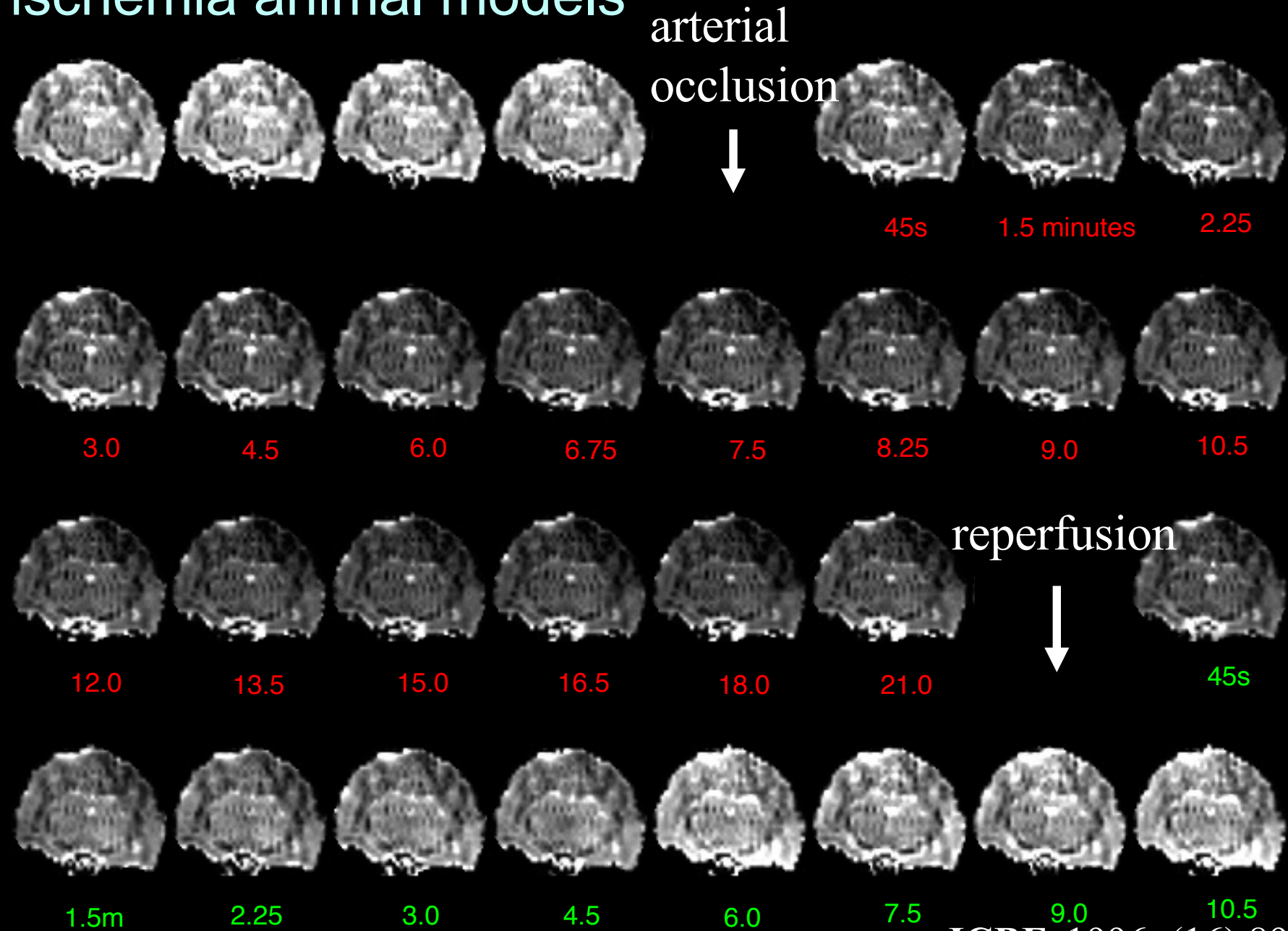
# Early Detection of Stroke by Diffusion MRI

---



[Mosley et.al, Magn Reson Med. 1990 May;14\(2\):330-46.](#)

# Kinetic of diffusion changes in reversible complete ischemia animal models

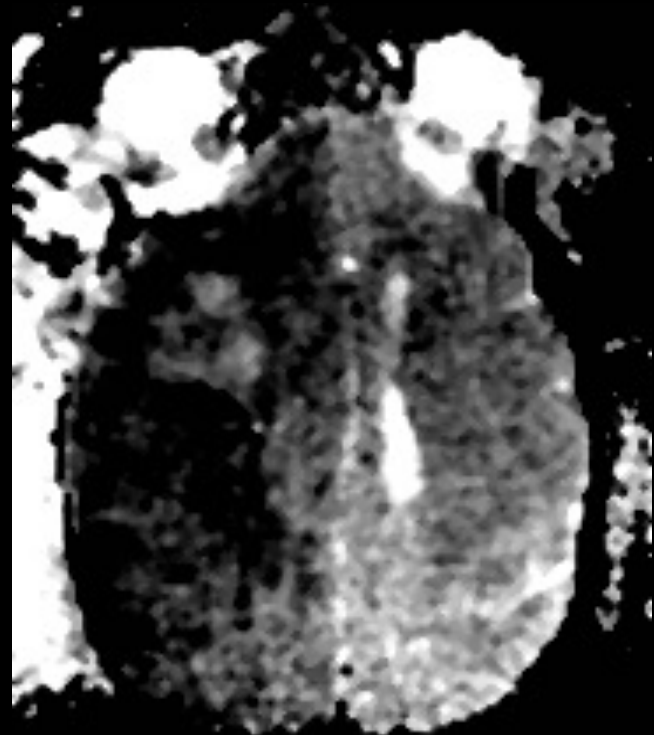




# Tissue characterization in stroke

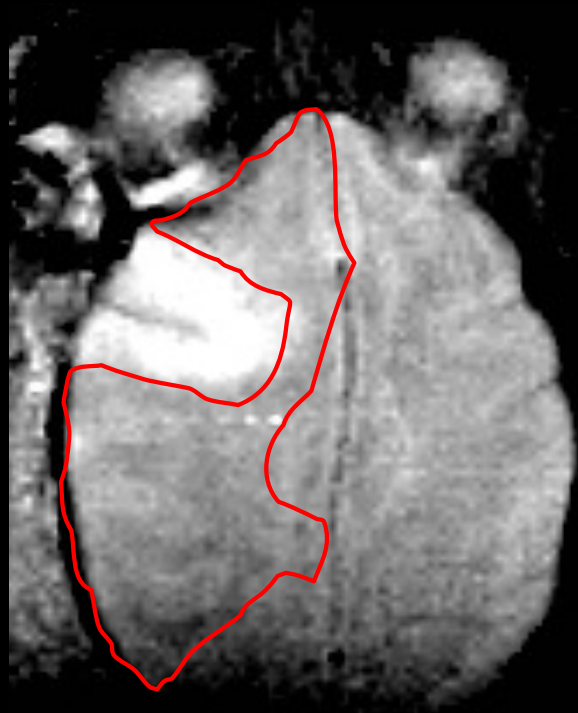


T2-weighted MRI



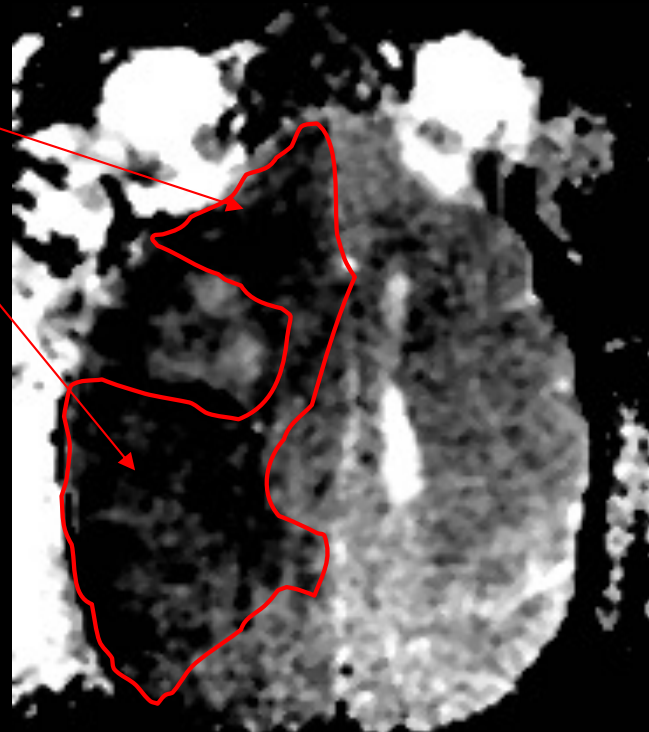
Trace (D)

# Tissue characterization in stroke



T2-weighted MRI

Acute  
Ischemia  
or stroke



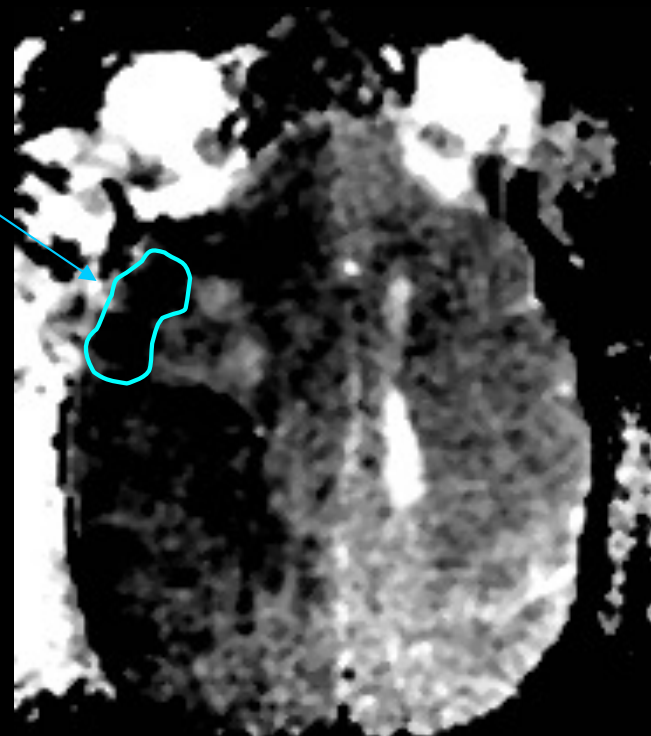
Trace (D)

# Tissue characterization in stroke



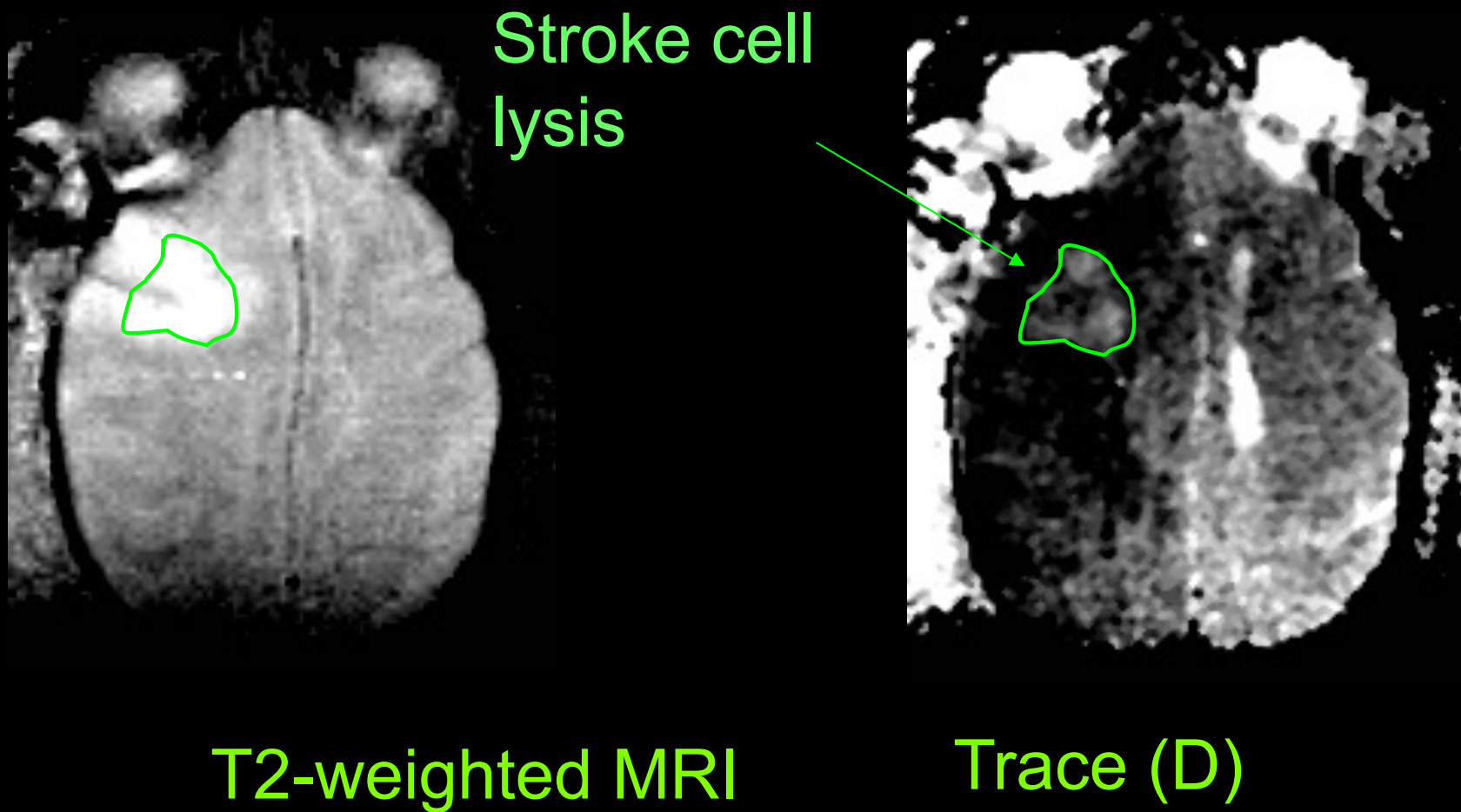
T2-weighted MRI

Stroke  
intact  
cells



Trace (D)

# Tissue characterization in stroke

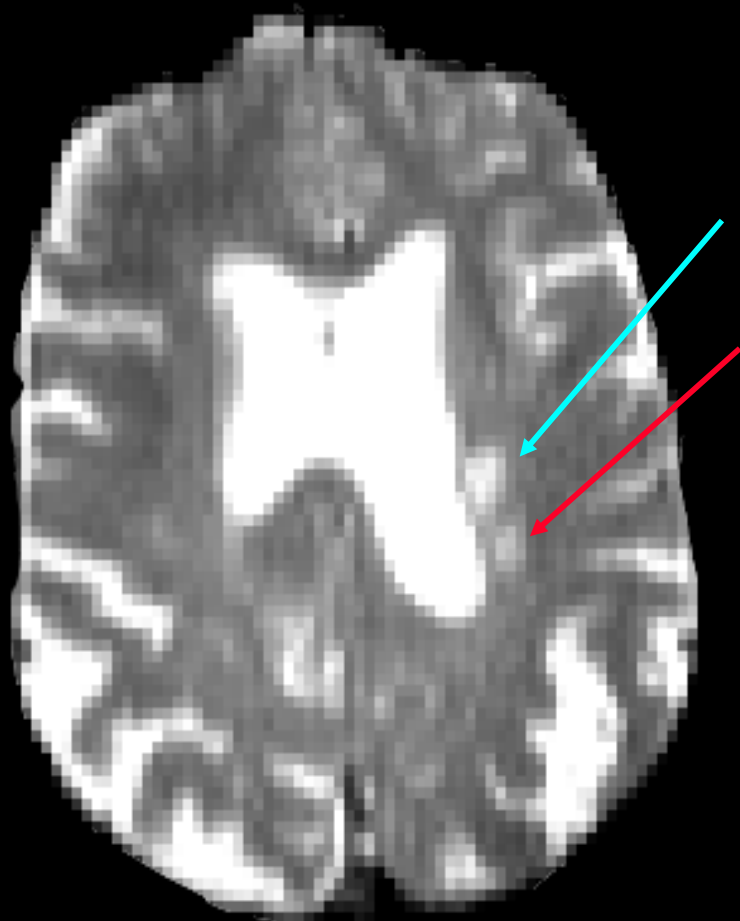


# SUMMARY. Tissue characterization in brain ischemia and stroke.

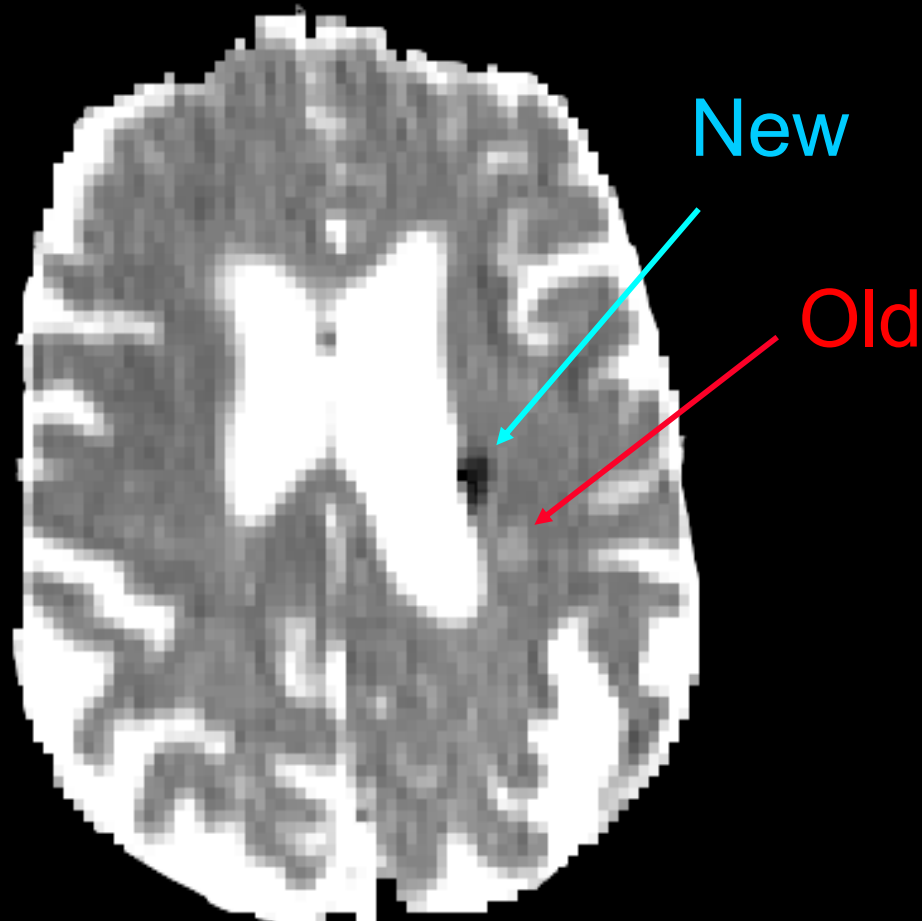
## T2WI      Diffusion

- |  |   |            |
|--|---|------------|
| • <b>Reduced perfusion</b>                     | = | =          |
| • <b>Ischemia</b>                              | = | - Trace(D) |
| • <b>Acute infarct</b><br>(no vasogenic edema) | = | - Trace(D) |
| • <b>Subacute infarct</b><br>(vasogenic edema) | + | - Trace(D) |
| • <b>Chronic infarct</b><br>(cell lysis)       | + | + Trace(D) |
| • <b>Healthy tissue</b><br>(vasogenic edema)   | + | + Trace(D) |

# Trace(**D**) differentiates between recent and old infarcts



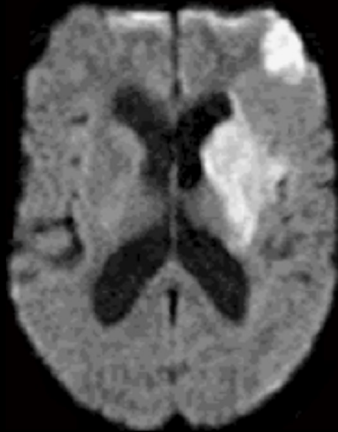
T2-weighted MRI



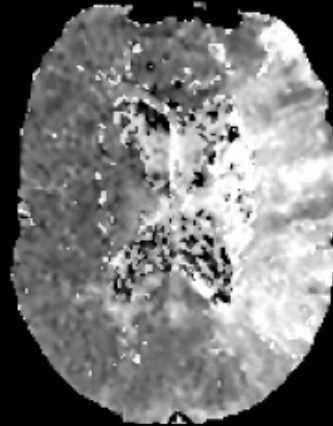
Trace(**D**)

# Documenting tissue plasminogen activator(tPA) treatment outcome with diffusion and perfusion MRI

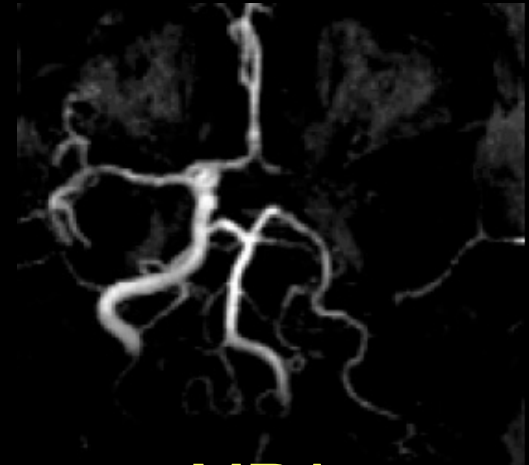
Pre tPA



DWI

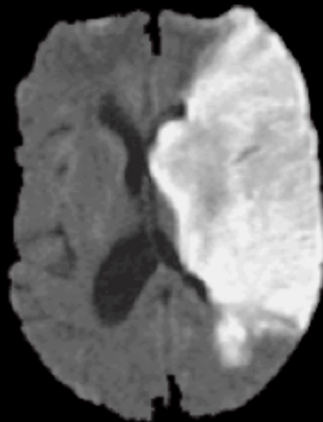


MTT

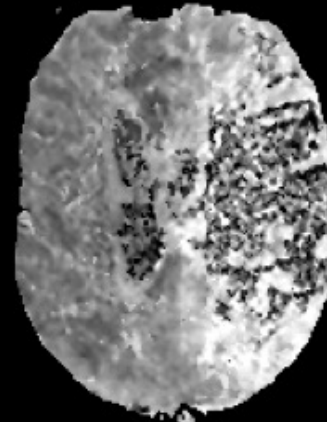


MRA

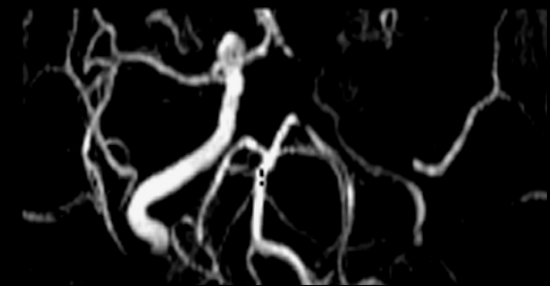
Post tPA



DWI



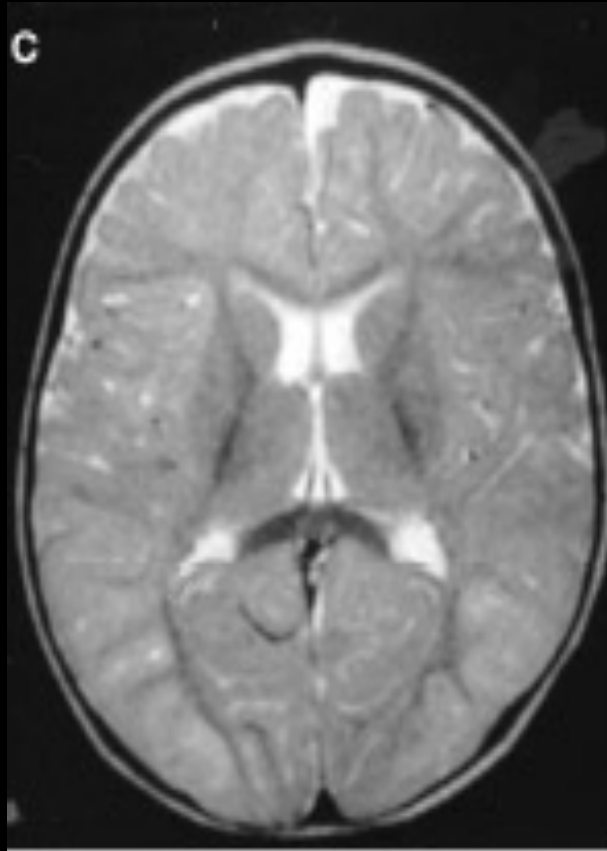
MTT



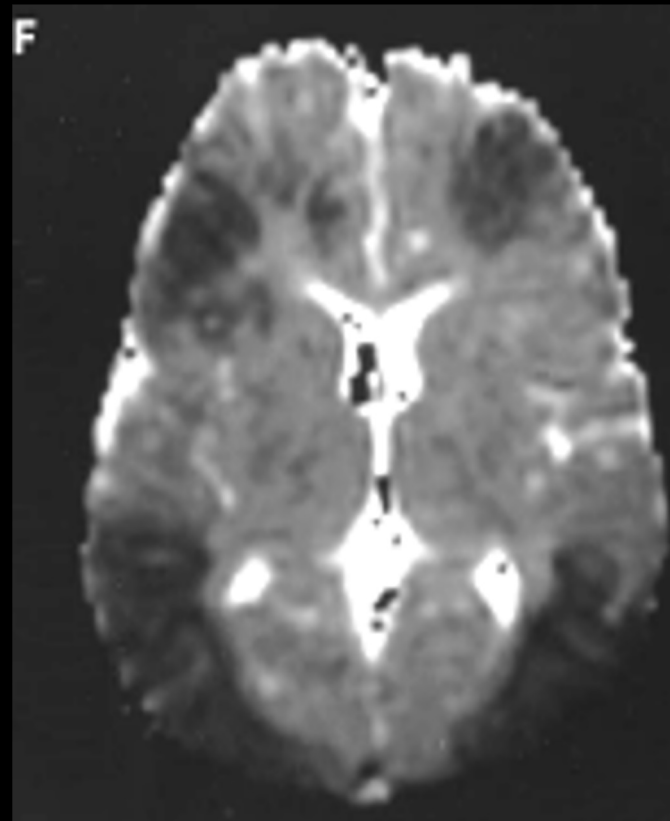
MRA

# TRAUMATIC BRAIN INJURY





T2WI



Trace(D)

7.5-month old boy who reportedly fell off the bed onto a carpeted floor. Scan performed 1 day after presentation.

# Biophysical hypothesis for Trace (or ADC) reduction in ischemia

In the normal brain: 80% intracellular water

$$ADC_{total} = ADC_{intra} * f_{intra} + ADC_{extra} * f_{extra}$$

Following ischemia: Na/K ATP-ase failure causes cell swelling

10% shift of water:  $f_{extra} \rightarrow f_{intra}$

Results in a 30-50% decrease in  $ADC_{total}$

Compartment shift hypothesis:

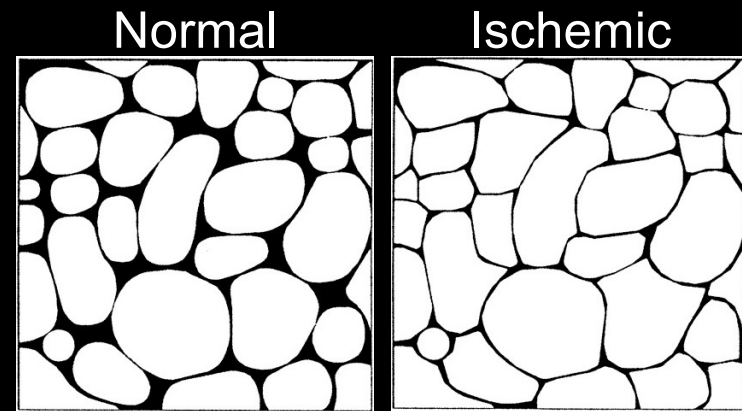
$$\text{Intrinsic } ADC_{intra} \ll ADC_{extra}$$

Extracellular tortuosity hypothesis:

$ADC_{extra}$  decrease

Intracellular restriction hypothesis:

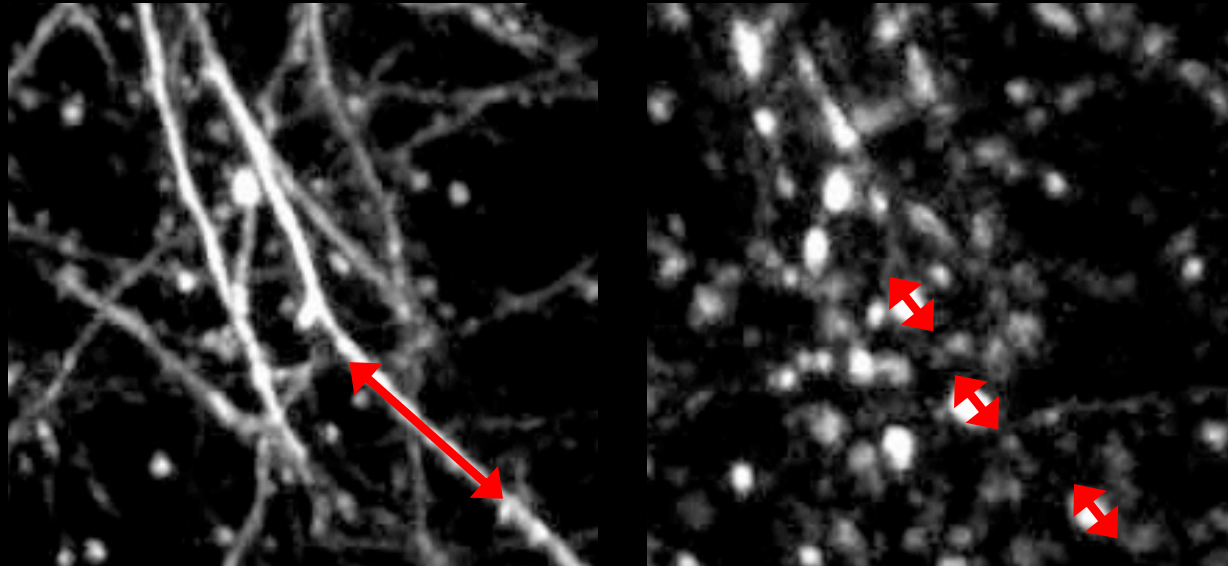
Diffusivity of Cs<sup>+</sup> (intracellular surrogate) decreased by ~75% following global ischemia. (Goodman, et al. *MRM* 2008)



Chen KC. & Nicholson C. *PNAS* 2000

# Hypothesis by Matt Budde, et al., PNAS, 2010

Neurite beading is sufficient to decrease  $ADC_{\text{intra}}$  by restricting water mobility along each neurite.



## Approach

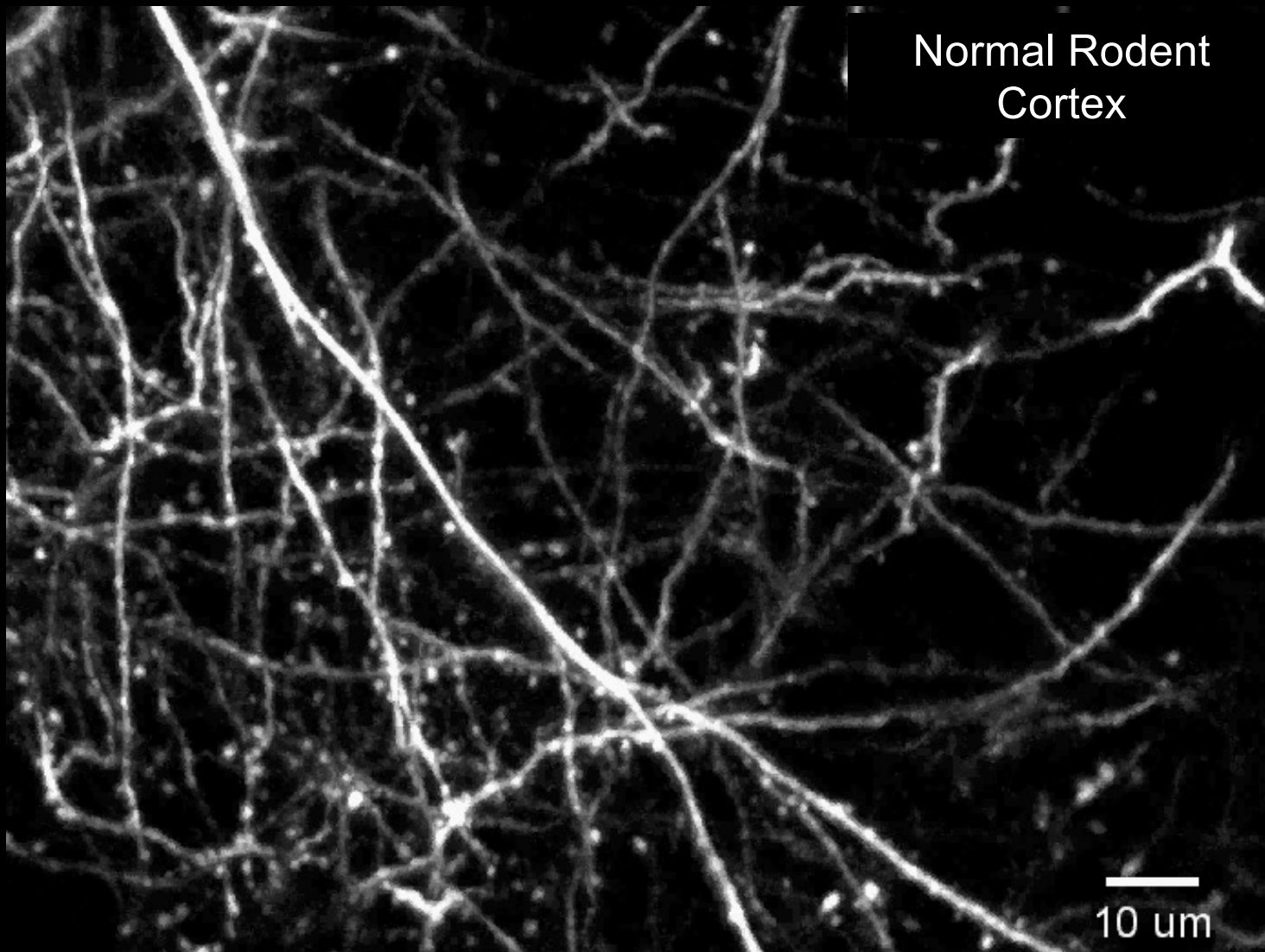
Derive a biophysical model of beading in neurites

Simulate diffusion MR experiment in 3D geometrical surfaces

Validate model in mammalian tissues

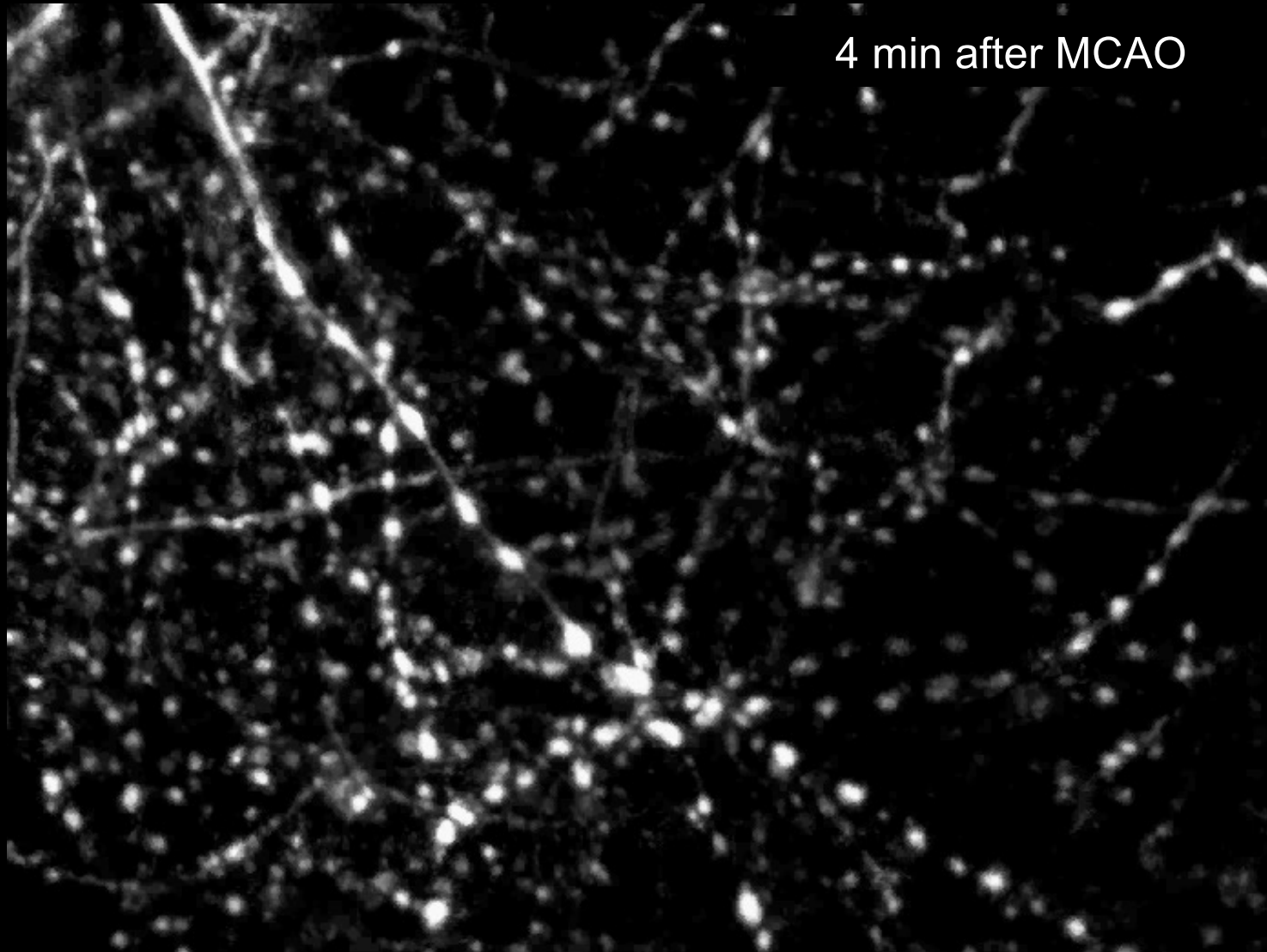
# What can we learn from other imaging modalities?

**In vivo two-photon microscopy** (Murphy T, et al. *J Neurosci* 2008)



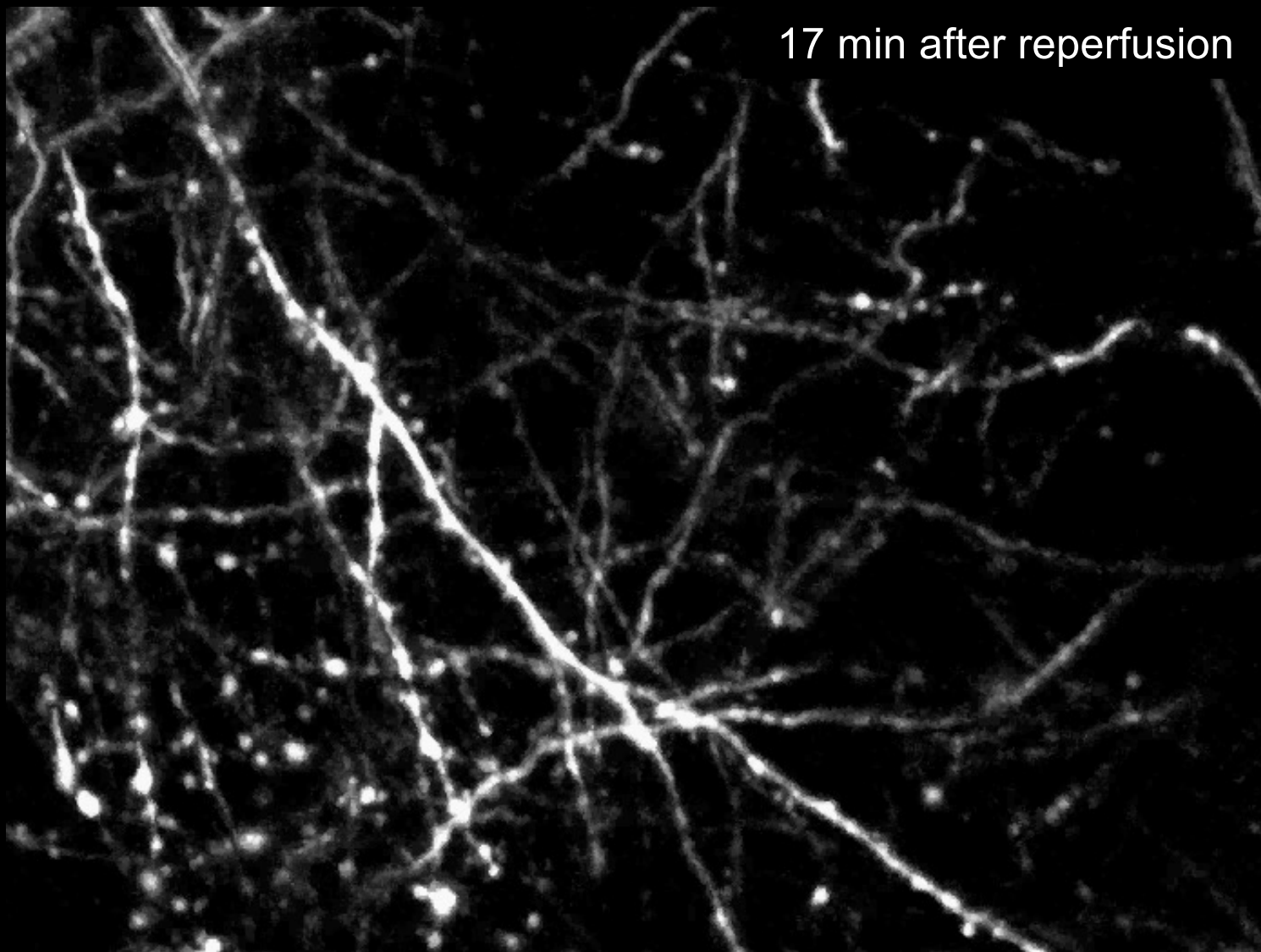
Slide courtesy of Matt Budde

# Neurite beading occurs abruptly after ischemia...



Slide courtesy of Matt Budde

...and resolves upon reperfusion.



17 min after reperfusion

Slide courtesy of Matt Budde

# Diffusion anisotropy (shape of displacement profile)

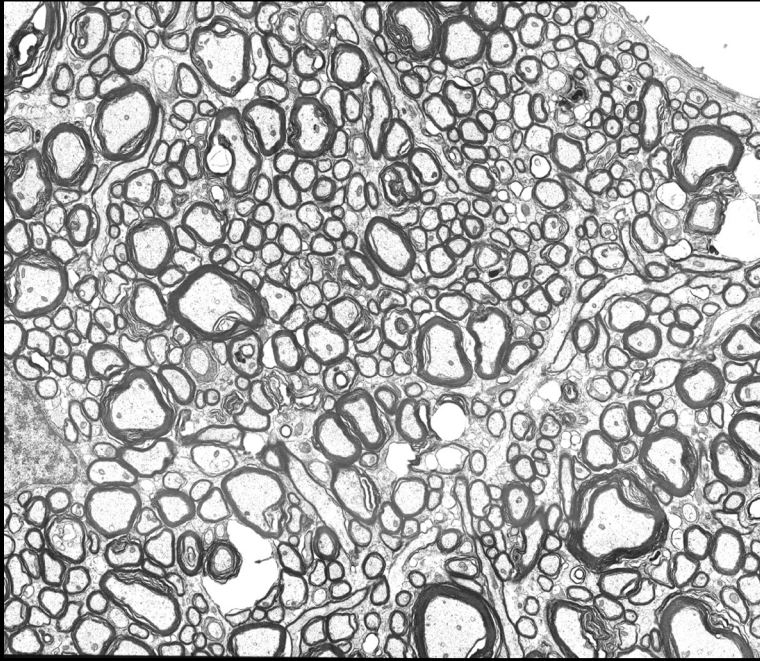


- Diffusion anisotropy is highly variable in normal white matter

- Differences in anisotropy reflect differences in white matter architecture

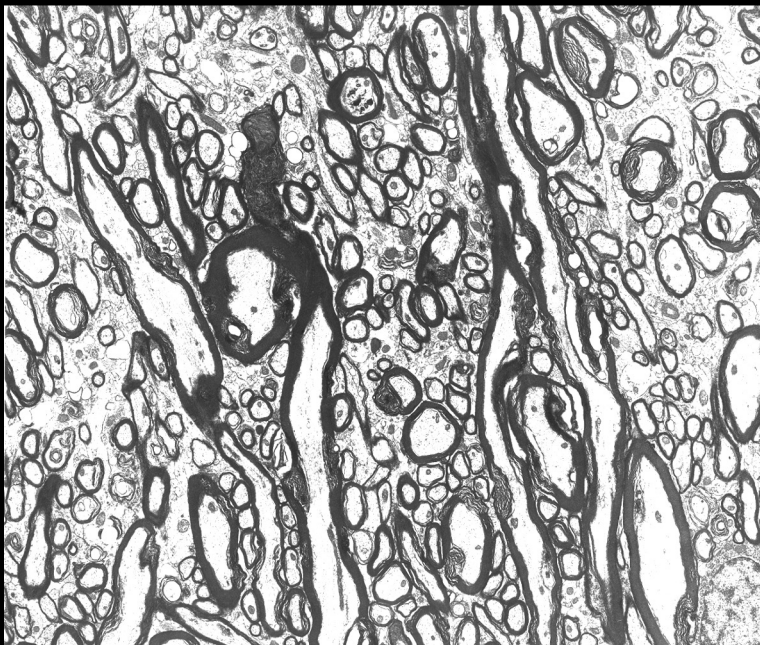
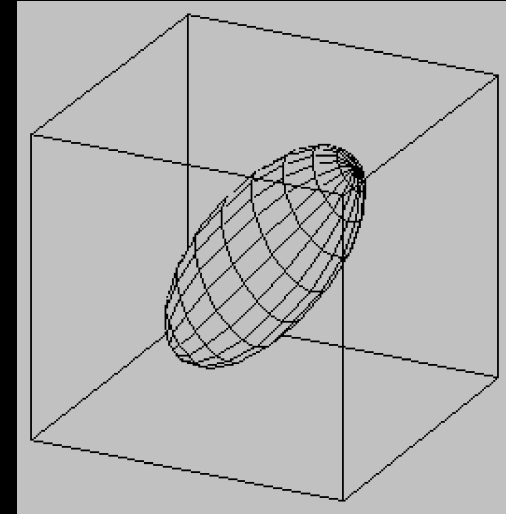
T2 weighted image   Anisotropy map

Intra-voxel orientational coherence of white matter fibers is an important factor in determining diffusion anisotropy



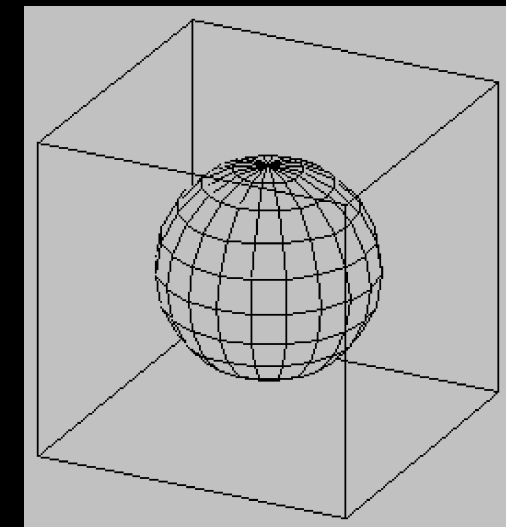
White matter  
(Corpus callosum)

anisotropic  
diffusion



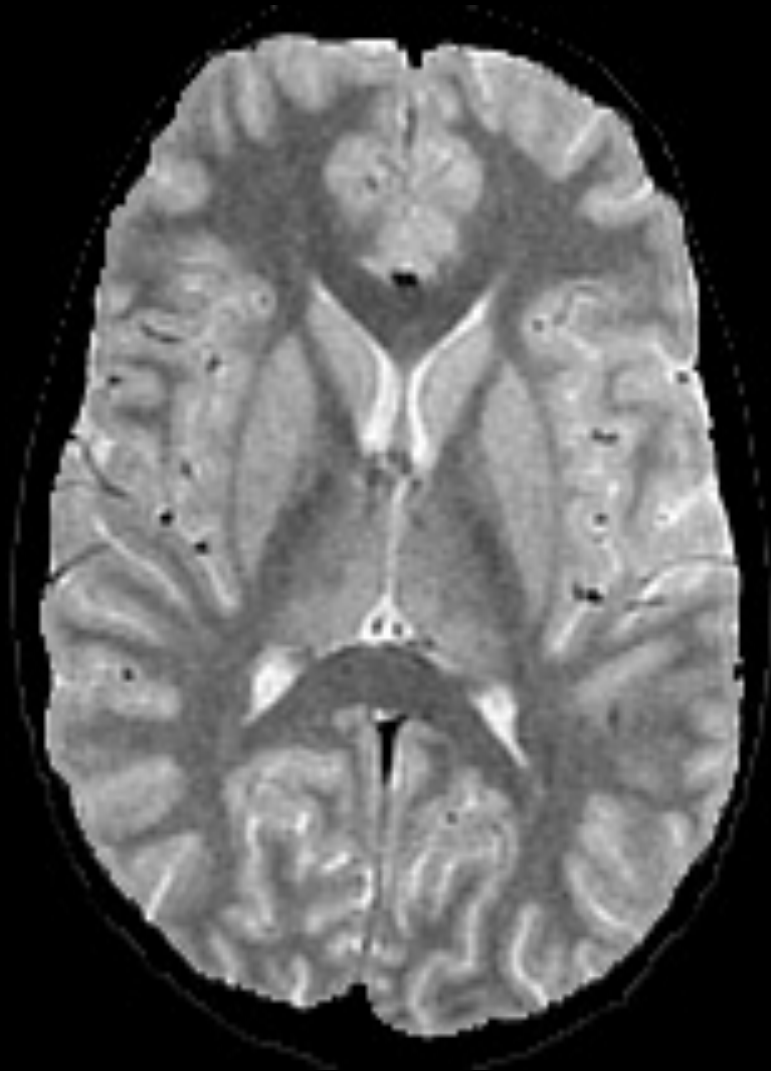
Subcortical  
White matter

more isotropic  
diffusion

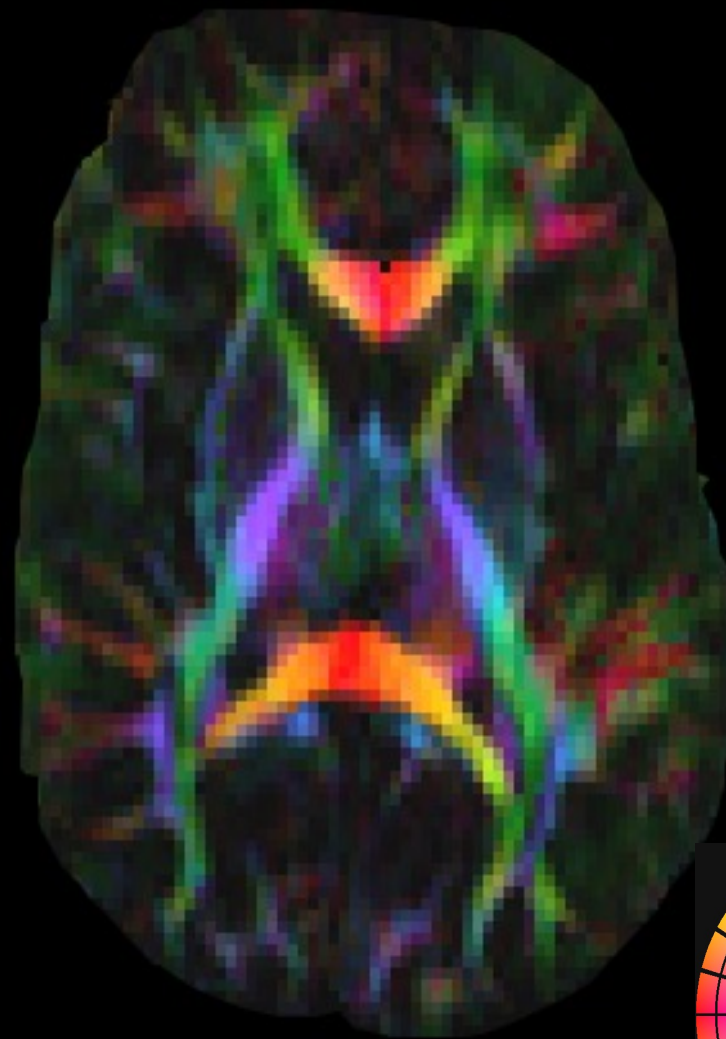




# Fiber orientation



T2 weighted image



Color fiber orientation map

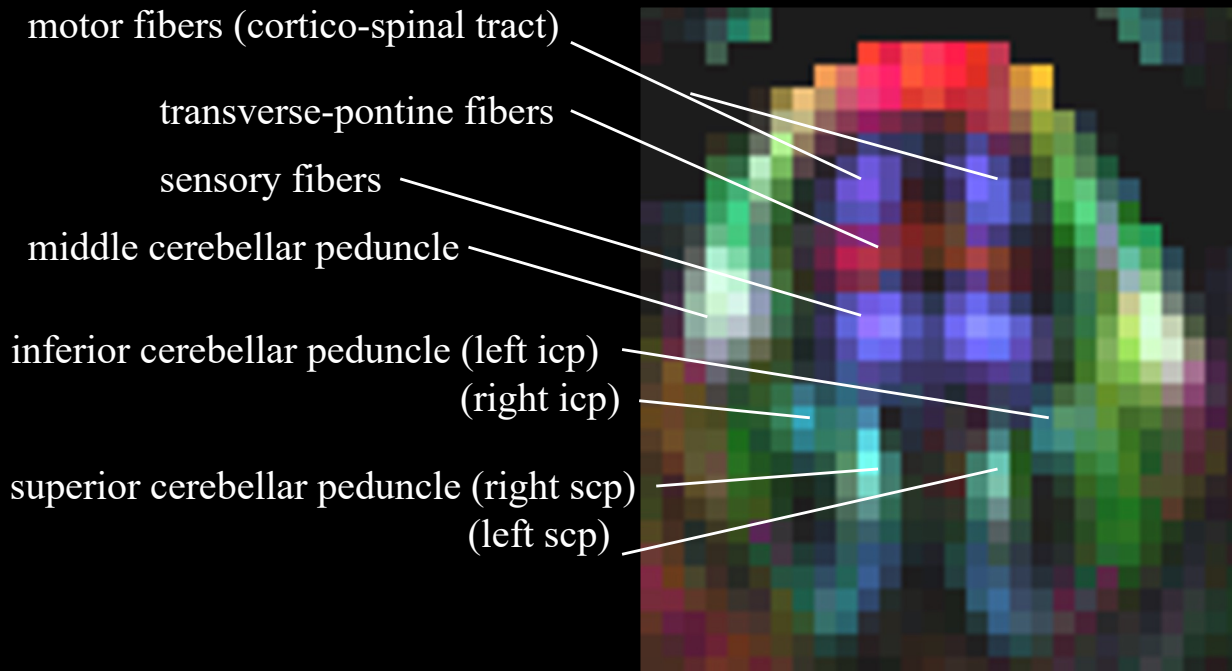


Pajevic and Pierpaoli, MRM 1999

# DTI vs. conventional structural MRI

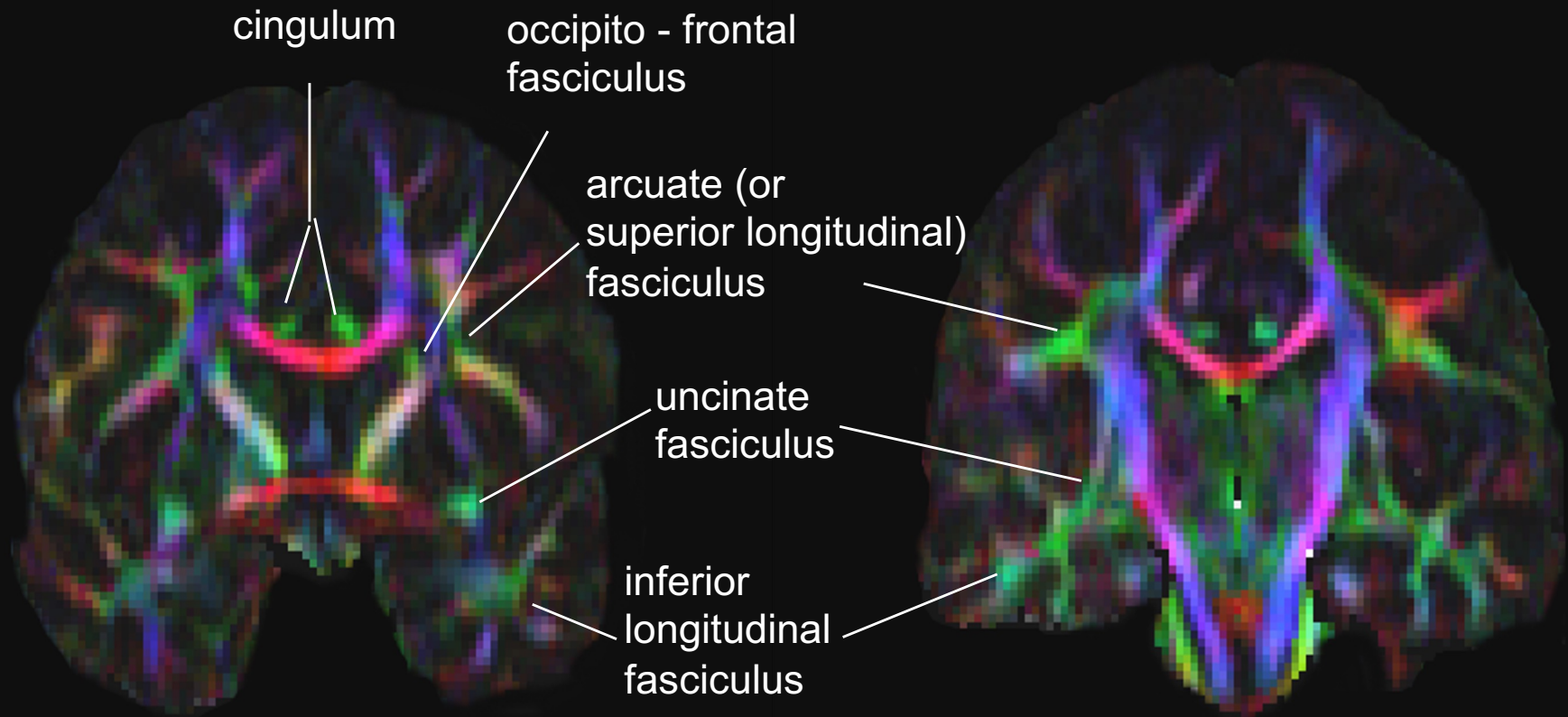


High resolution  
T2-weighted  
structural MRI



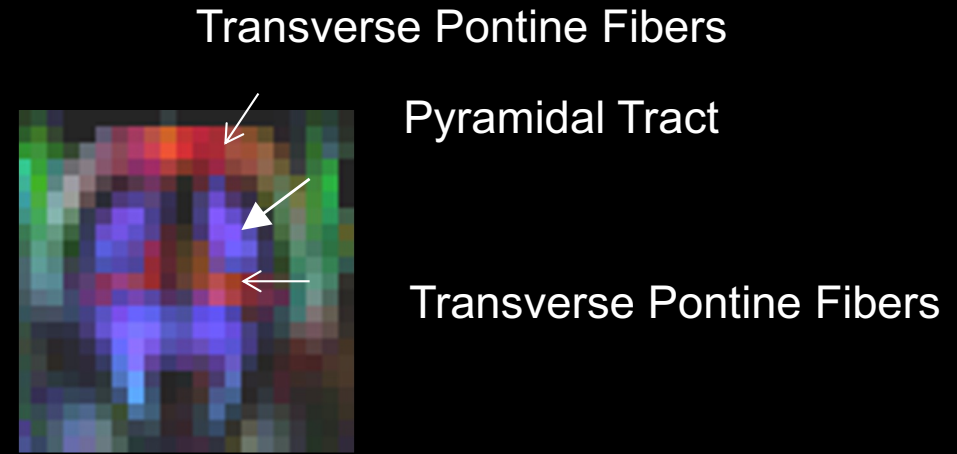
DTI fiber  
orientation map

# Color maps of Association Pathways

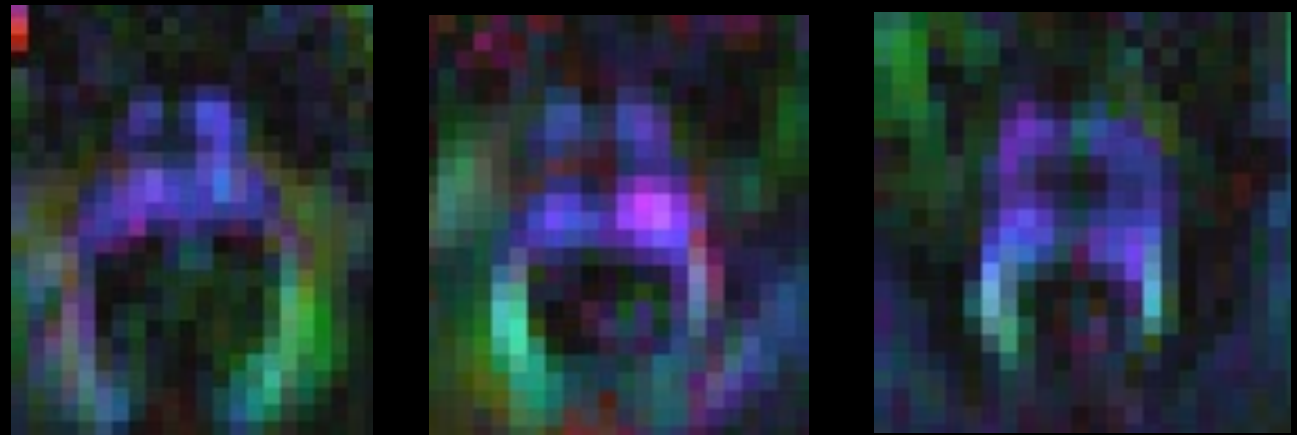


# Degeneration of pontocerebellar pathways in Multiple System Atrophy

Healthy subject

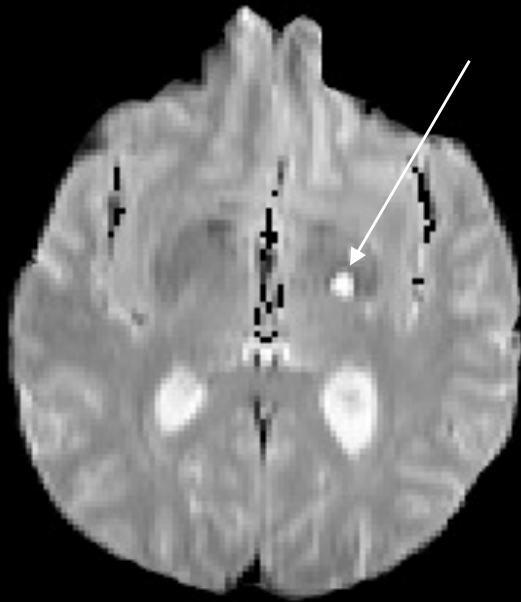


MSA patient

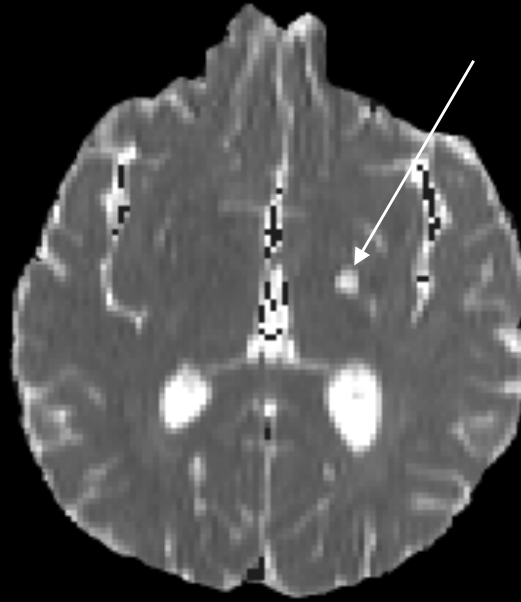


# SECONDARY WHITE MATTER DEGENERATION

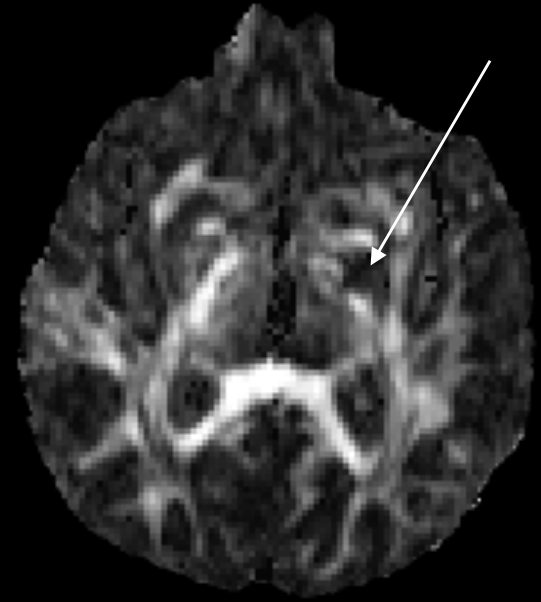
## Primary lesion in the Internal Capsule



T2WI

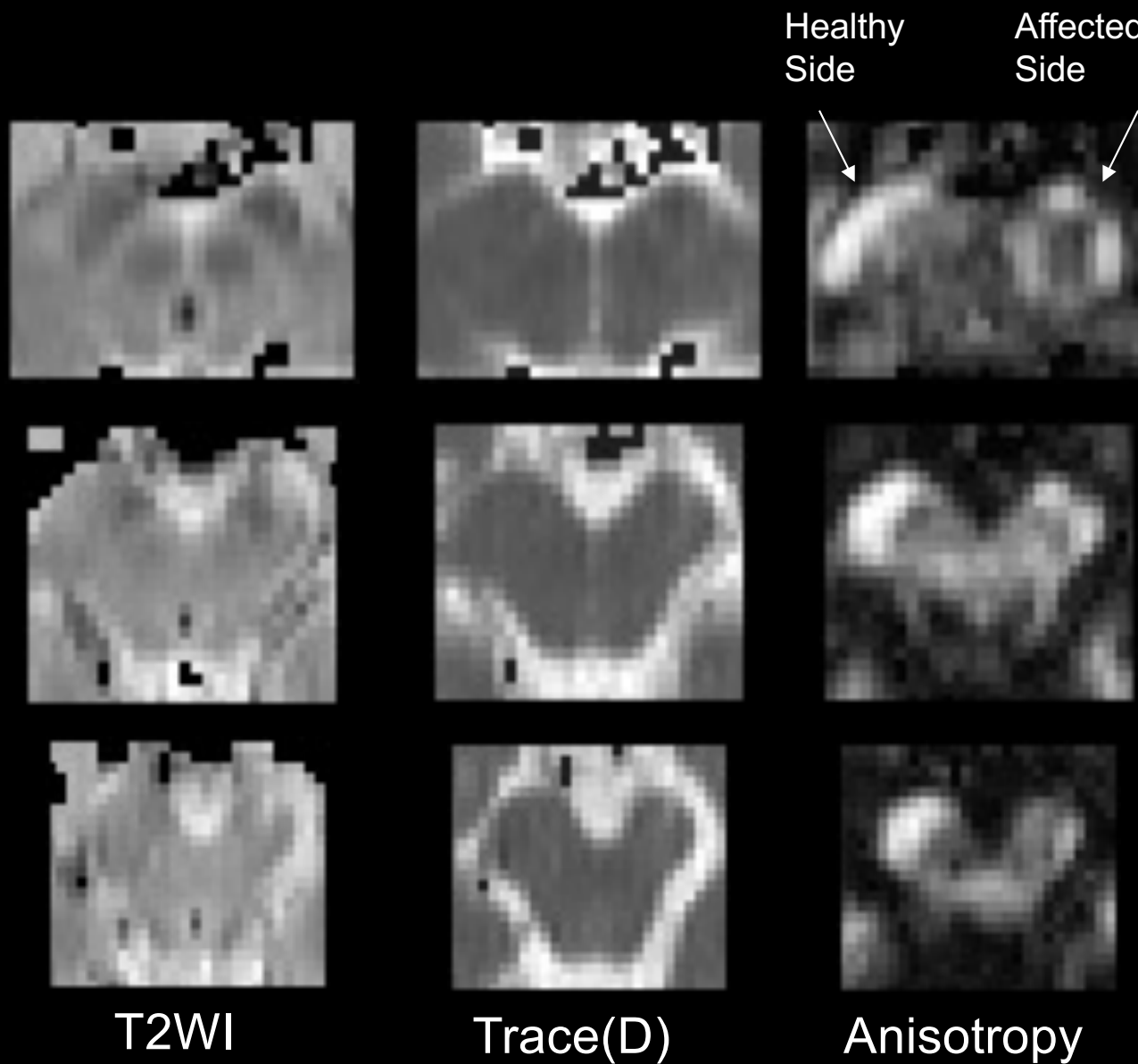


Trace(D)



Anisotropy

# Secondary degeneration in the Cerebral Peduncle



# Secondary degeneration in the Rostral Pons

Healthy  
Side

Affected  
Side



T2WI

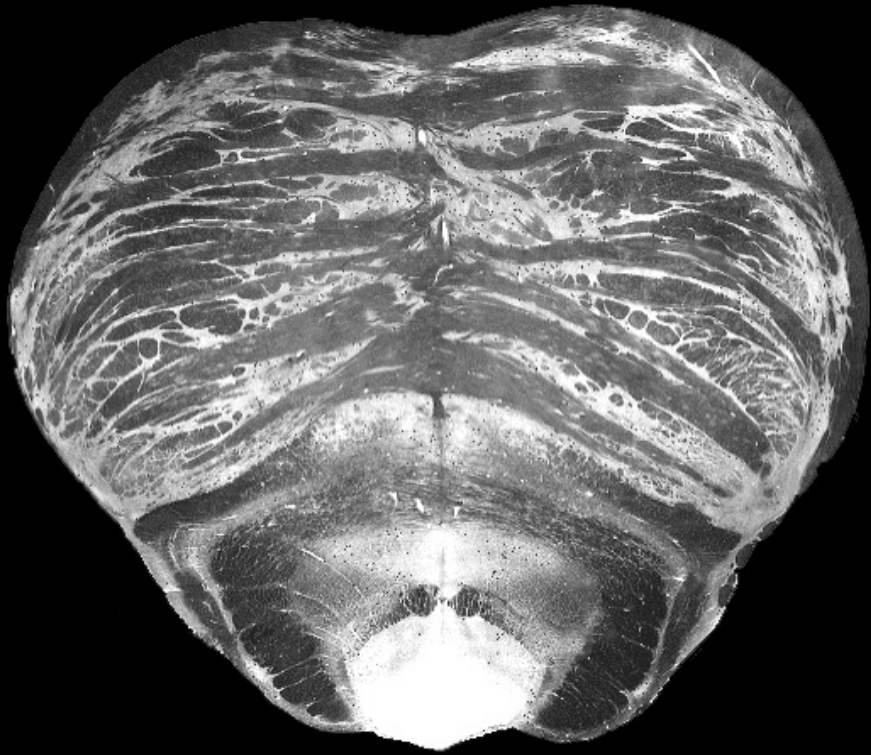


Trace(D)



Anisotropy

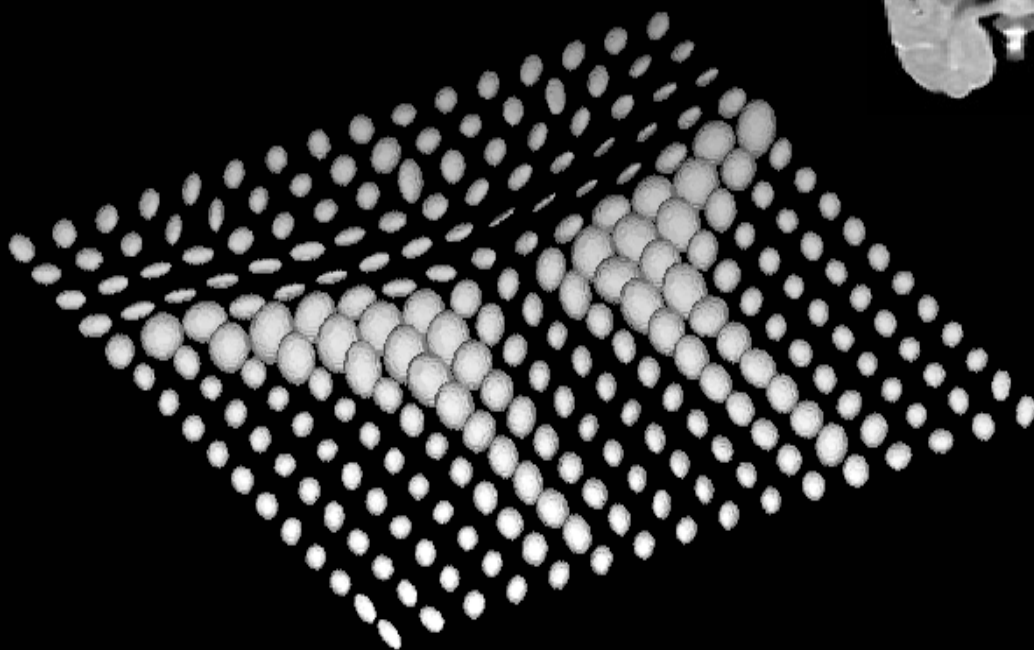
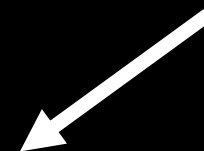
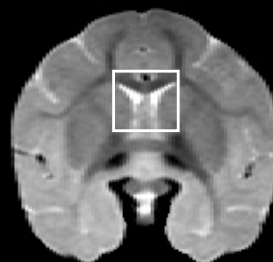
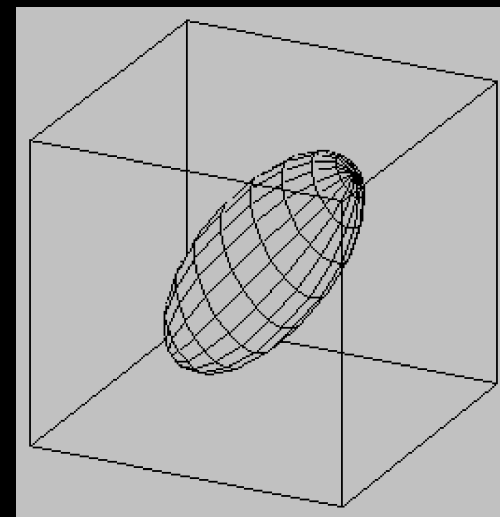
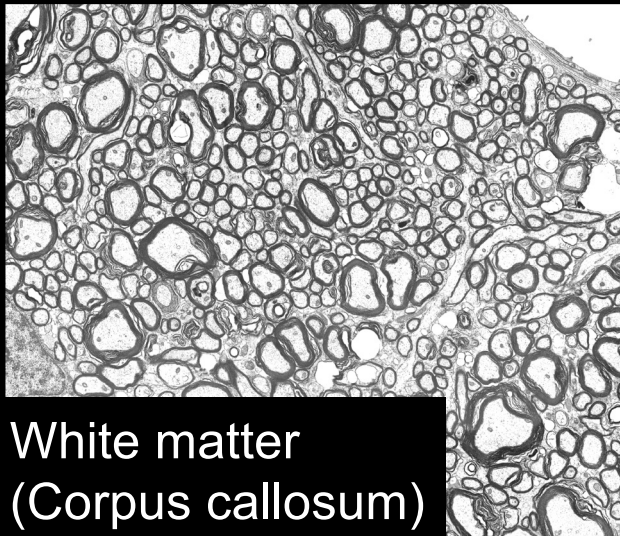




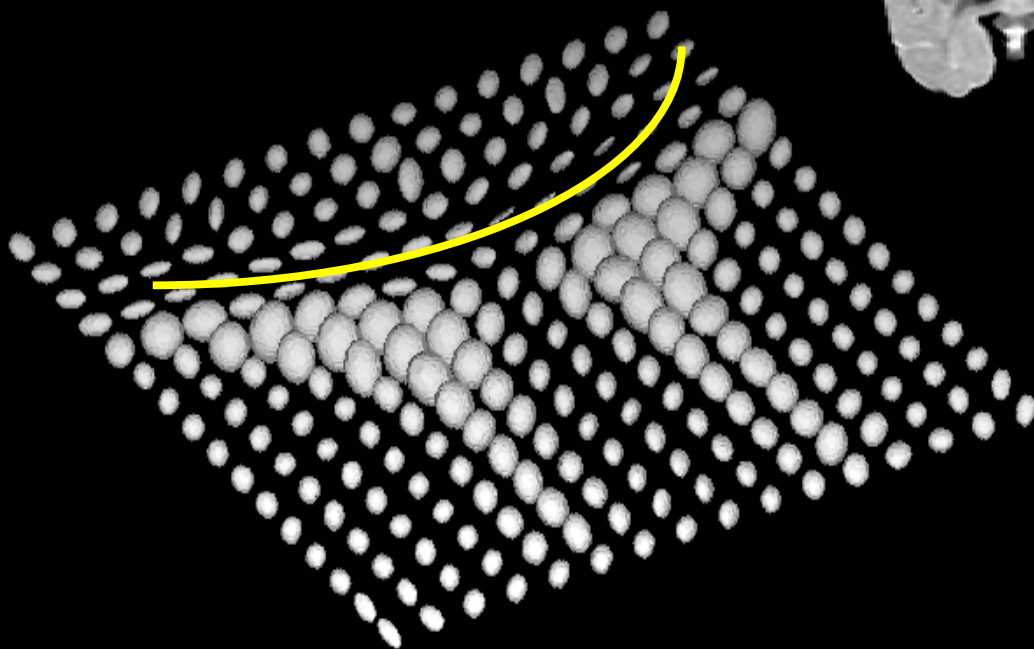
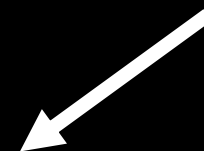
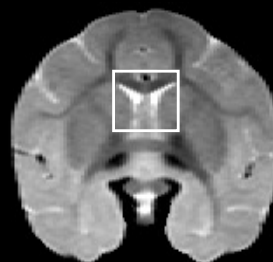
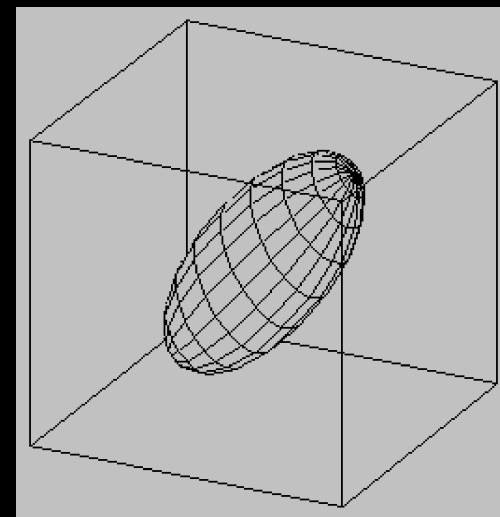
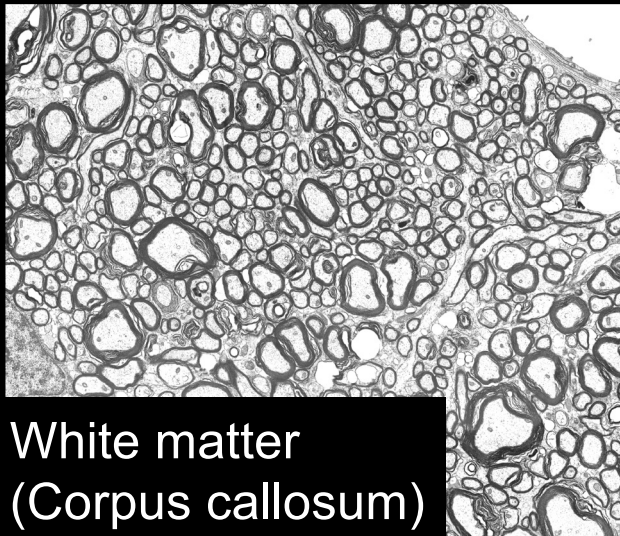
# Summary of findings in Wallerian degeneration

|  | <b>Primary lesion</b>                             | <b>Wallerian degeneration<br/>in regions of isolated<br/>fiber bundles</b> | <b>Wallerian degeneration<br/>in regions of intersecting<br/>pathways</b>   |
|--|---|--|---|
| $D_{av} = \text{Trace}(\mathbf{D})/3$  | Large increase                                    | Small increase   | Small increase  |
| <b>Diffusion anisotropy</b>  | Large decrease                                    | Large decrease   | Small decrease. No<br>changes or slight increase<br>possible  |
| <b>Diffusivity parallel to<br/>the fibers (<math>\lambda_1</math>)</b>                                     | Increase  | Decrease   | Small change  |
| <b>Diffusivity<br/>perpendicular to the<br/>fibers (<math>\lambda_2</math> and <math>\lambda_3</math>)</b> | Increase  | Increase   | Small change  |
| <b>Apparent fiber<br/>orientation (<math>\epsilon_1</math>)</b>  | Inconsistent changes due<br>to loss of anisotropy | Inconsistent changes due<br>to loss of anisotropy                          | Consistent changes<br>dictated by the orientation<br>of remaining pathways<br>unaffected by Wallerian<br>degeneration |

# Diffusion MRI “tractography”



# Diffusion MRI “tractography”



# Deterministic Diffusion MRI tractography

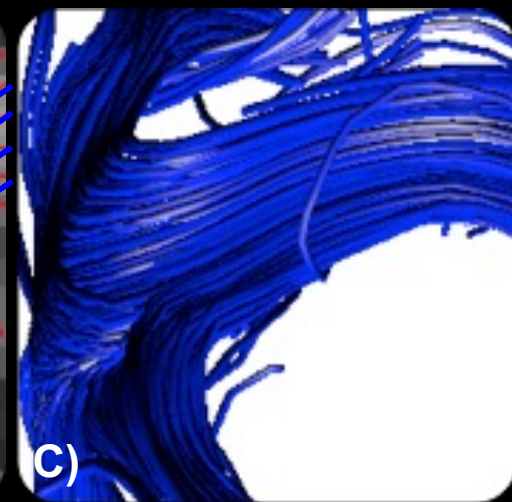
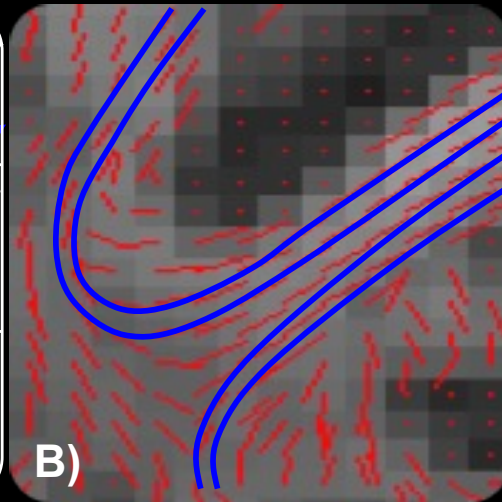
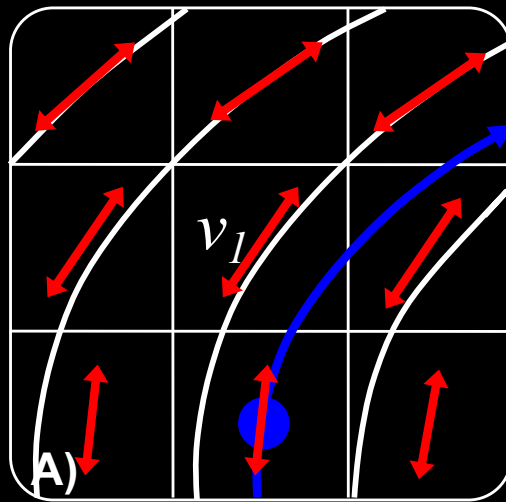
Seminal contributions:

Conturo *et al.* PNAS, 1999

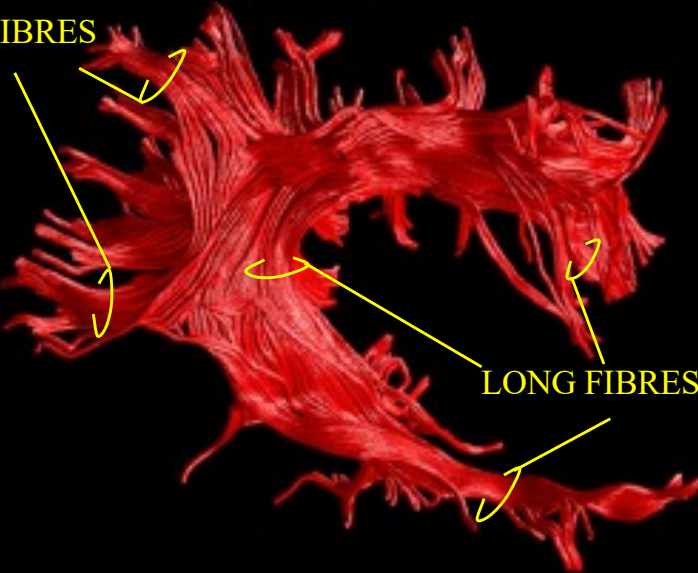
Mori *et al.* Annals Neurology, 1999

Basser *et al.*, MRM 2000

Pupon *et al.*, Neuroimage, 2000



SHORT  
FIBRES

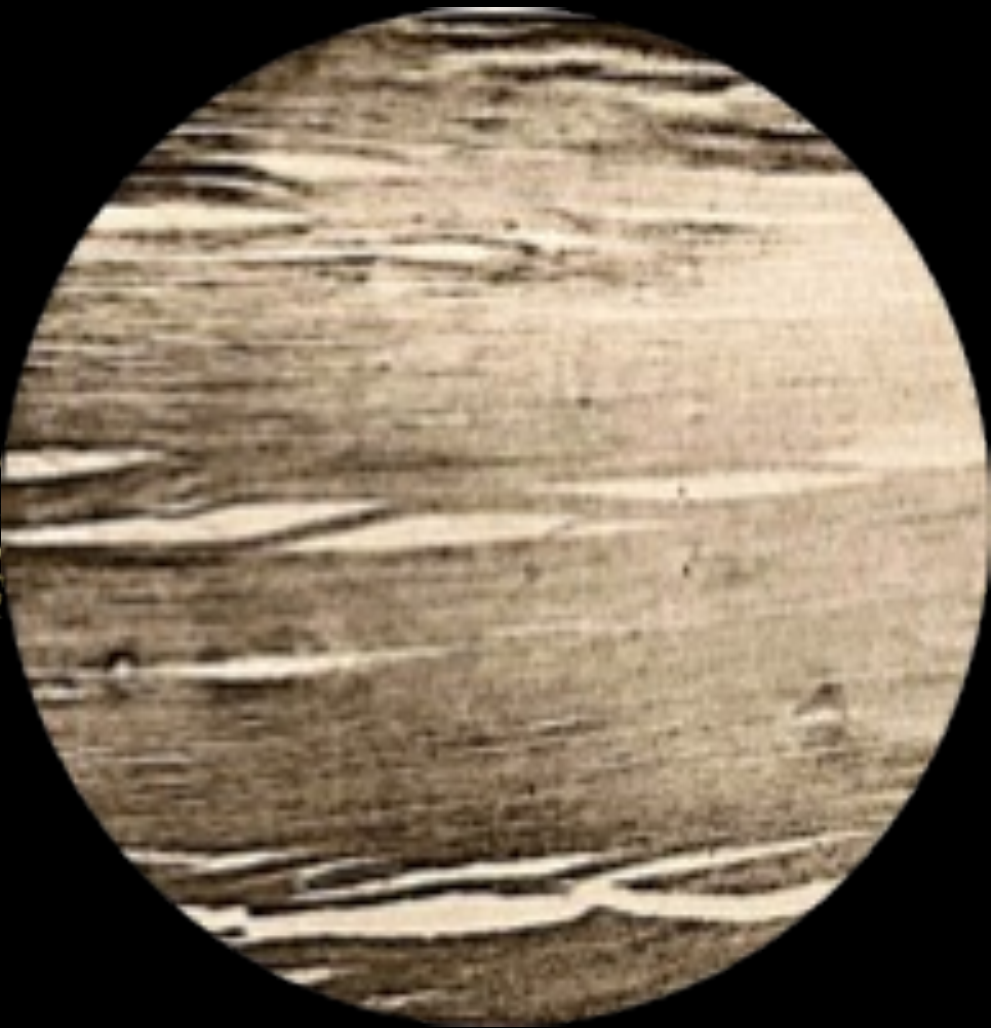


Virtual In-Vivo Dissection



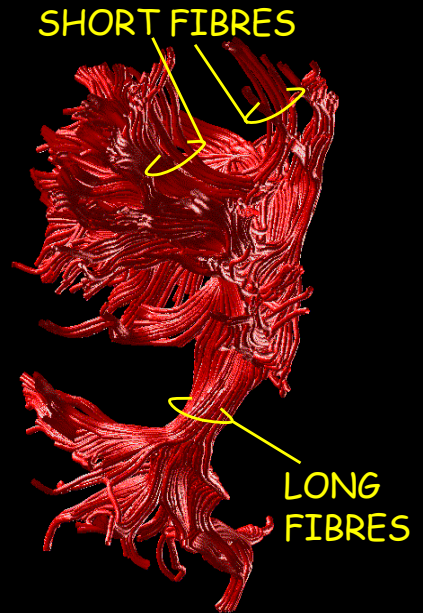
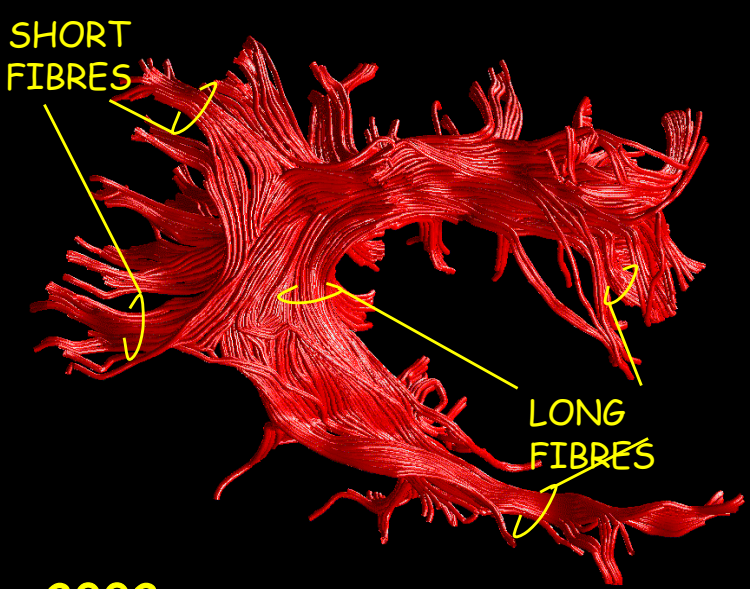
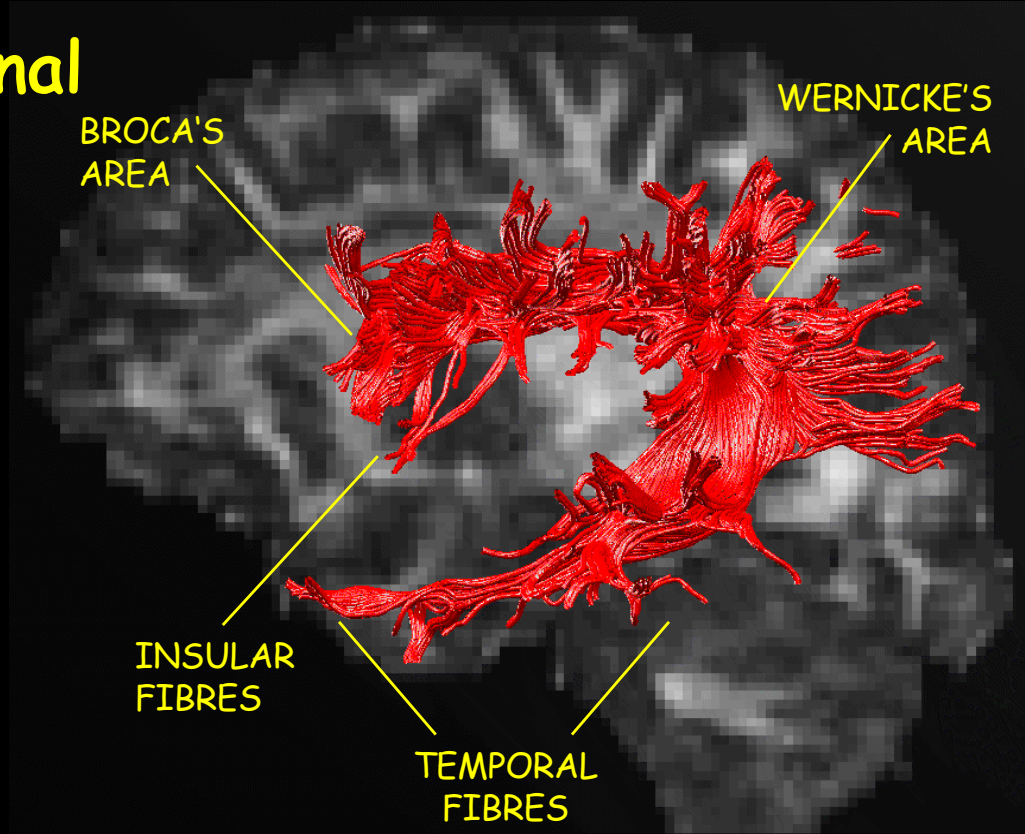
Post-Mortem Dissection

# The Klingler method of tract dissection



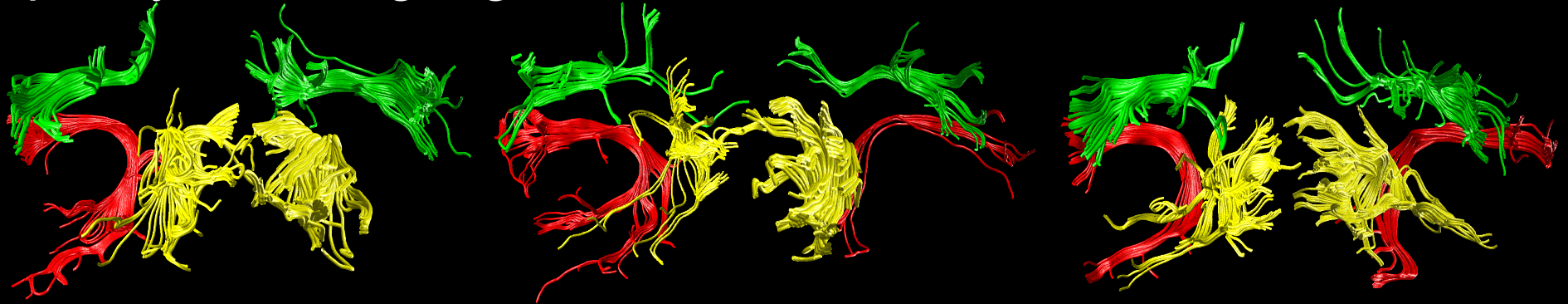
From Catani's chapter in Diffusion MRI (Oxford University Press)

# Superior Longitudinal Fasciculus





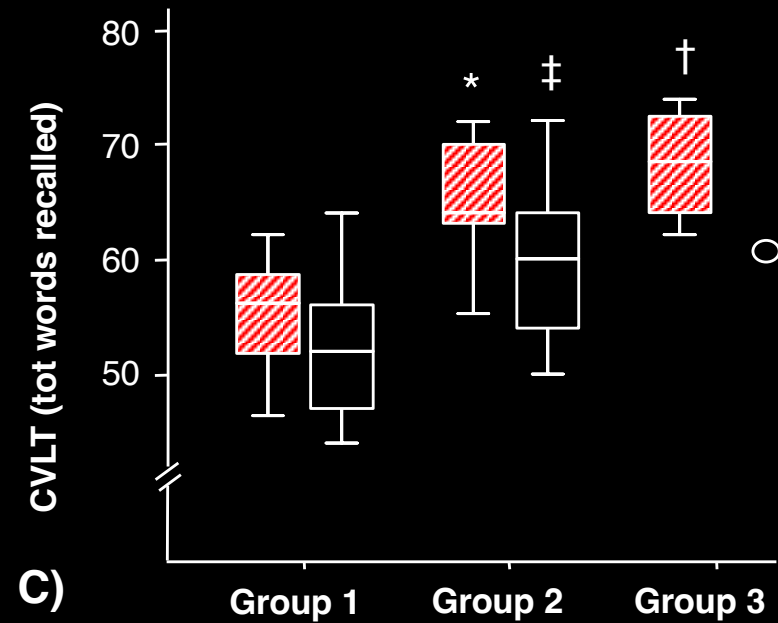
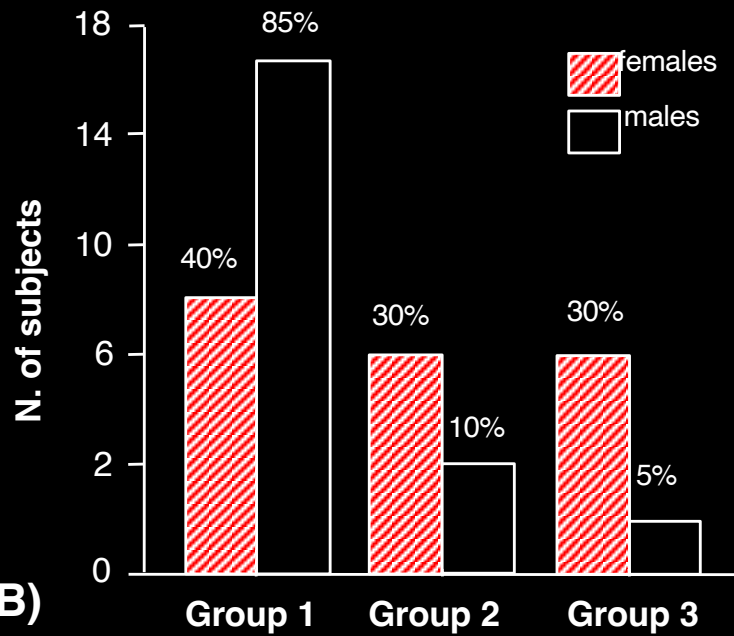
# perisylvian language networks Catani et al PNAS 2007



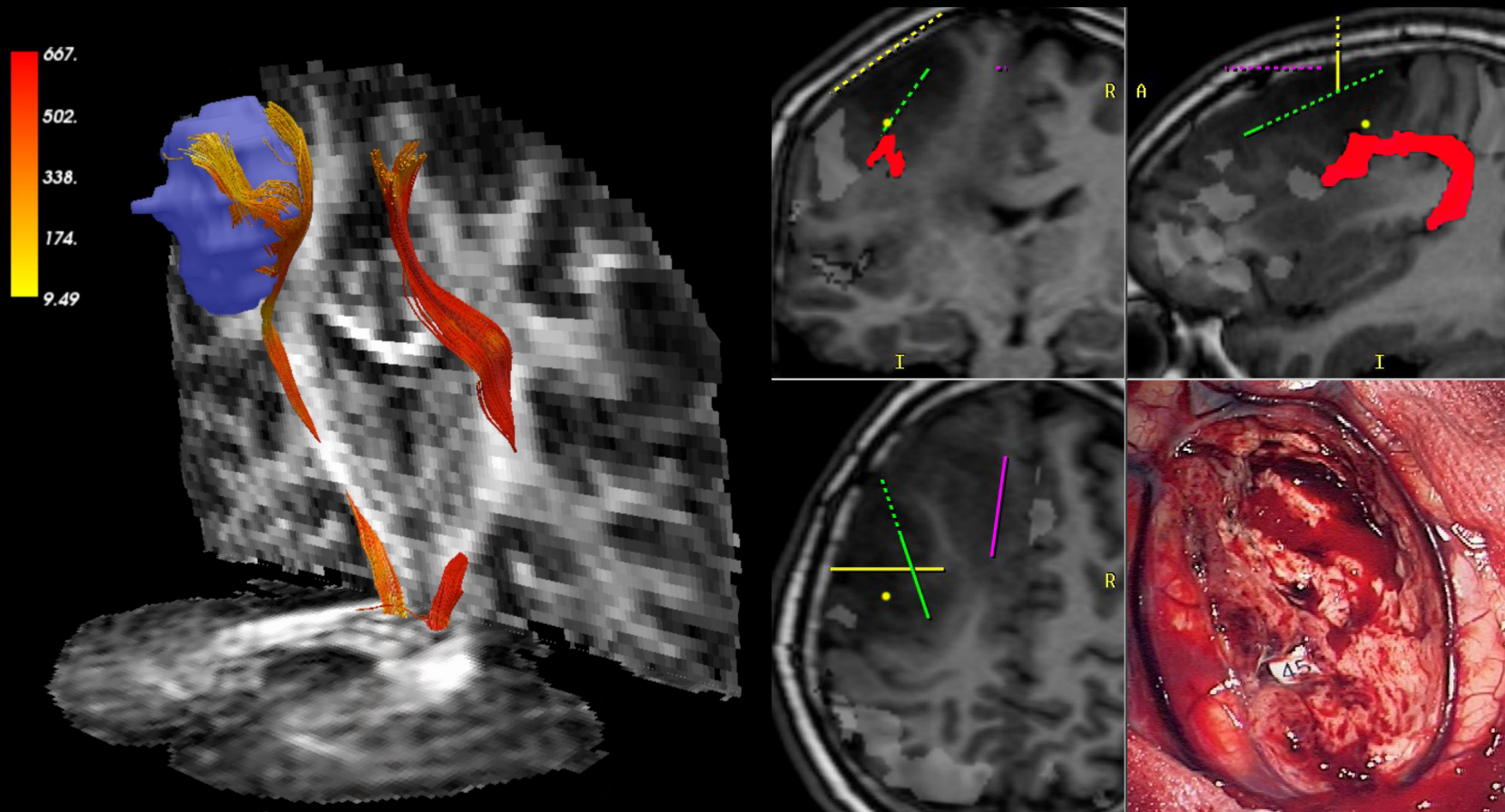
**A) Group 1** strong left lateralization (~60%)

**Group 2** bilateral, left lateralization (~20%)

**Group 3** bilateral, symmetrical (~20%)



# DT\_MRI tractography in presurgical assessment of tumors



# Probabilistic Diffusion MRI tractography

Seminal contributions:

Pajevic and Basser, 2000

Behrens *et al.*, 2003

Parker *et al.*, 2003

Lazar *et al.*, 2005

Jones *et al.*, 2005

# Probabilistic Diffusion MRI tractography

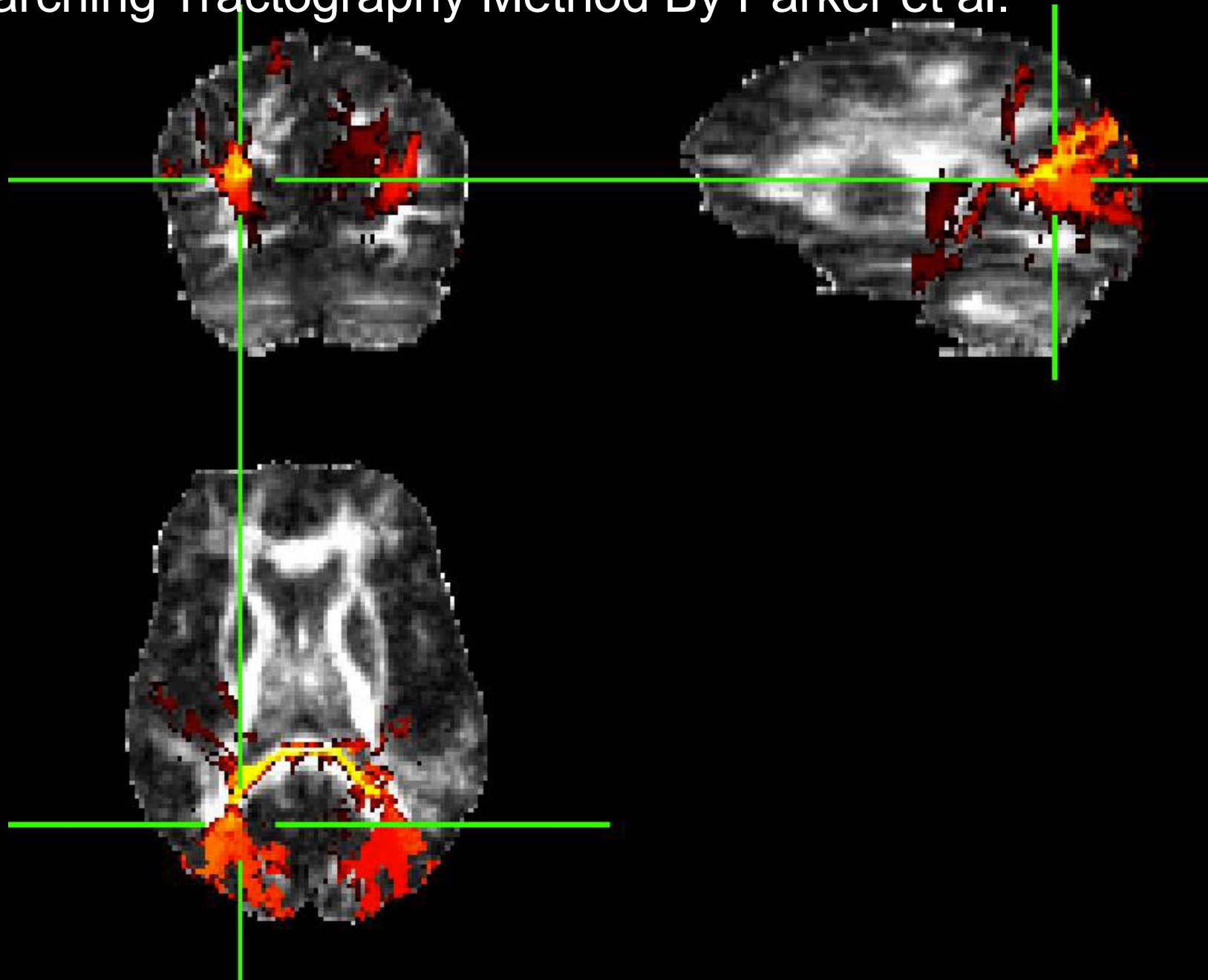
## Key Concepts:

Taking into account uncertainty (effects of noise)

Still considering a single fiber population in a voxel

Provides information on reproducibility of tracts,  
but it does not improve anatomical accuracy

Example of probabilistic tractography using the Fast Marching Tractography Method By Parker et al.



# Tractography from HARDI methods

# Spherical harmonics

L. Frank, 2000

## q-space, DSI

P. T. Callaghan, et al 1988

D. G. Cory and A. N. Garroway 1990

M. D. King, 1994

Y. Assaf and Y. Cohen, 1999

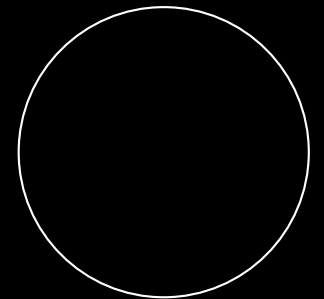
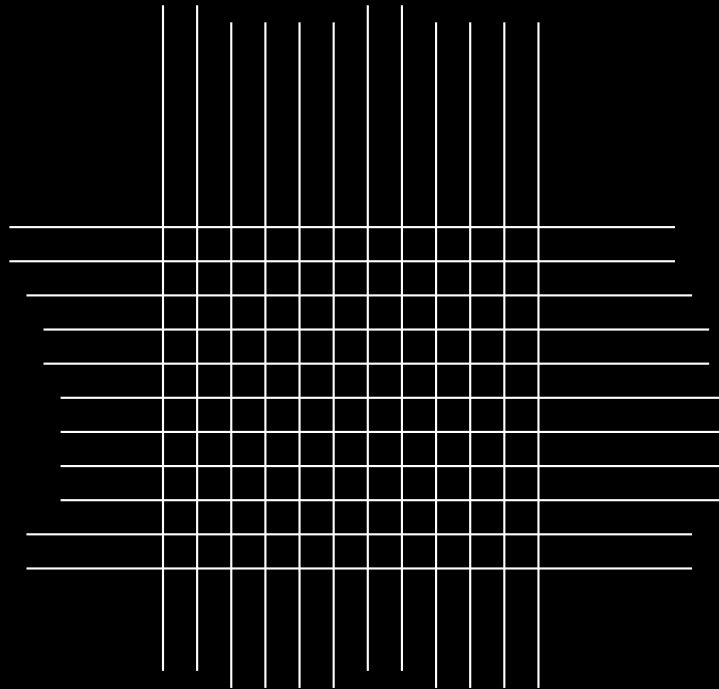
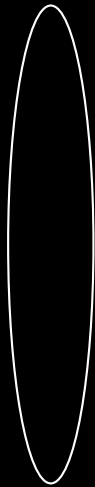
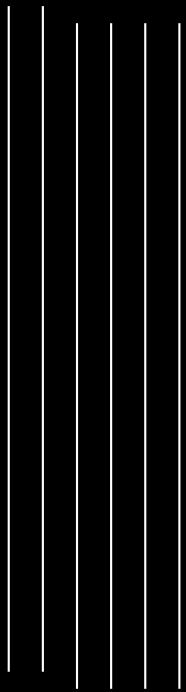
DS Tuch, JW Belliveau, TG Reese, VJ Wedeen, 1998

VJ Wedeen, 2000

---

# Multiple fiber populations in a voxel

## Diffusion tensor model

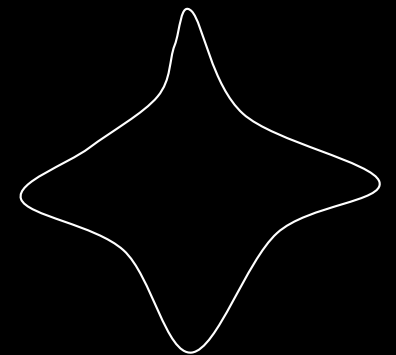
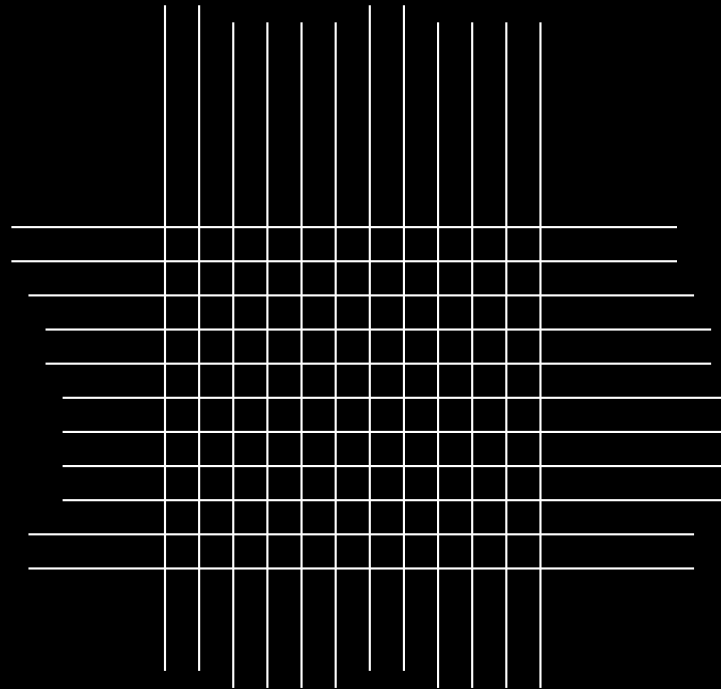
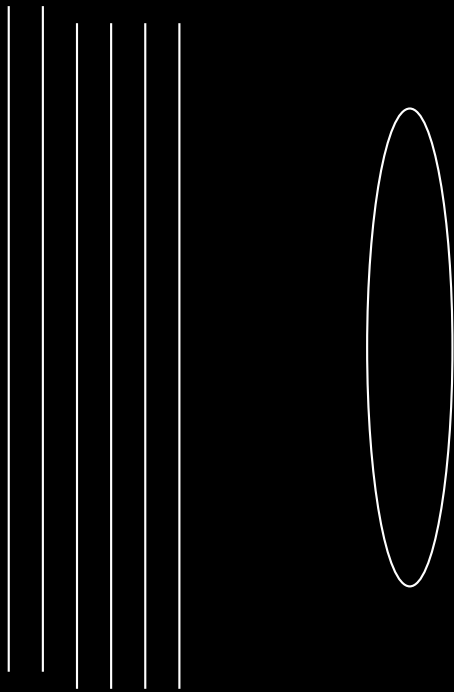




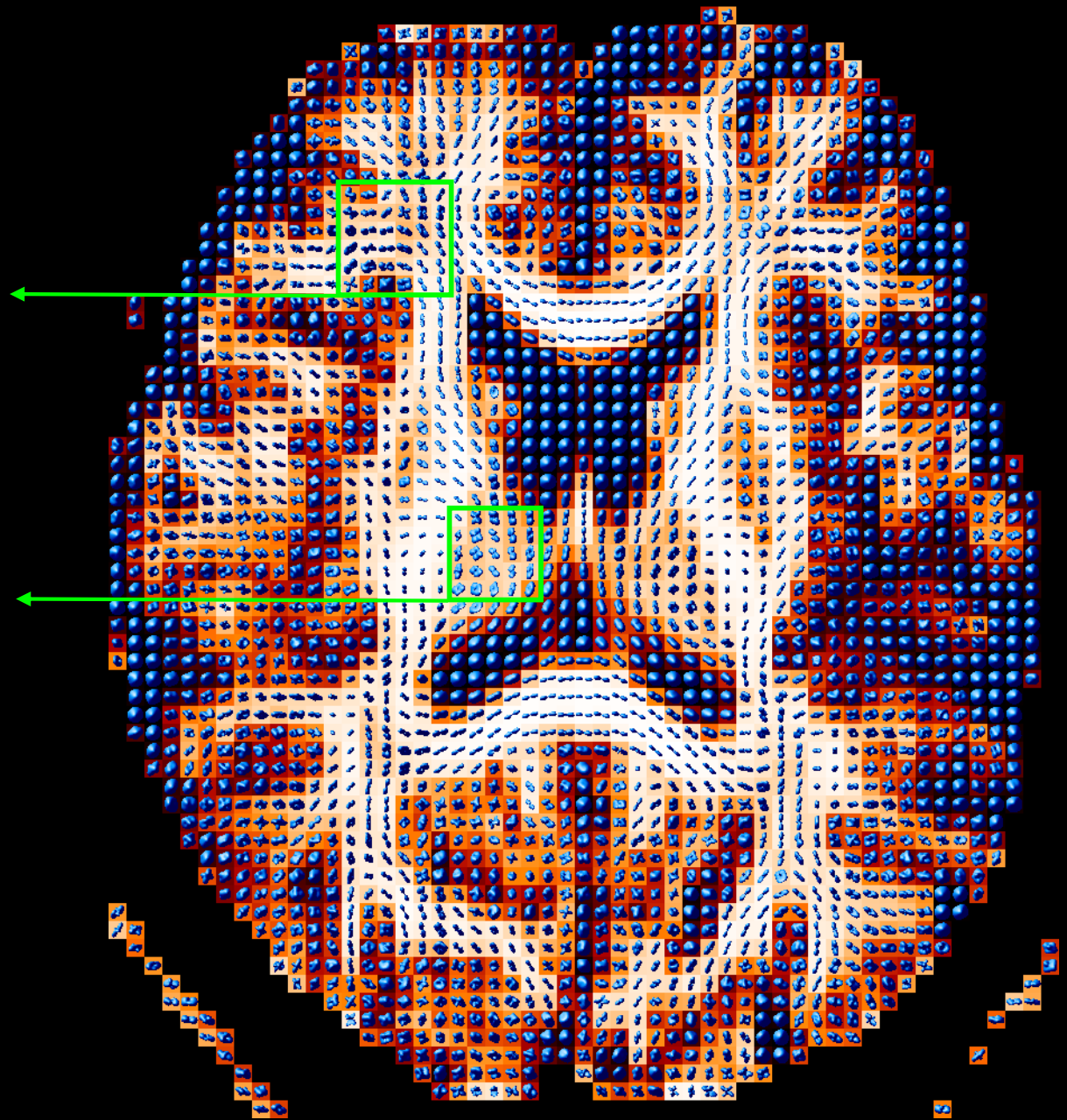
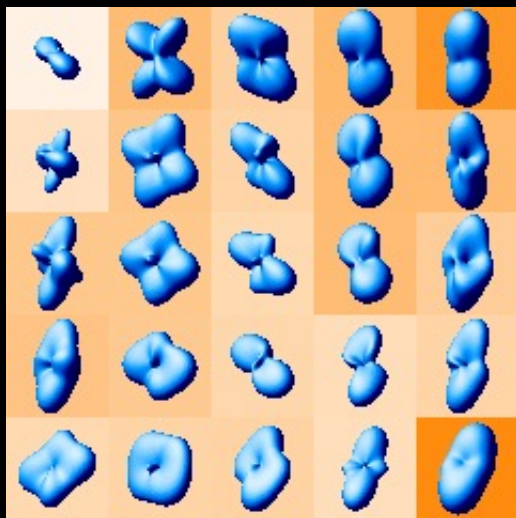
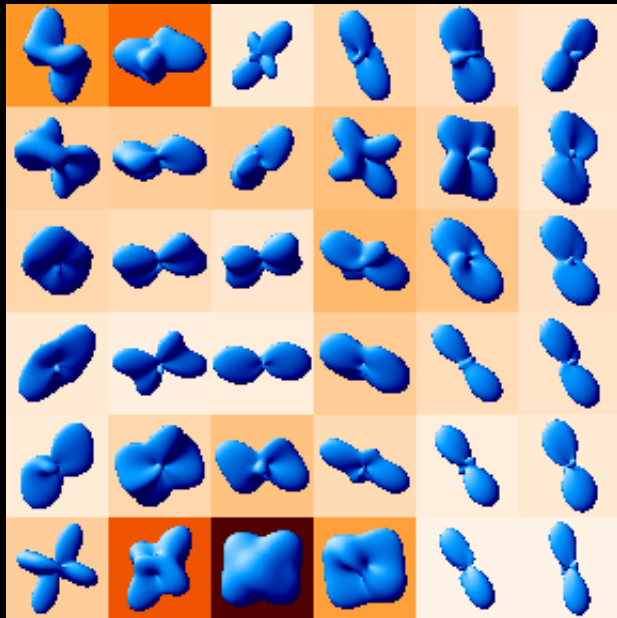
# Multiple fiber populations in a voxel

Model “independent”: q-space, DSI

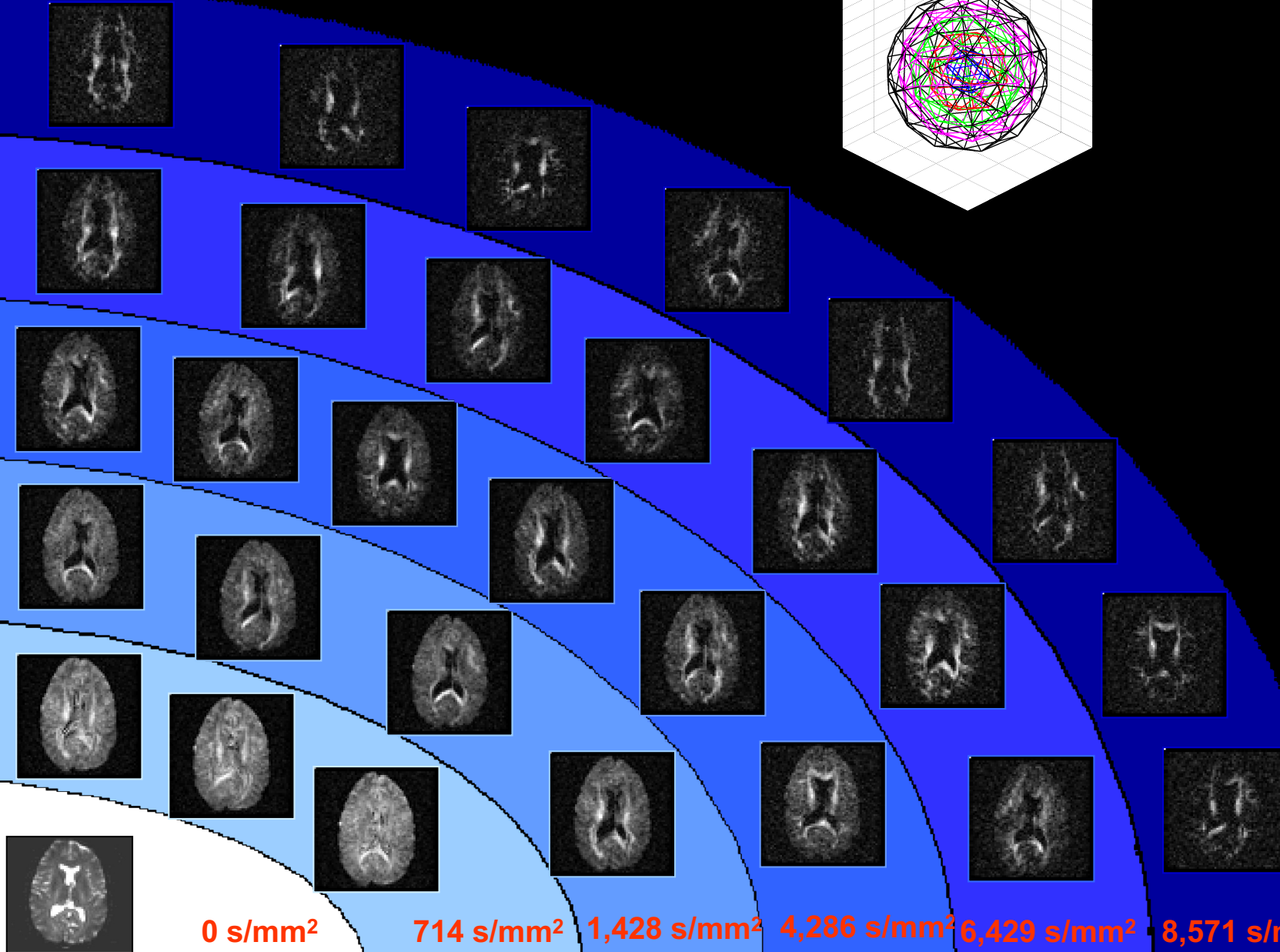
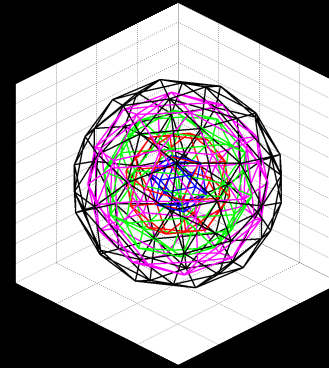
Higher order models: spherical harmonics



# Diffusion Orientation Transform - Results



# Solving multiple fiber populations



0 s/mm<sup>2</sup>

714 s/mm<sup>2</sup>

1,428 s/mm<sup>2</sup>

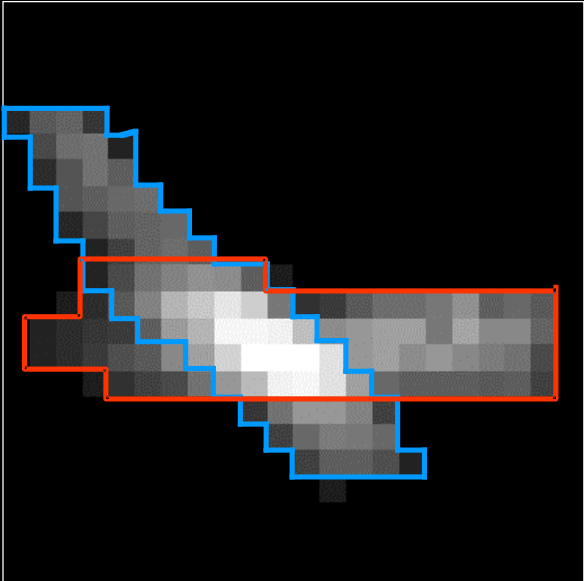
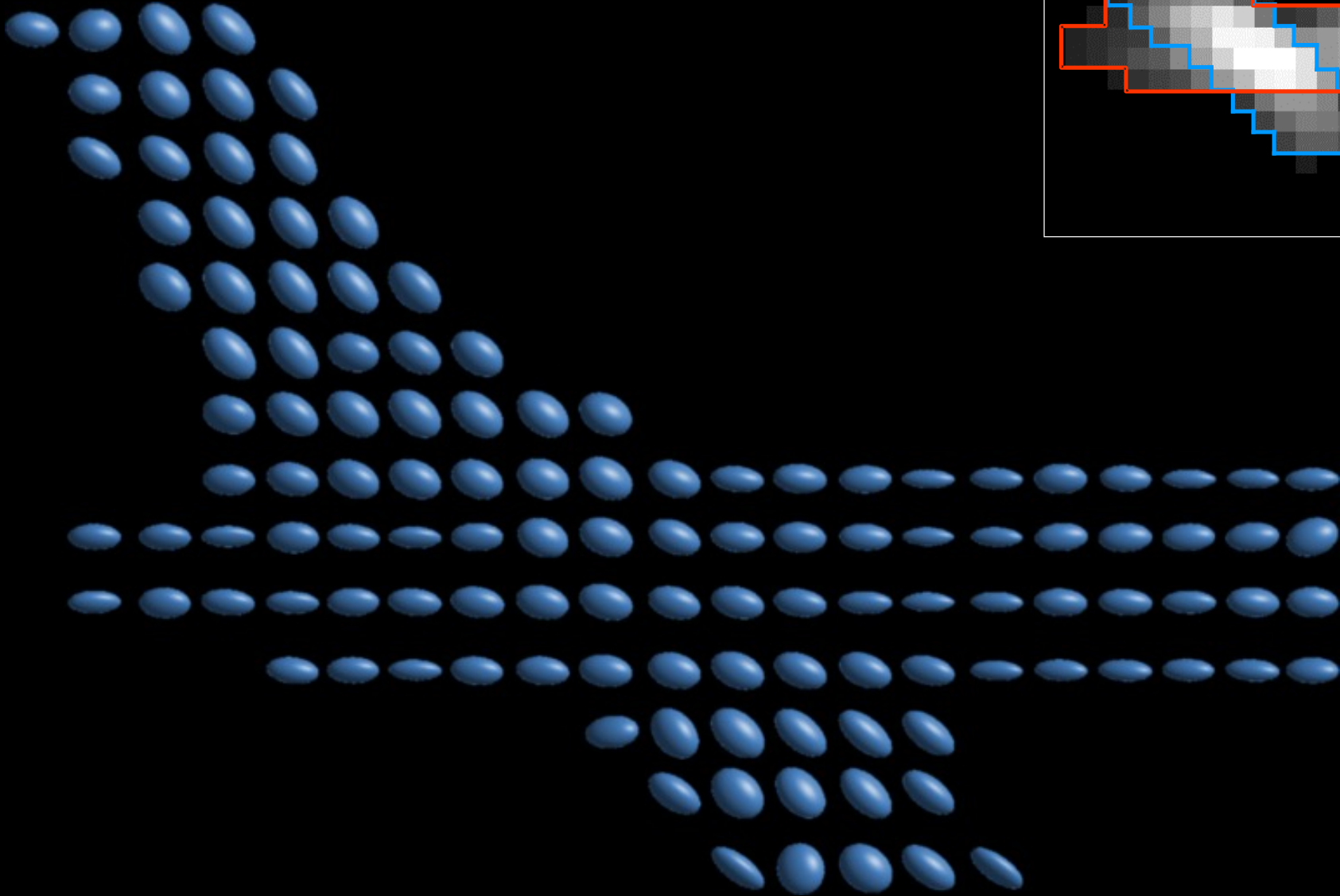
4,286 s/mm<sup>2</sup>

6,429 s/mm<sup>2</sup>

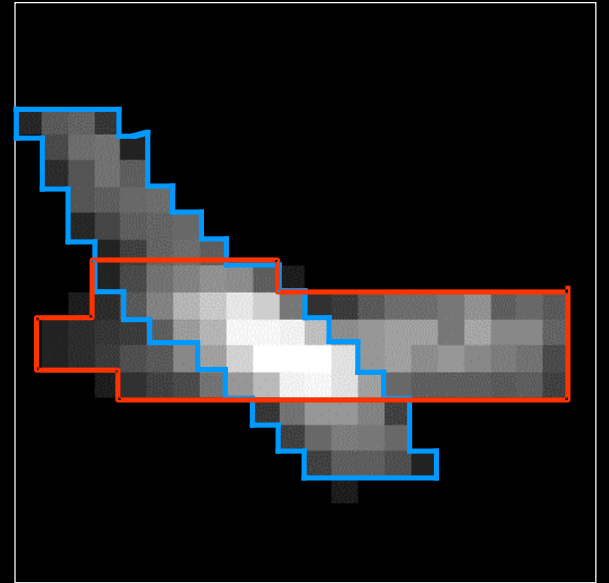
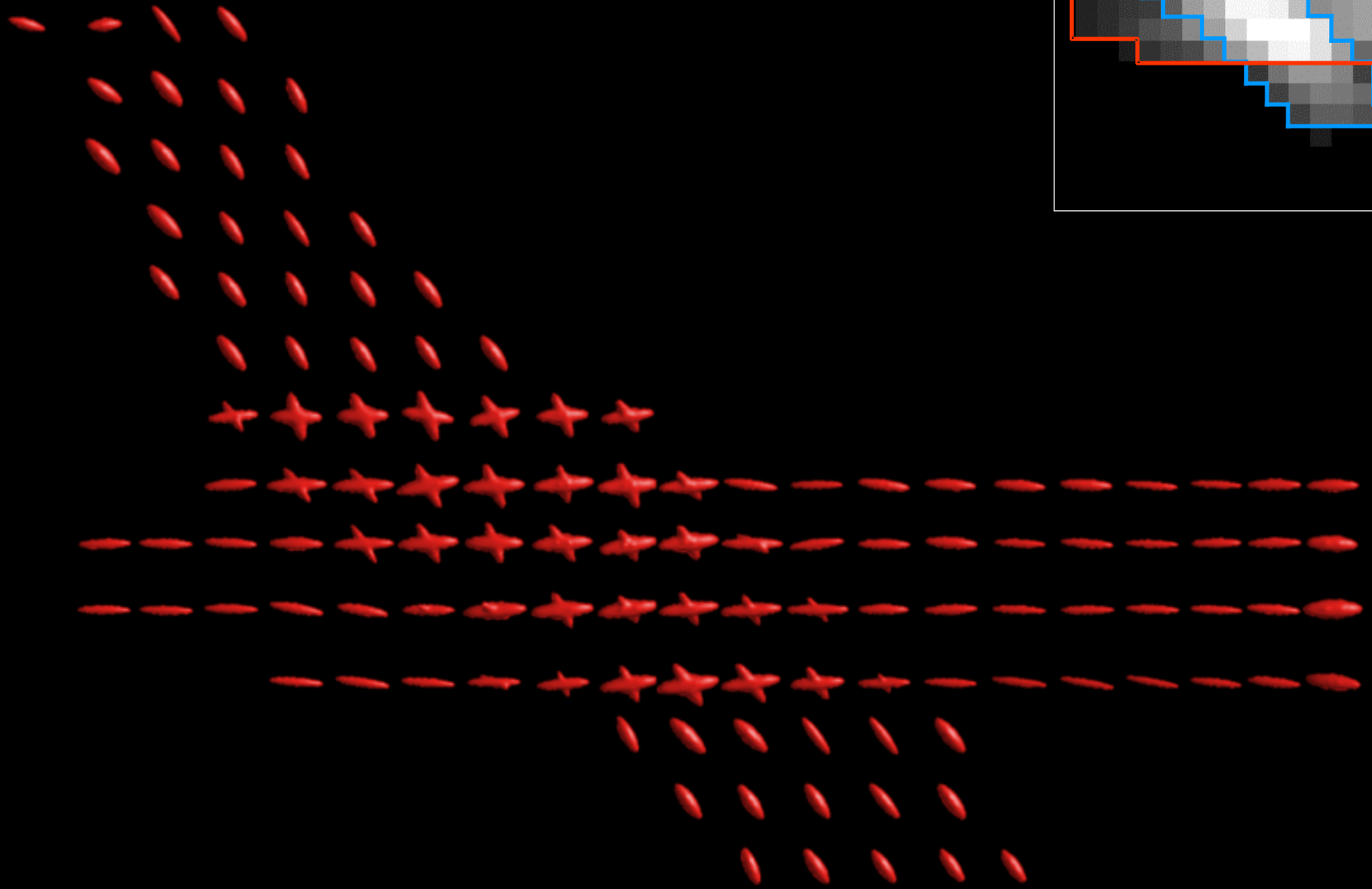
8,571 s/mm<sup>2</sup>

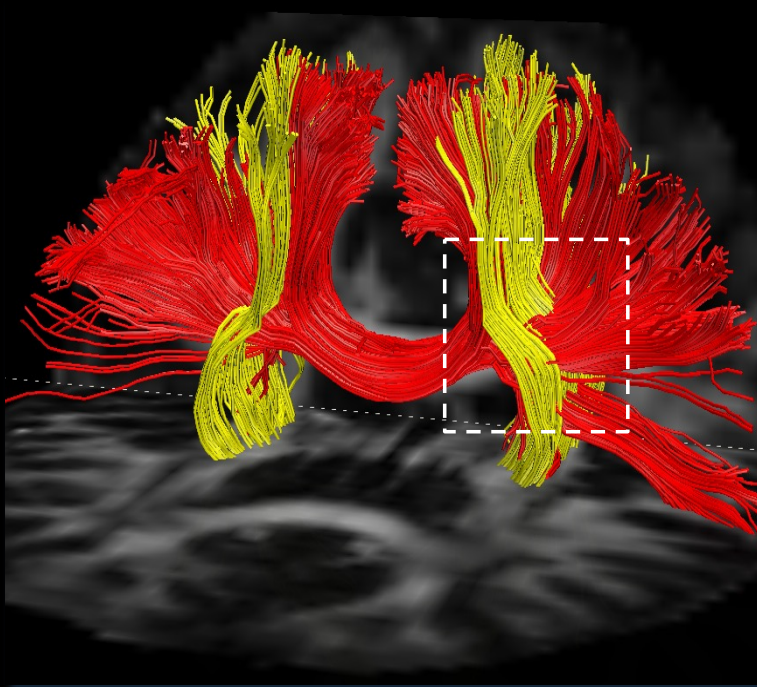
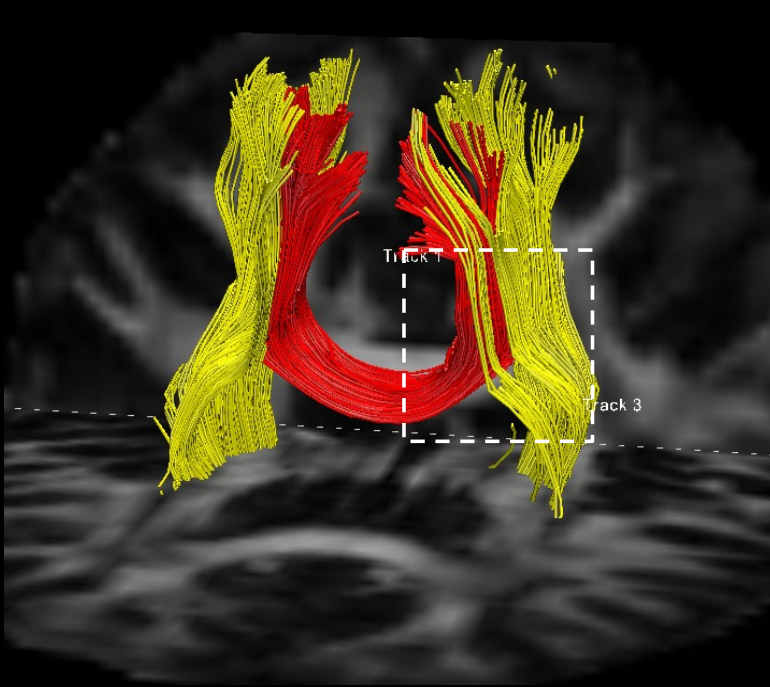
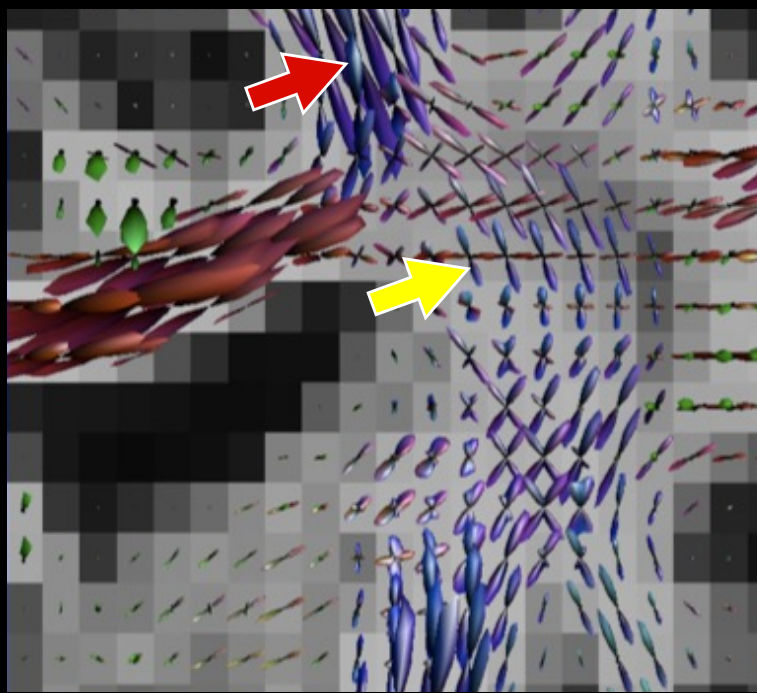
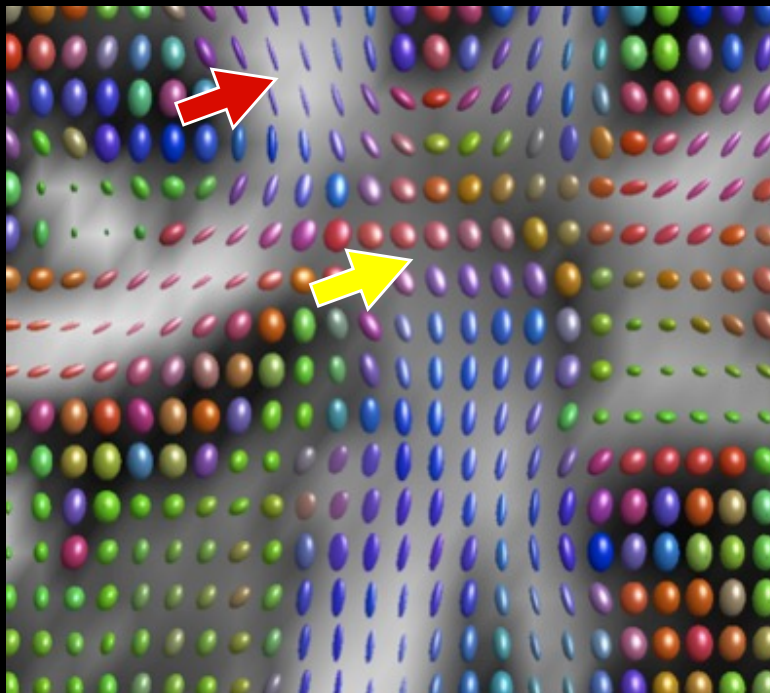
Courtesy of  
Yaniv Assaf

# Hindered Compartment



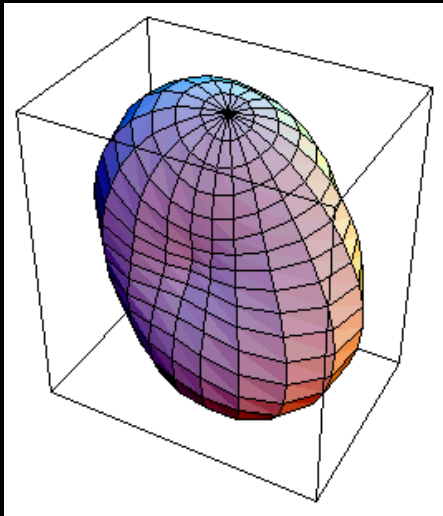
# Restricted Compartment



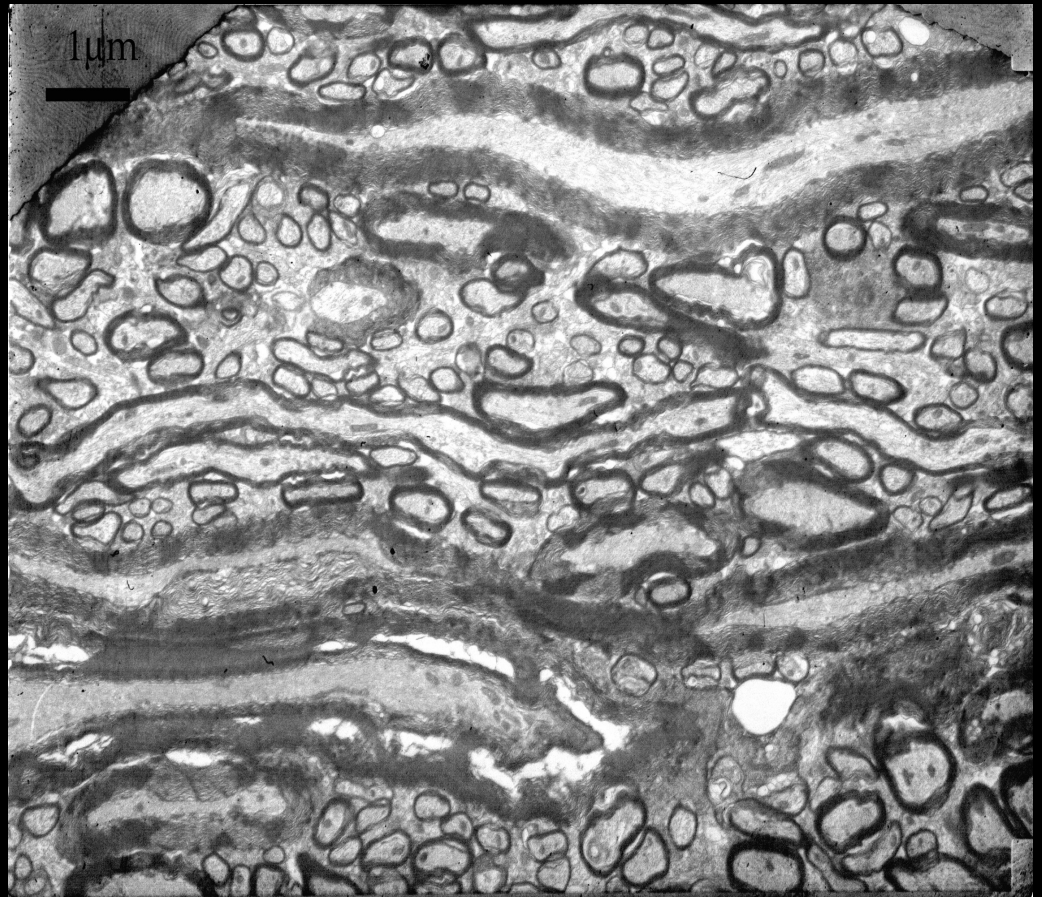


# Challenges in using diffusion MRI tractography

Knowledge of the diffusion propagator in each voxel is sufficient to trace white matter fibers reliably ?



?





# Anatomical Validation of Diffusion MRI tractography

Human brain: a-priori anatomical knowledge by experts

Animal brain: tracers

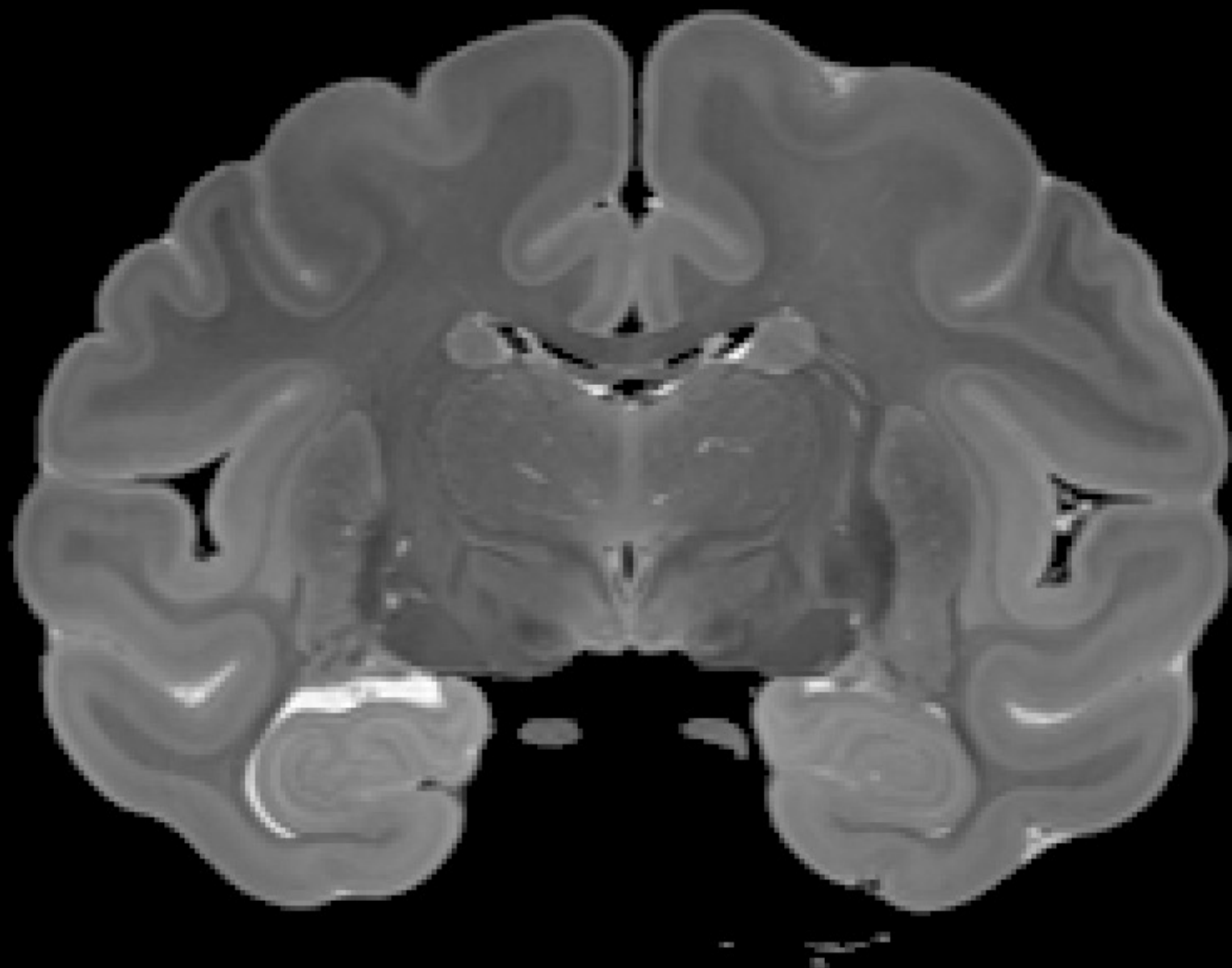
- Tractography validation in animal models:
  - Macaque (Schmahmann et al., 2007)
  - Macaque (Jbabdi et al., 2013)
  - Minipig (Dyrby et al., 2007)
  - Mice (Jiang et al., 2005)
- However....
  - Studies are qualitative
  - Focused on sensitivity (True positives), ignoring specificity (False positives)
  - Using constraints: e.g. way points, multiple ROIs
  - Empirical search of best parameters

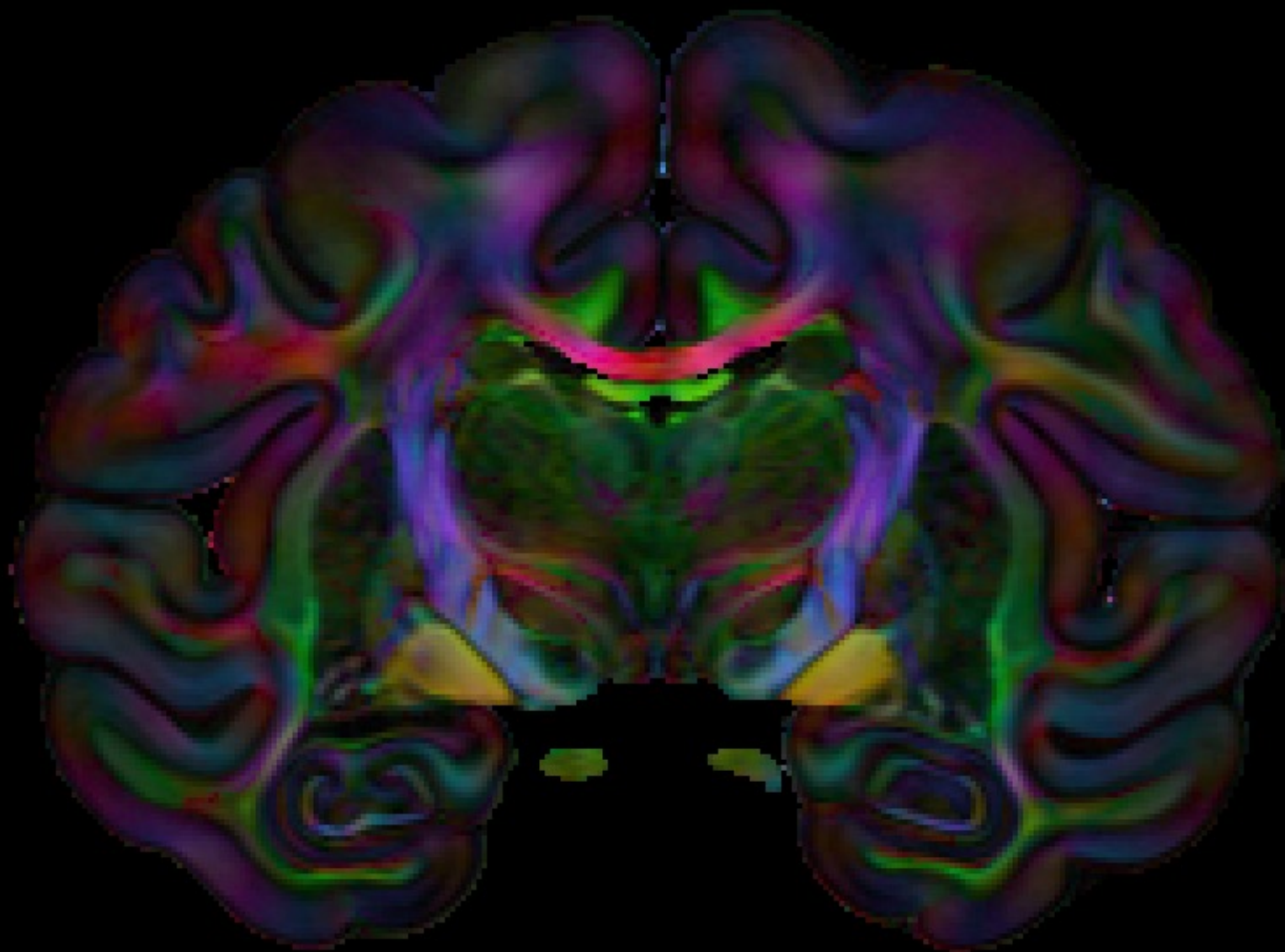
# Anatomical accuracy of brain connections derived from diffusion MRI tractography is inherently limited

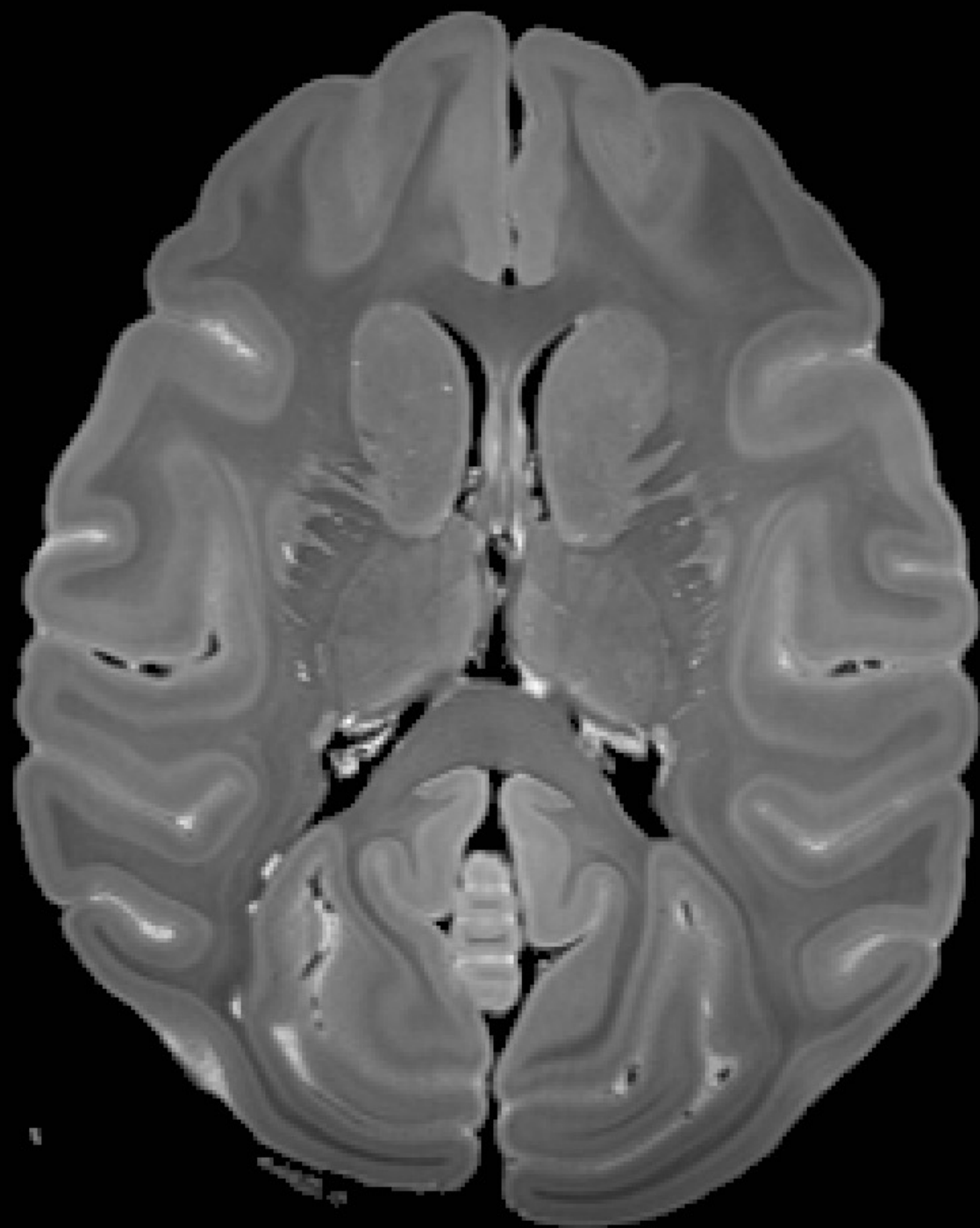
Cibu Thomas<sup>a,b,1</sup>, Frank Q. Ye<sup>c,d</sup>, M. Okan Irfanoglu<sup>a,b</sup>, Pooja Modi<sup>a</sup>, Kadharbatcha S. Saleem<sup>e</sup>, David A. Leopold<sup>c,d</sup>, and Carlo Pierpaoli<sup>a,b</sup>

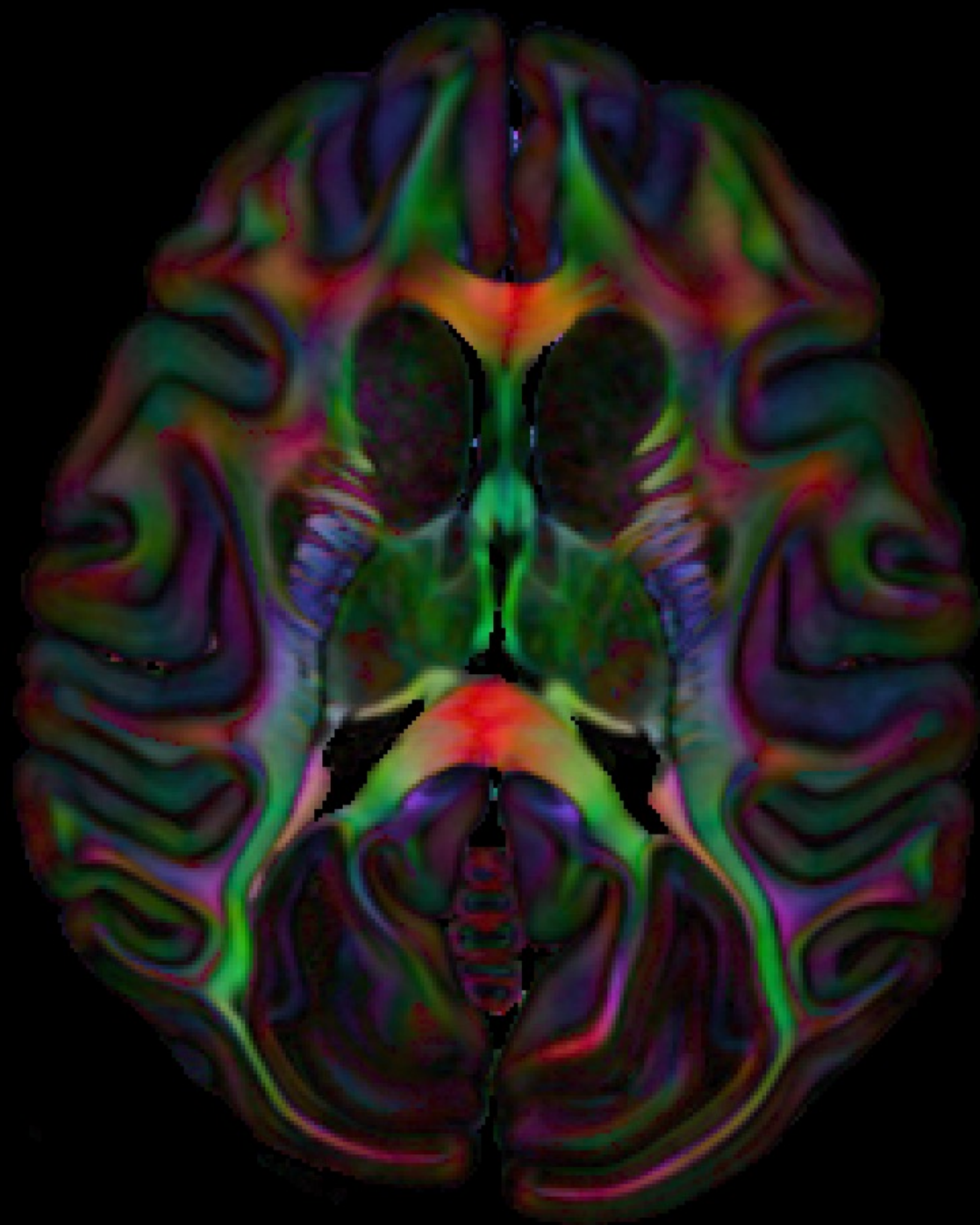
<sup>a</sup>Program on Pediatric Imaging and Tissue Sciences, Eunice Kennedy Shriver National Institute of Child Health and Human Development, Bethesda, MD, 20892; <sup>b</sup>Center for Neuroscience and Regenerative Medicine, Uniformed Services University of the Health Sciences, Bethesda, MD 20814; <sup>c</sup>Neurophysiology Imaging Facility, National Institute of Mental Health, National Institute of Neurological Disorders and Stroke, and National Eye Institute, Bethesda, MD 20892; <sup>d</sup>Section on Cognitive Neurophysiology and Imaging and <sup>e</sup>Section on Cognitive Neuroscience, Laboratory of Neuropsychology, National Institute of Mental Health, Bethesda, MD, 20892

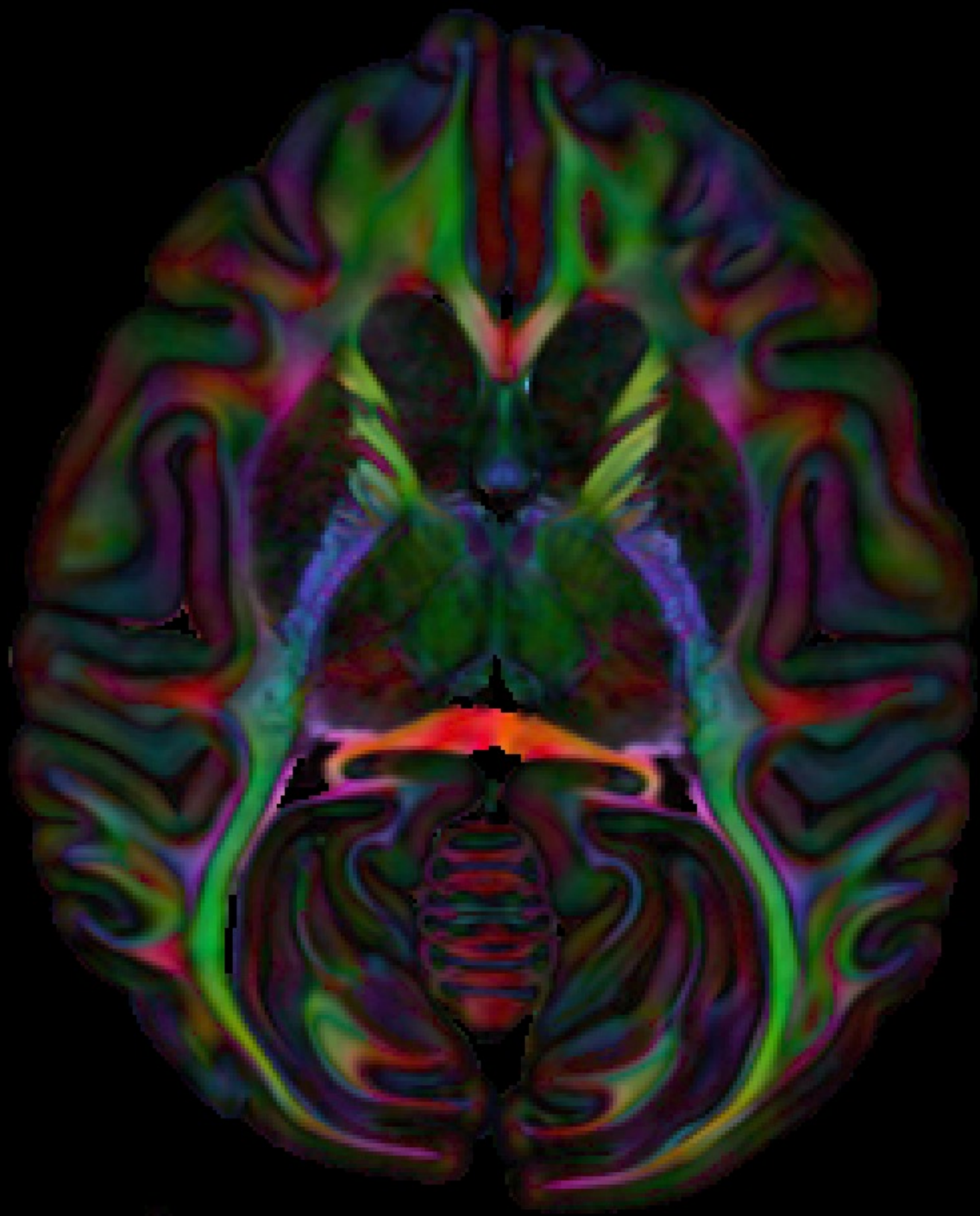
Edited\* by Leslie G. Ungerleider, National Institute of Mental Health, Bethesda, MD, and approved September 22, 2014 (received for review March 26, 2014)



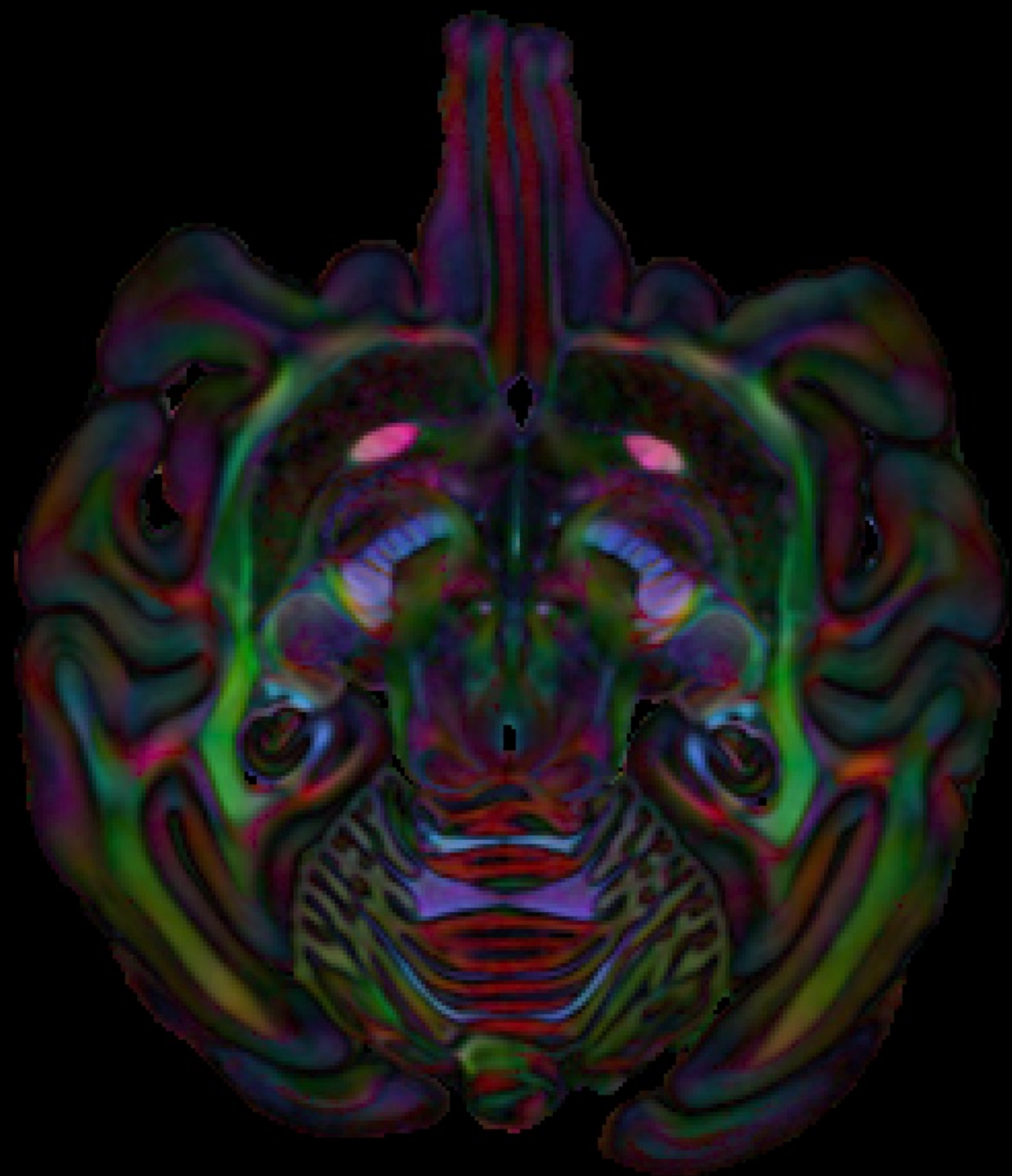


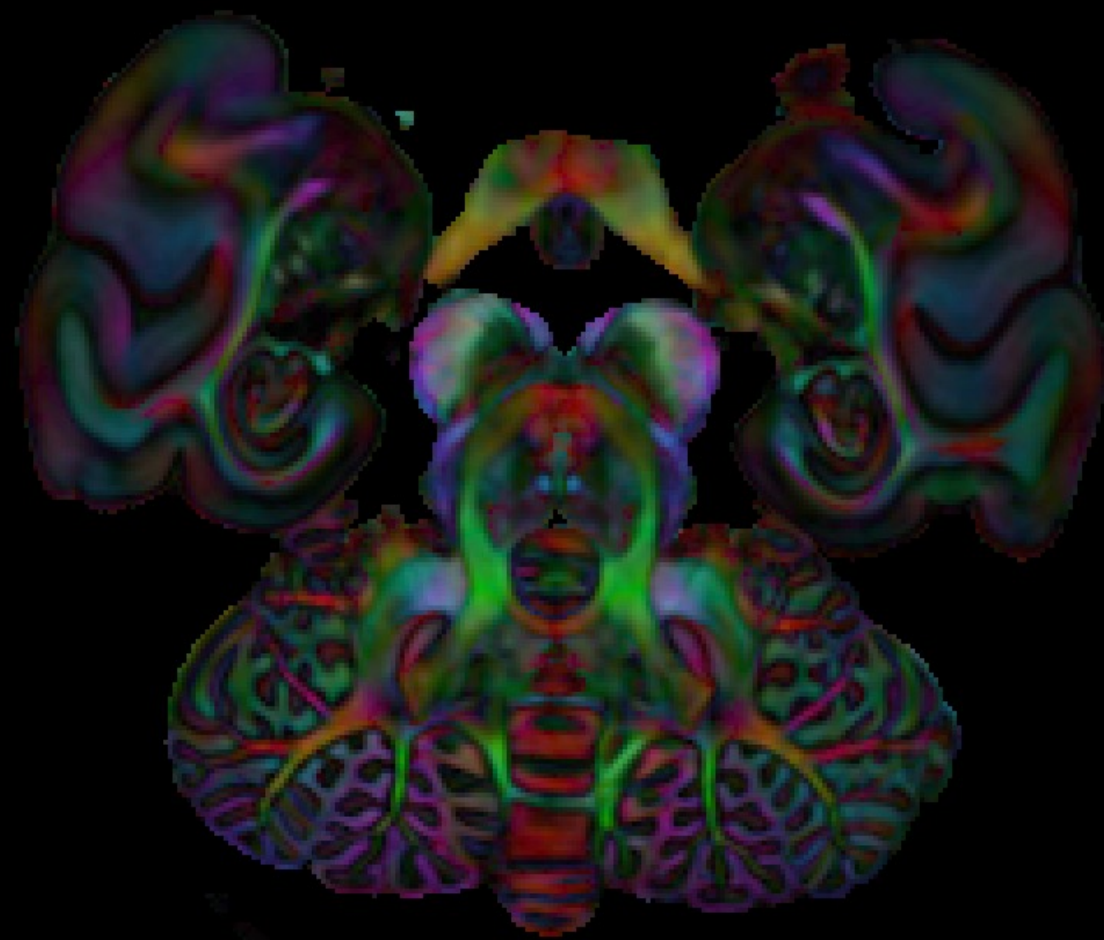












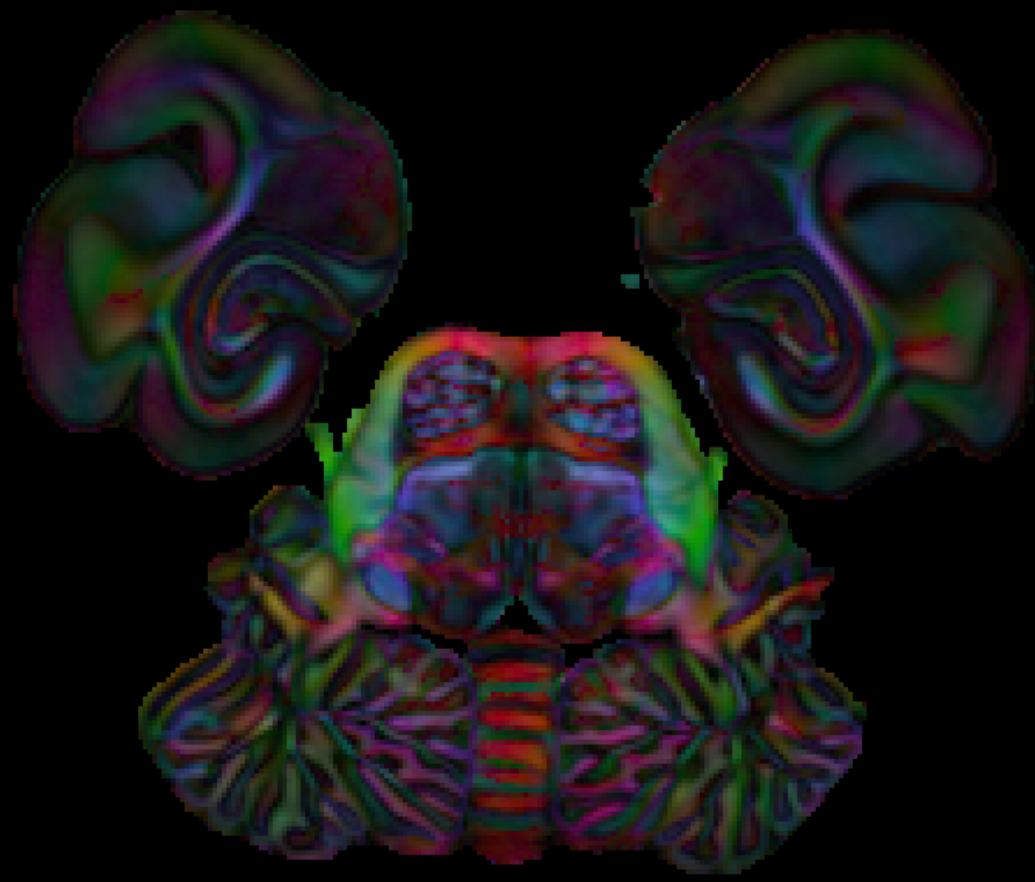
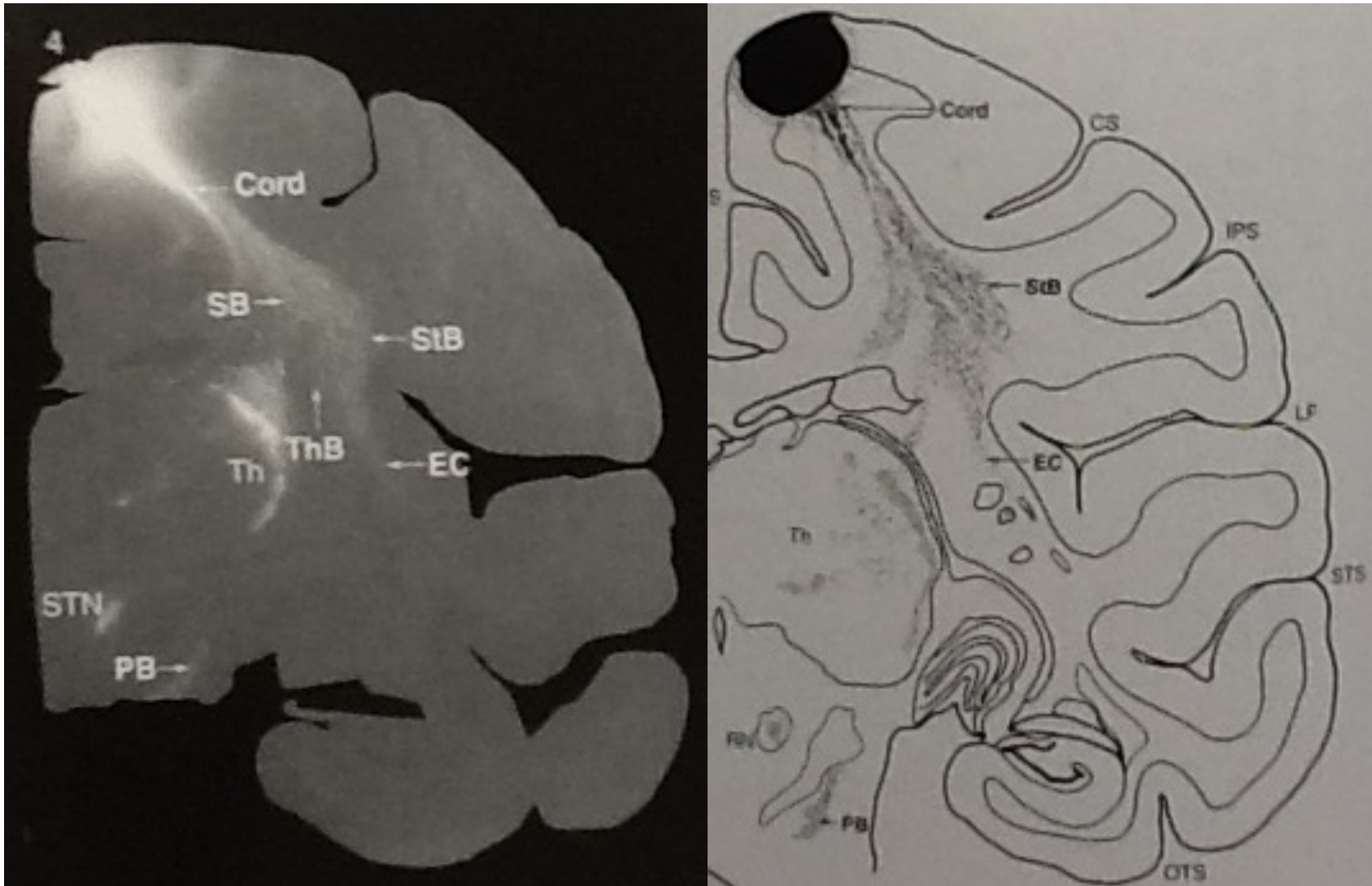
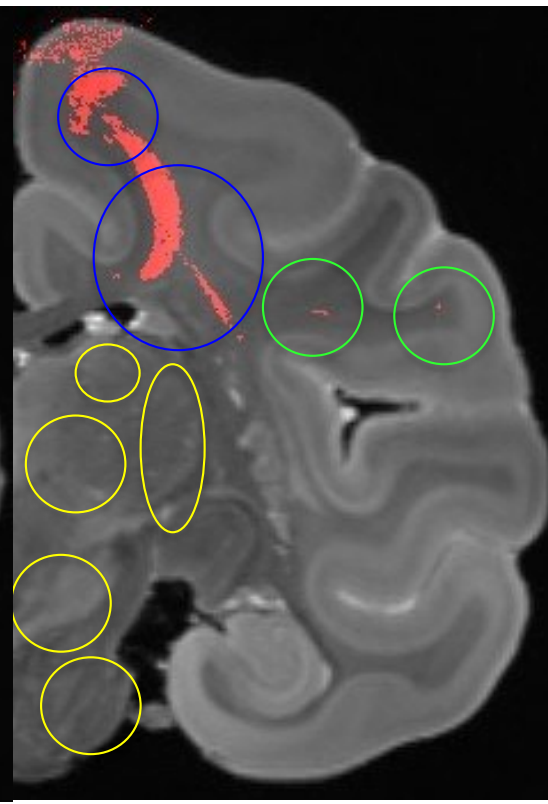
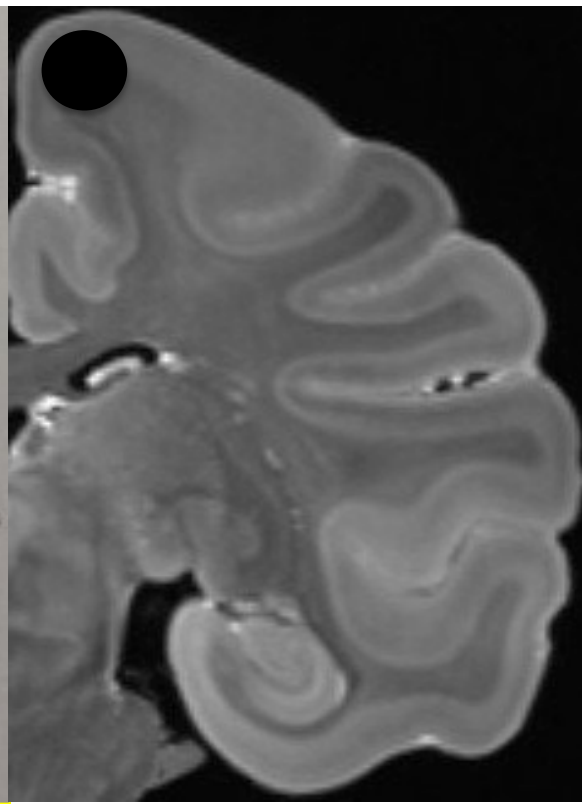


Figure 1: A 3D visualization of a brain with a colorful, wavy pattern overlaid on it, set against a black background.



Left: Cord = Paired Cord of fibers that split into callosal fibers and coronal radiata fibers;  
 EC: External Capsule; Th: Thalamus; ThB: Thalamic Bundle; SB: Subcortical Bundle;  
 StB: Striatal Bundle; PB: Pontine Bundle; STN: Subthalamic Nucleus.

Right: CS: Central Sulcus, IPS: Intraparietal Sulcus; LF: Lateral Fissure; STS: Superior Temporal Sulcus; OTS: Occipitotemporal Sulcus



site of the tracer injection  
(Pre central gyrus)

The same region was  
seeded for tractography  
in a different monkey

Results of tractography

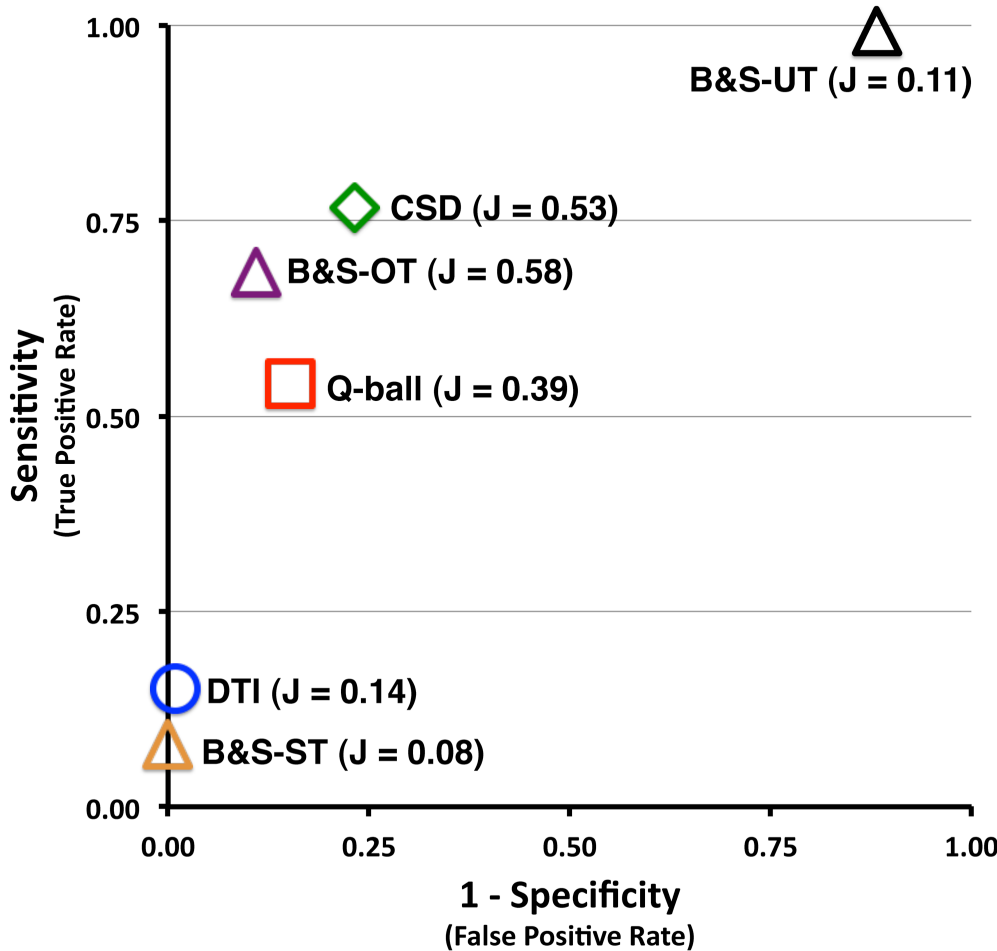
Blue circles – True positives  
Green circles – False Positives  
Yellow circles – False Negatives

*Note: This slice is 11 slices  
(2.25 mm) anterior to the  
seeded coronal slice*

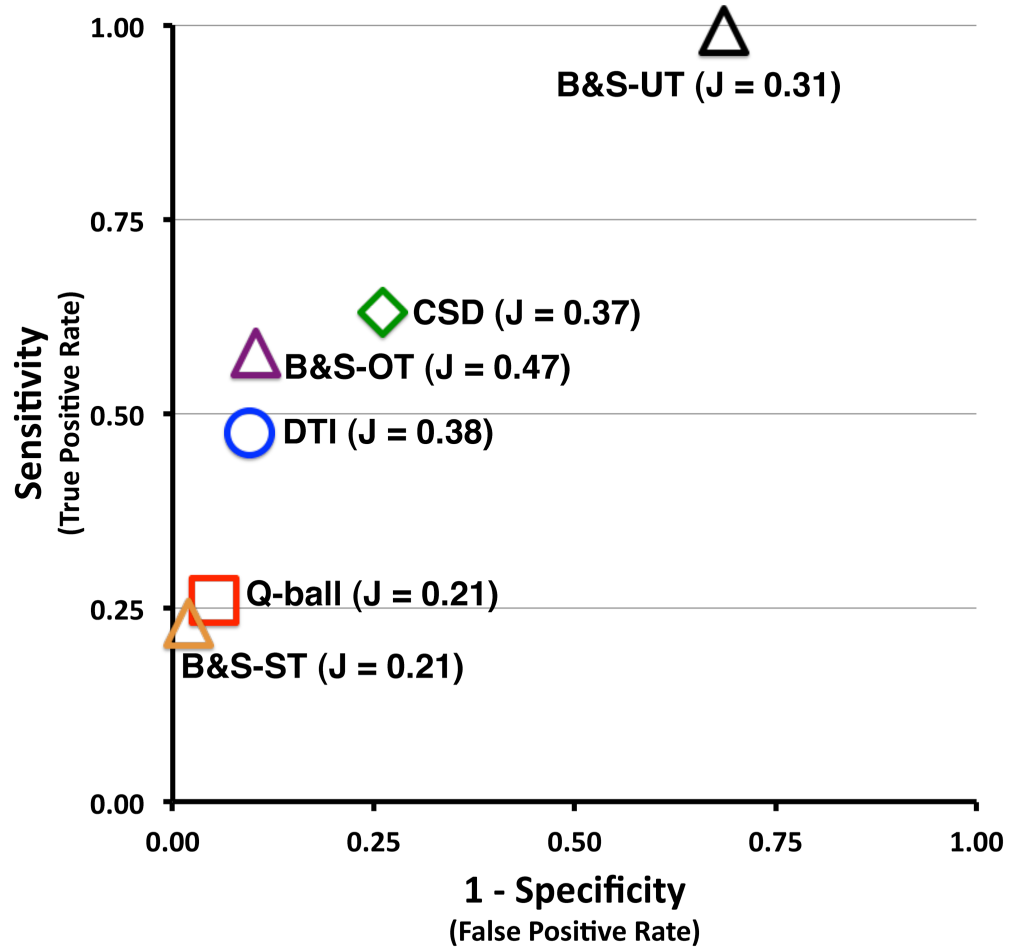
# The anatomical accuracy of brain connections derived from Diffusion MRI Tractography is inherently limited *Thomas et al.*

PNAS

## a) Gray Matter ROI: PCG



## b) Gray Matter ROI: V4

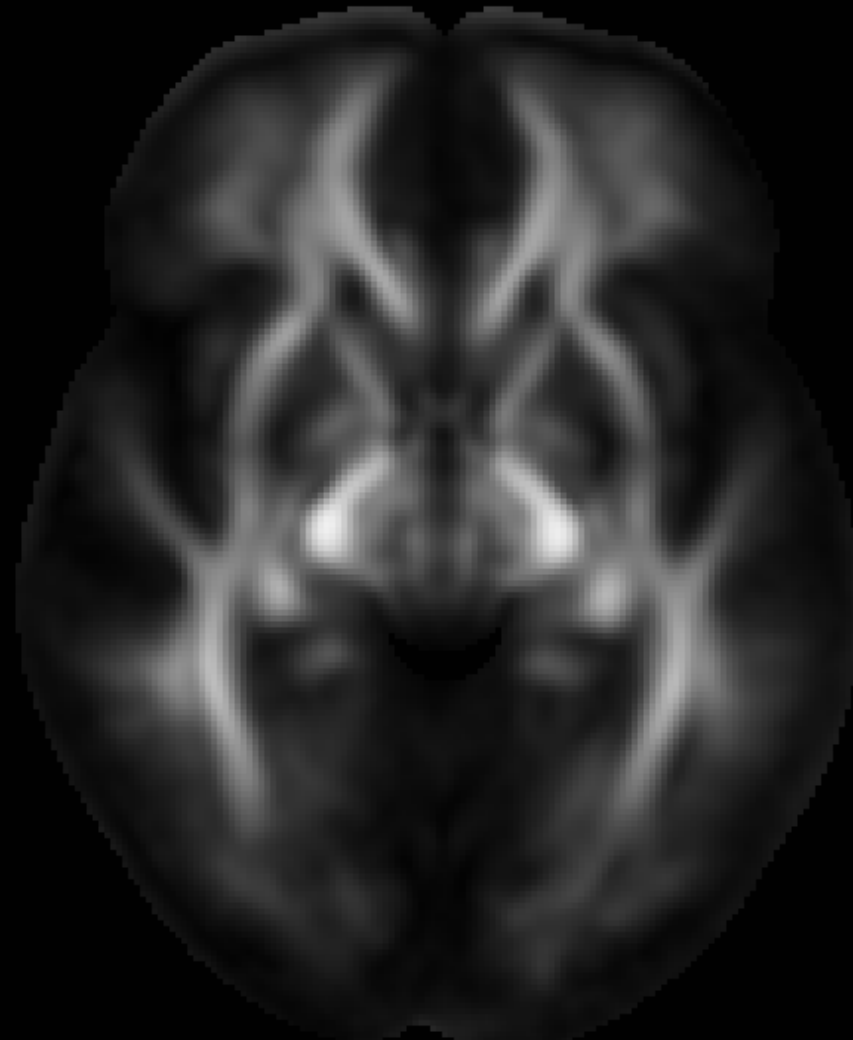


Population-based atlases

Normative databases

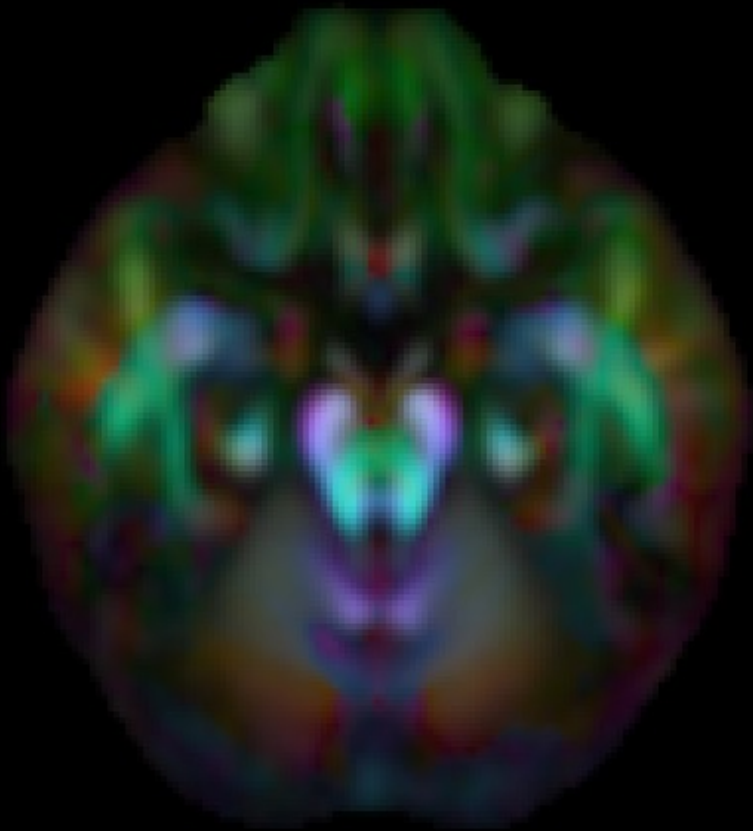


20 Subject Deformable  
Atlas

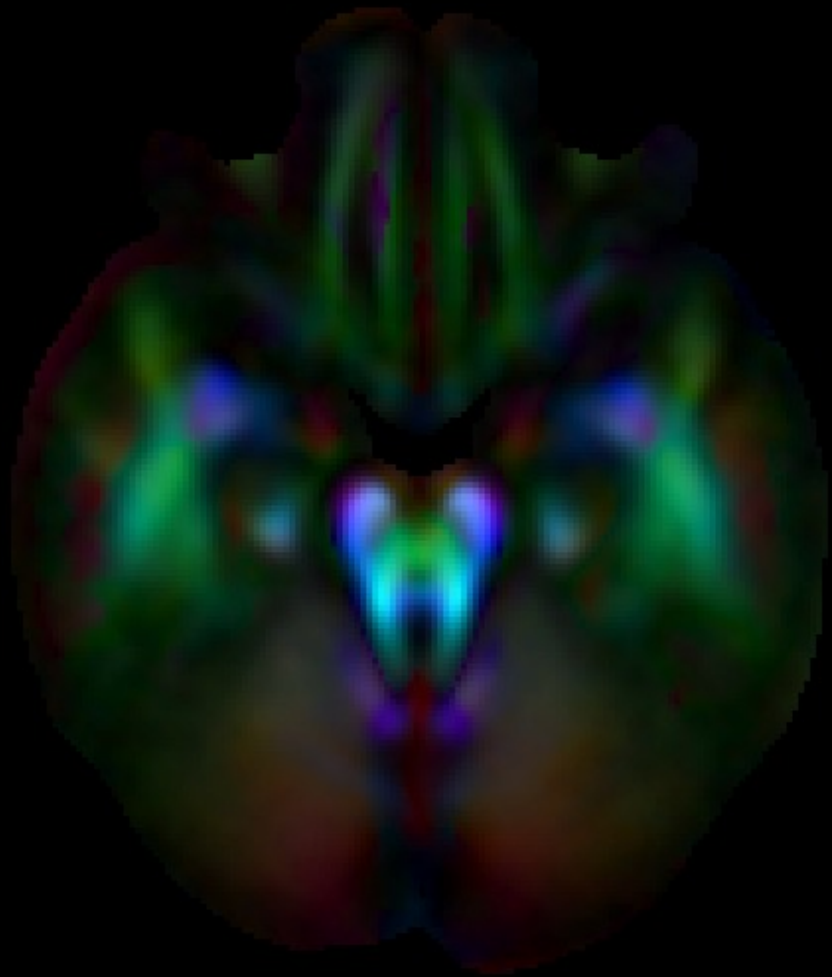


ICBM 81 DTI Affine Atlas

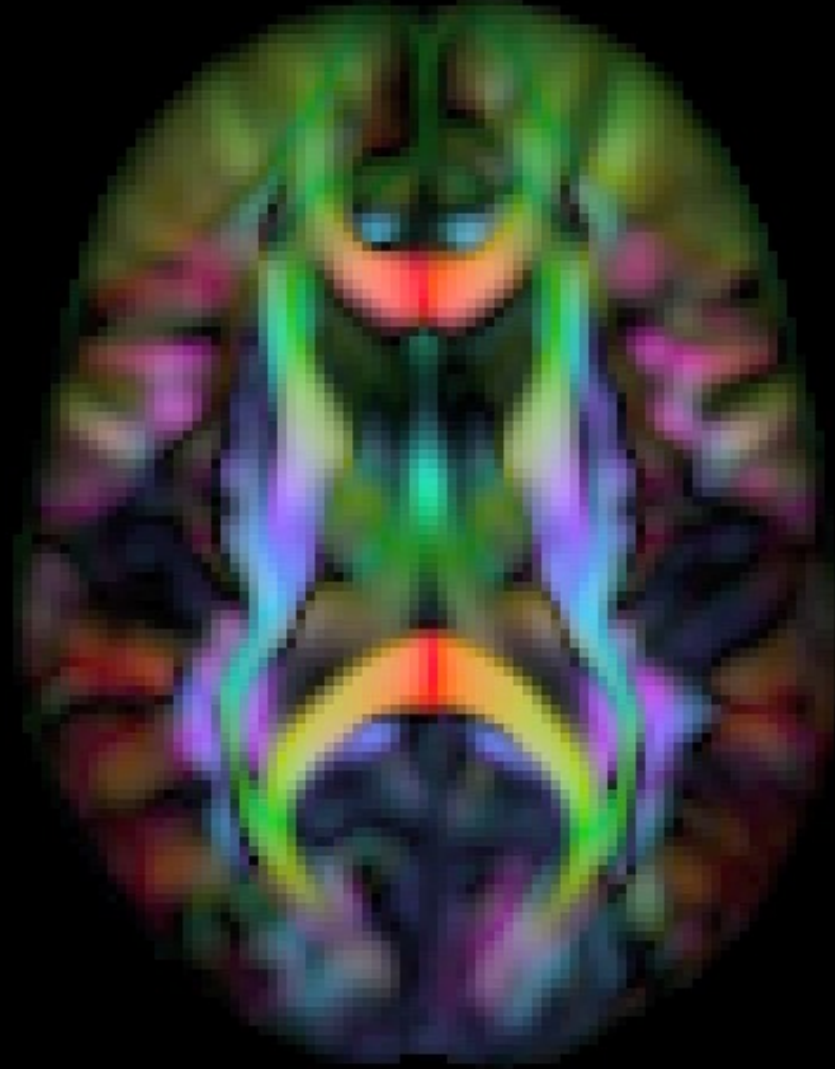
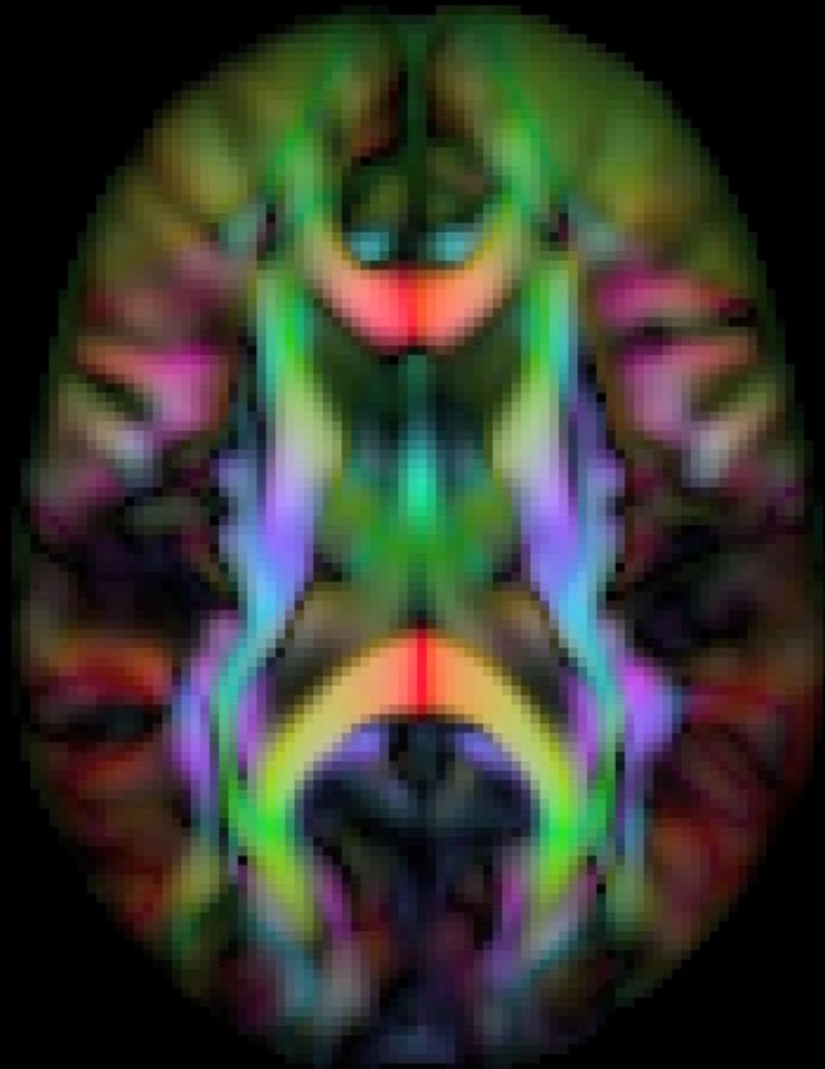




20 Subject Deformable  
Atlas

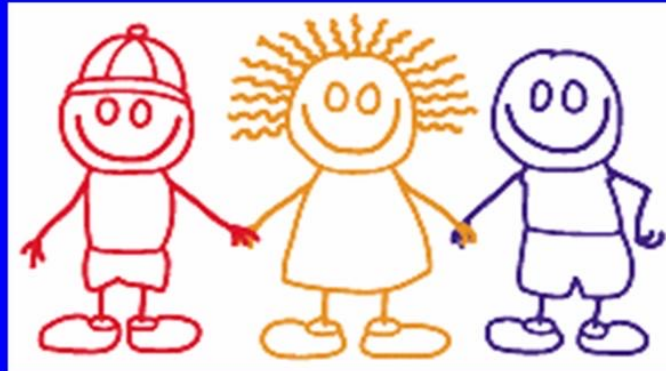


ICBM 81 DTI Affine Atlas



# NIH MRI Study of Normal Brain Development

[www.NIH-PediatricMRI.org](http://www.NIH-PediatricMRI.org)



The MRI Study of Normal Brain Development



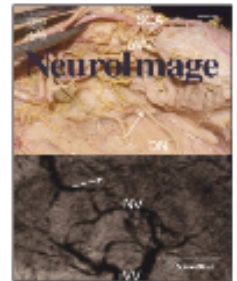


ELSEVIER

Contents lists available at [ScienceDirect](#)

## NeuroImage

journal homepage: [www.elsevier.com/locate/ynimg](http://www.elsevier.com/locate/ynimg)



## The diffusion tensor imaging (DTI) component of the NIH MRI study of normal brain development (PedsDTI)

Lindsay Walker <sup>a</sup>, Lin-Ching Chang <sup>a,1</sup>, Amritha Nayak <sup>a</sup>, M. Okan Irfanoglu <sup>a</sup>, Kelly N. Botteron <sup>b</sup>, James McCracken <sup>c</sup>, Robert C. McKinstry <sup>d</sup>, Michael J. Rivkin <sup>e</sup>, Dah-Jyuu Wang <sup>f</sup>, Judith Rumsey <sup>g</sup>, Carlo Pierpaoli <sup>a,\*</sup>, the Brain Development Cooperative Group

<sup>a</sup> Program on Pediatric Imaging and Tissue Sciences, NICHD, NIH, Bethesda, MD, USA

<sup>b</sup> Washington University in St. Louis, Department of Psychiatry, Saint Louis, MO, USA

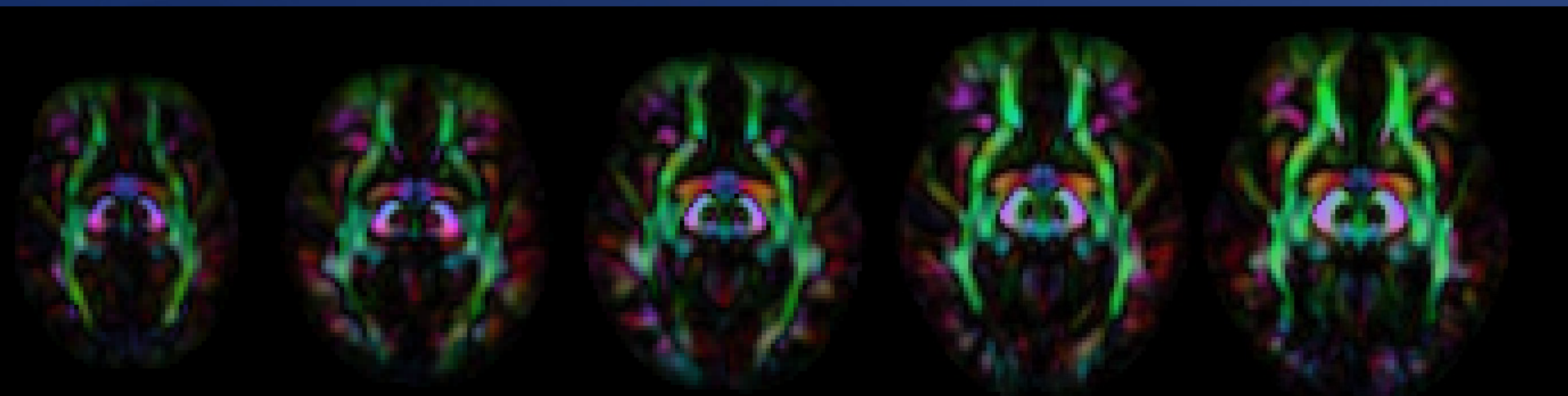
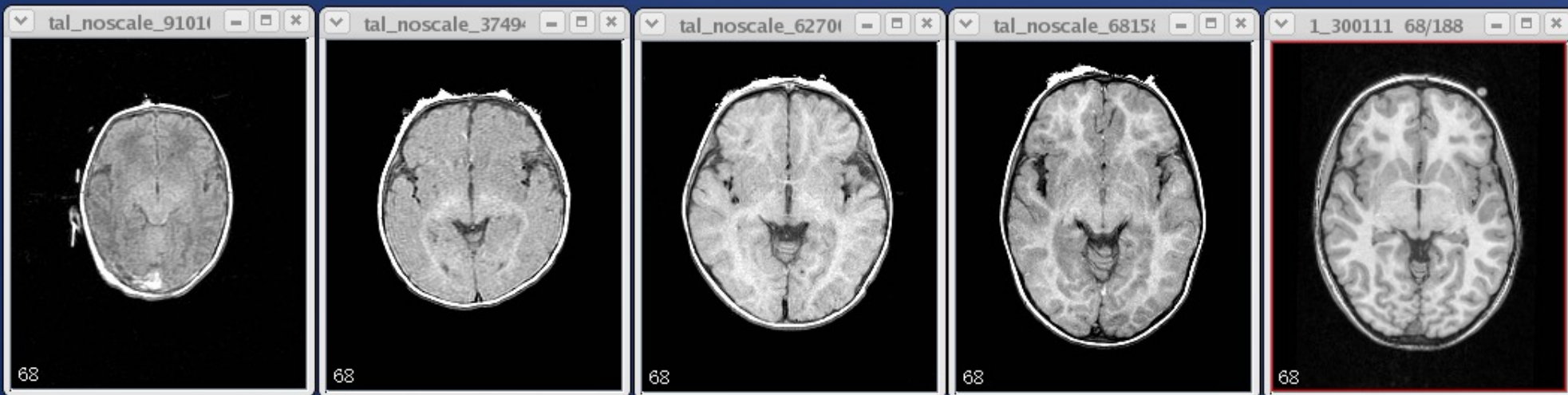
<sup>c</sup> Department of Child Psychiatry, University of California in Los Angeles, Los Angeles, CA, USA

<sup>d</sup> Mallinckrodt Institute of Radiology, Washington University School of Medicine, St. Louis, MO, USA

<sup>e</sup> Departments of Neurology, Psychiatry and Radiology, Boston Children's Hospital, Boston, MA, USA

<sup>f</sup> The Children's Hospital of Philadelphia, Philadelphia, PA, USA

<sup>g</sup> Clinical Neuroscience Research Branch, Division of Translational Research, NIMH, NIH, Bethesda, MD, USA



0-3  
months

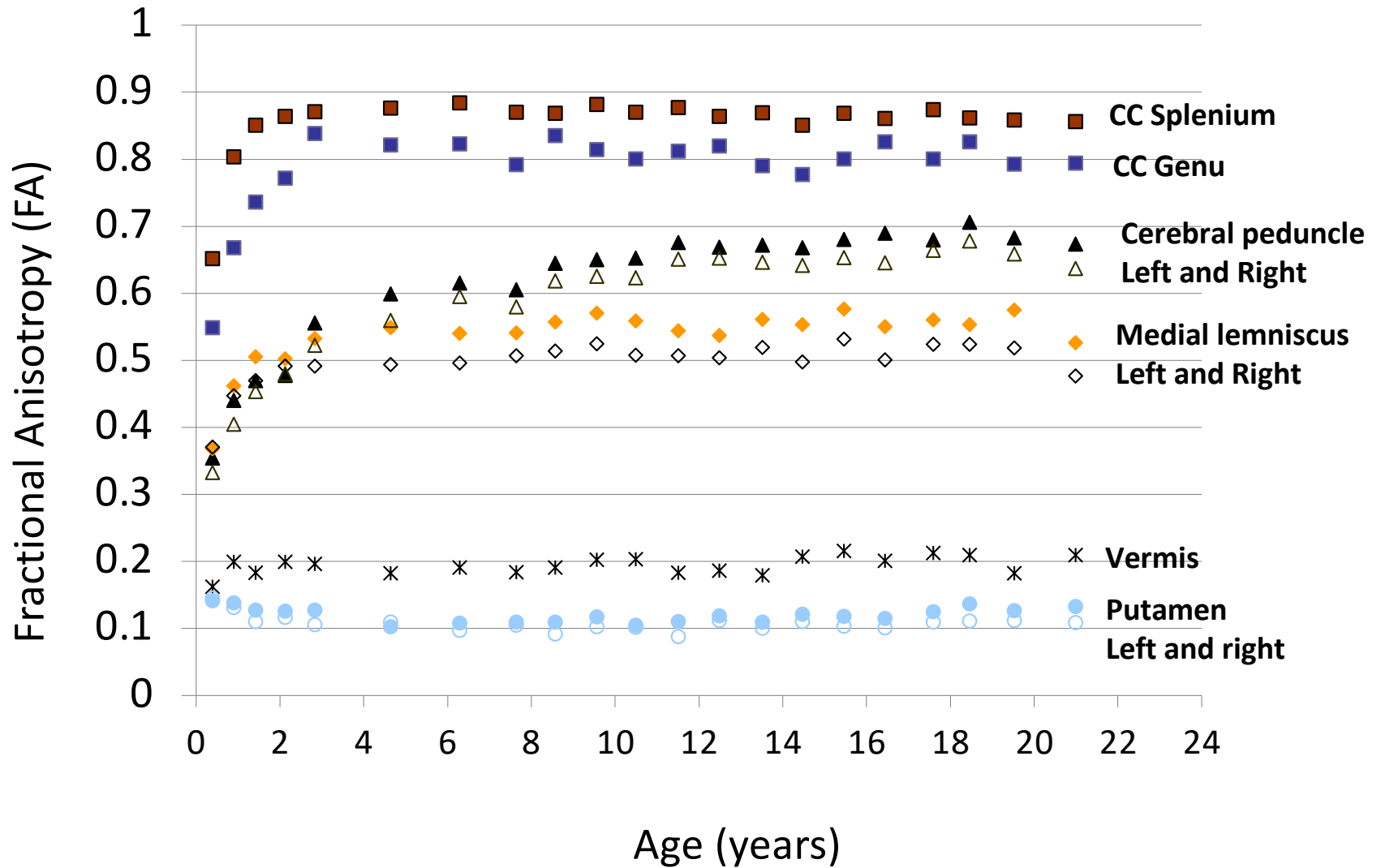
6-12  
months

18  
months

2-4  
years

10  
years

# Developmental trajectories



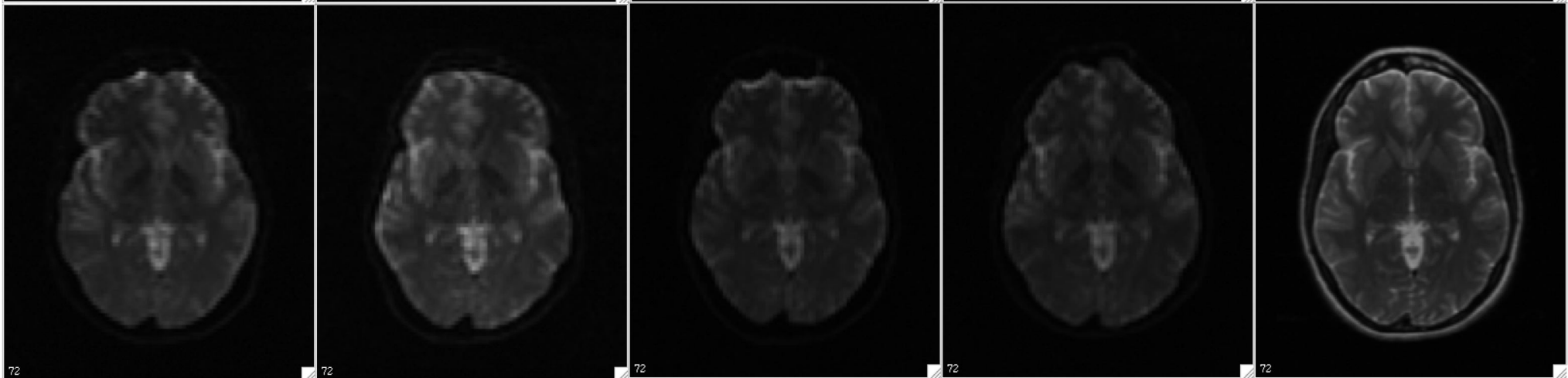
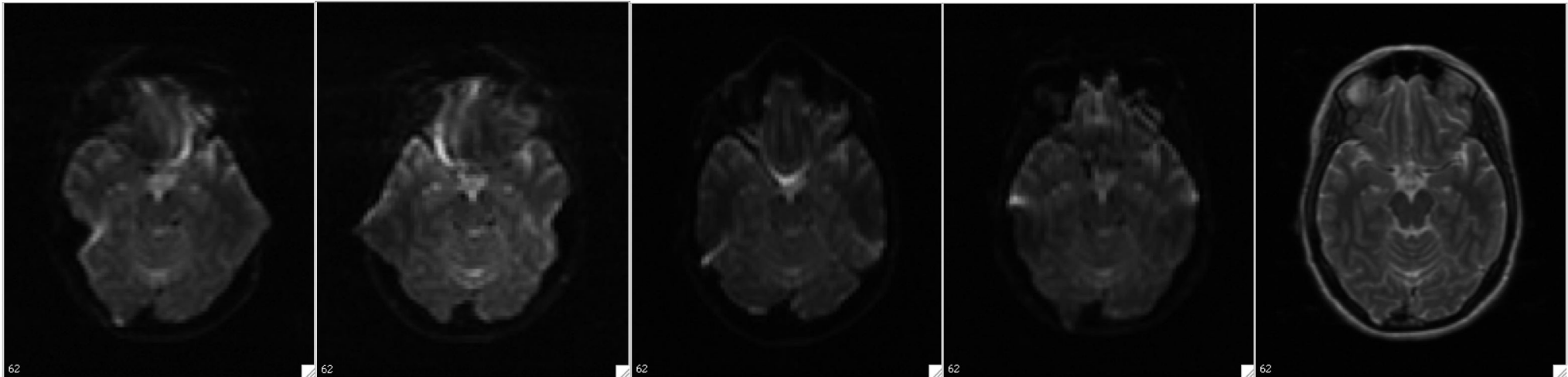
Accuracy and reproducibility

Analysis of confounds

Physiological noise

# Image quality issues in clinical Diffusion MRI:

## EPI Distortions



R/L-P

R/L-M

A/P-P

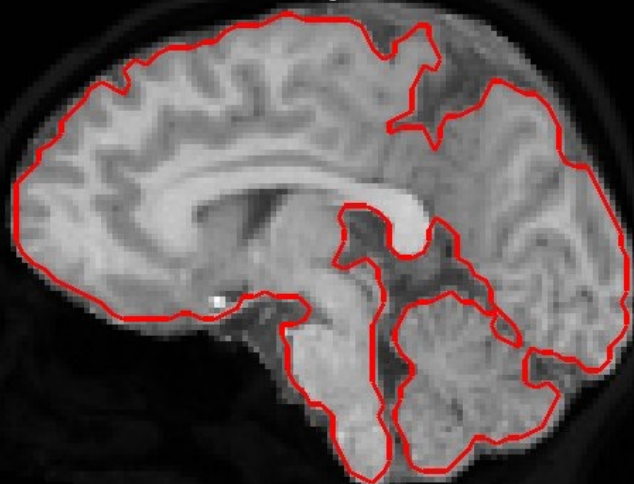
A/P-M

T2-FSE

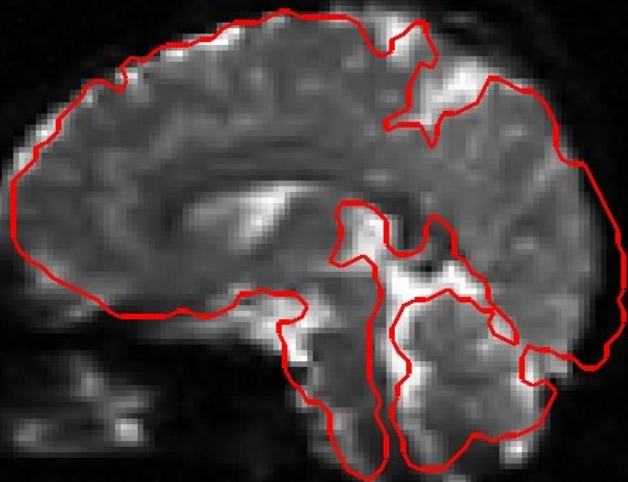


# Image quality issues in clinical Diffusion MRI:

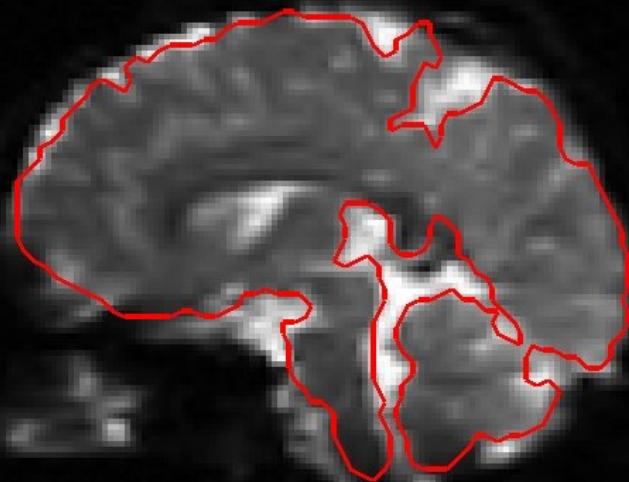
T1 Target



before correction



after correction

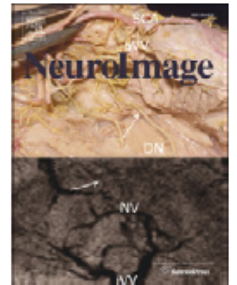




Contents lists available at [SciVerse ScienceDirect](#)

NeuroImage

journal homepage: [www.elsevier.com/locate/ynimg](http://www.elsevier.com/locate/ynimg)



## Effects of image distortions originating from susceptibility variations and concomitant fields on diffusion MRI tractography results

M. Okan Irfanoglu <sup>a,b,\*</sup>, Lindsay Walker <sup>a,b</sup>, Joelle Sarlls <sup>c</sup>, Stefano Marengo <sup>d</sup>, Carlo Pierpaoli <sup>a</sup>

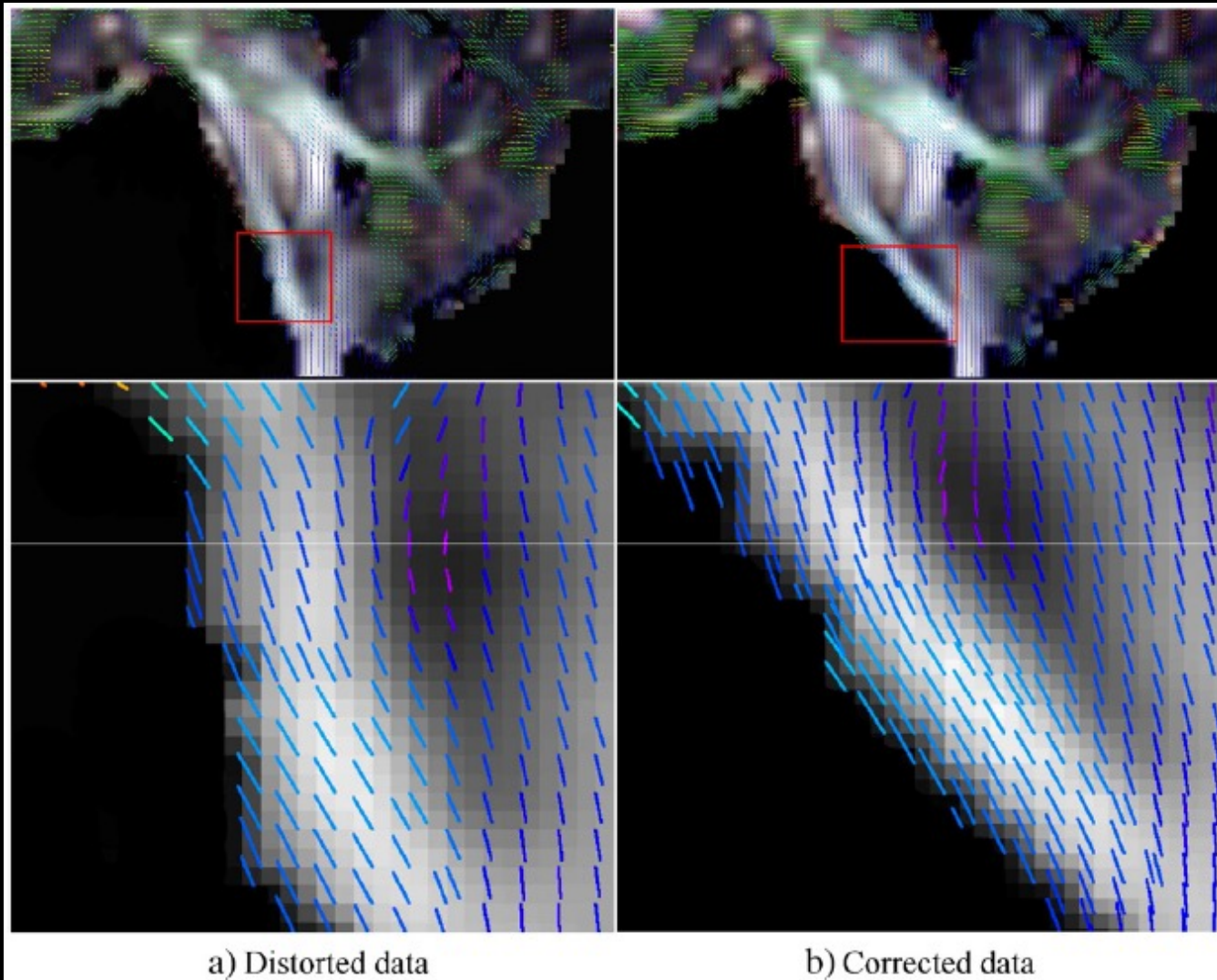
<sup>a</sup> Program on Pediatric Imaging and Tissue Sciences, NICHD, National Institutes of Health, Bethesda, MD, 20892, USA

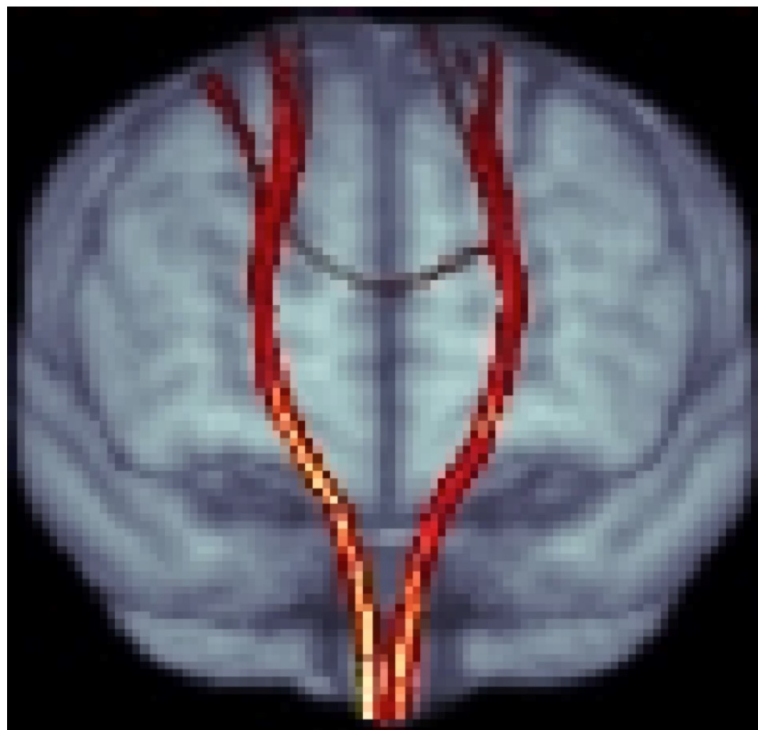
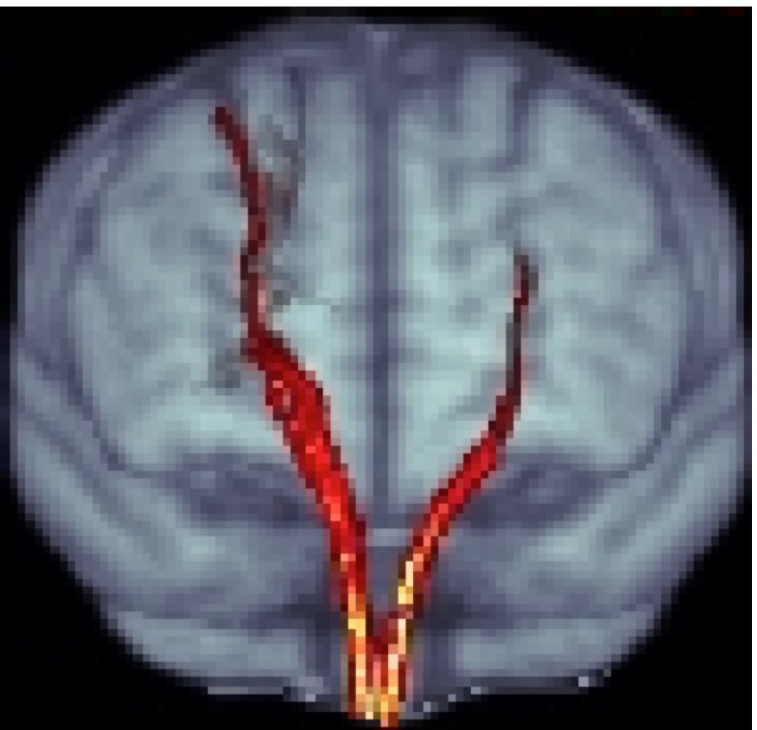
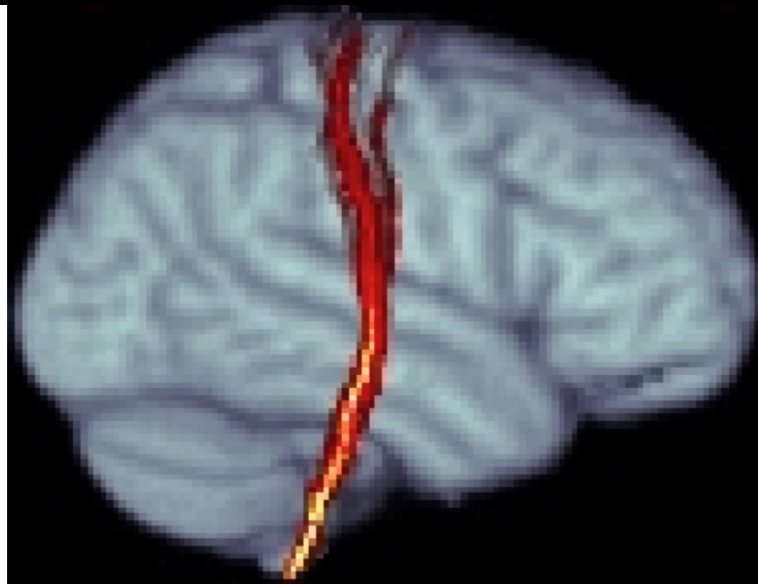
<sup>b</sup> Center for Neuroscience and Regenerative Medicine, Uniformed Services University of the Health Sciences, Bethesda, MD 20814, USA

<sup>c</sup> National Institute of Neurological Disorders and Stroke, National Institutes of Health, Bethesda, Maryland, USA

<sup>d</sup> Section on Clinical Studies, National Institute of Mental Health, National Institute of Health, Bethesda, MD, 20892, USA

# EPI distortions & Tensors





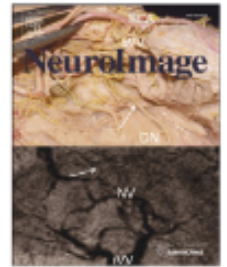
Before correction

After correction



Contents lists available at ScienceDirect

NeuroImage

journal homepage: [www.elsevier.com/locate/ynimg](http://www.elsevier.com/locate/ynimg)

## DR-BUDDI (Diffeomorphic Registration for Blip-Up blip-Down Diffusion Imaging) method for correcting echo planar imaging distortions



M. Okan Irfanoglu<sup>a,b,\*</sup>, Pooja Modi<sup>a</sup>, Amritha Nayak<sup>a,b</sup>, Elizabeth B. Hutchinson<sup>a,b</sup>, Joelle Sarlls<sup>c</sup>, Carlo Pierpaoli<sup>a</sup>

<sup>a</sup> Section on Tissue Biophysics and Biomimetics, National Institute of Child Health and Human Development, National Institutes of Health, Bethesda 20892, USA

<sup>b</sup> Center for Neuroscience and Regenerative Medicine, Uniformed Services University of the Health Sciences, Bethesda, MD 20814, USA

<sup>c</sup> NIH MRI Research Facility, National Institute of Neurological Disorders and Stroke, National Institutes of Health, Bethesda, MD 20892, USA

### ARTICLE INFO

#### Article history:

Accepted 19 November 2014

Available online 26 November 2014

#### Keywords:

Echo planar imaging

Diffusion tensor imaging

Reversed phase encoding

Diffeomorphic image registration

### ABSTRACT

We propose an echo planar imaging (EPI) distortion correction method (*DR-BUDDI*), specialized for diffusion MRI, which uses data acquired twice with reversed phase encoding directions, often referred to as blip-up blip-down acquisitions. *DR-BUDDI* can incorporate information from an undistorted structural MRI and also use diffusion-weighted images (DWI) to guide the registration, improving the quality of the registration in the presence of large deformations and in white matter regions. *DR-BUDDI* does not require the transformations for correcting blip-up and blip-down images to be the exact inverse of each other. Imposing the theoretical “blip-up blip-down distortion symmetry” may not be appropriate in the presence of common clinical scanning artifacts such as motion, ghosting, Gibbs ringing, vibrations, and low signal-to-noise. The performance of *DR-BUDDI* is evaluated with several data sets and compared to other existing blip-up blip-down correction approaches. The proposed method is robust and generally outperforms existing approaches. The inclusion of the DWIs in the correction process proves to be important to obtain a reliable correction of distortions in the brain stem. Methods that do not use DWIs may produce a visually appealing correction of the non-diffusion weighted images, but the directionally encoded color maps computed from the tensor reveal an abnormal anatomy of the white matter pathways.

© 2014 Elsevier Inc. All rights reserved.

# Software download: [www.tortoisedti.org](http://www.tortoisedti.org)

## TORTOISE

**Tolerably Obsessive Registration and Tensor Optimization Indolent Software Ensemble**

The current release is **TORTOISE V2.1.0**, available on the [download page](#)

[Click here](#) for version update information.

To get started with TORTOISE: [Quick Start Guide](#)

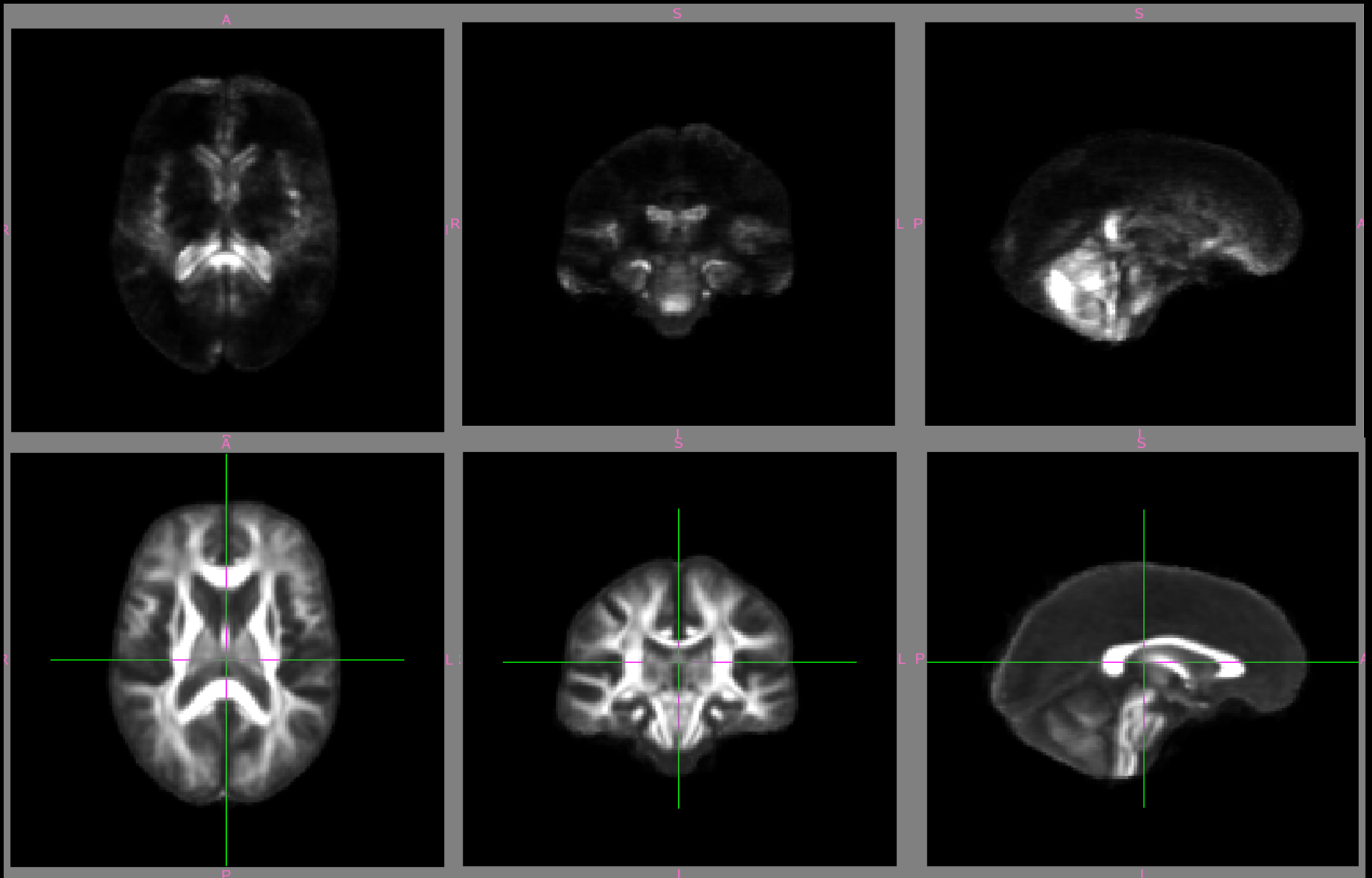
Please register to the **TORTOISEDTI Google group** for questions and help at:

<https://groups.google.com/forum/#!forum/tortoisedti>



# Outlier Rejection Probability Map

Lindsay Walker et al Neuroimage 2011



## Diffusion Tensor Imaging in Young Children with Autism: Biological Effects and Potential Confounds

Lindsay Walker, Marta Gozzi, Rhoshel Lenroot, Audrey Thurm, Babak Behseta, Susan Swedo, and Carlo Pierpaoli

**Background:** Diffusion tensor imaging (DTI) has been used over the past decade to study structural differences in the brains of children with autism compared with typically developing children. These studies generally find reduced fractional anisotropy (FA) and increased mean diffusivity (MD) in children with autism; however, the regional pattern of findings varies greatly.

**Methods:** We used DTI to investigate the brains of sedated children with autism ( $n = 39$ ) and naturally asleep typically developing children ( $n = 39$ ) between 2 and 8 years of age. Tract based spatial statistics and whole brain voxel-wise analysis were performed to investigate the regional distribution of differences between groups.

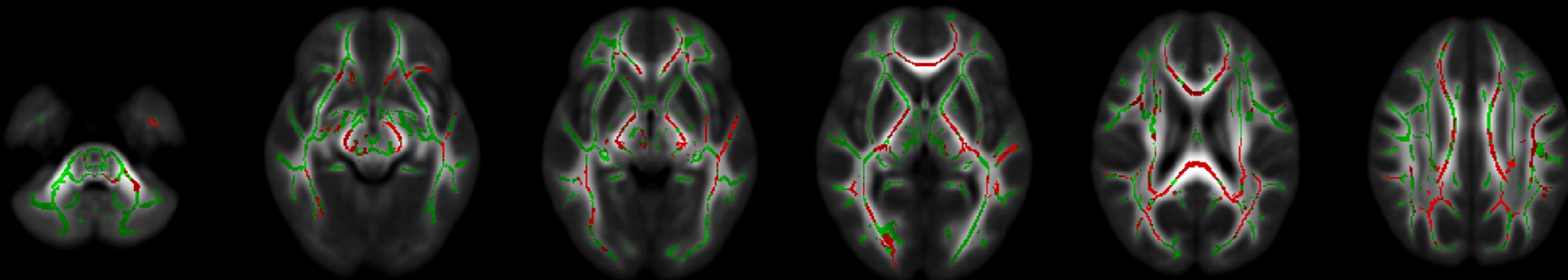
**Results:** In children with autism, we found significantly reduced FA in widespread regions and increased MD only in posterior brain regions. Significant age  $\times$  group interaction was found, indicating a difference in developmental trends of FA and MD between children with autism and typically developing children. The magnitude of the measured differences between groups was small, on the order of approximately 1%–2%. Subjects and control subjects showed distinct regional differences in imaging artifacts that can affect DTI measures.

**Conclusions:** We found statistically significant differences in DTI metrics between children with autism and typically developing children, including different developmental trends of these metrics. However, this study indicates that between-group differences in DTI studies of autism should be interpreted with caution, because their small magnitude make these measurements particularly vulnerable to the effects of artifacts and confounds, which might lead to false positive and/or false negative biological inferences.

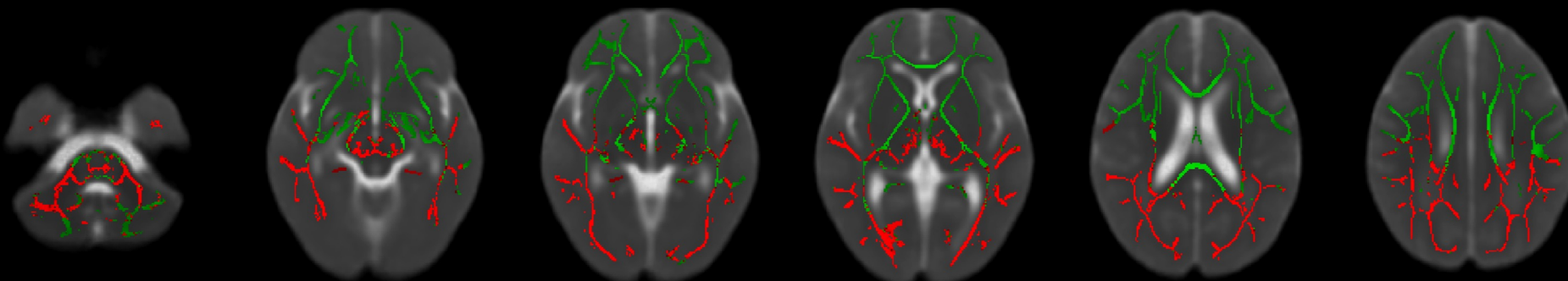


A) Clusters of significant differences in FA (TYP > AUT)

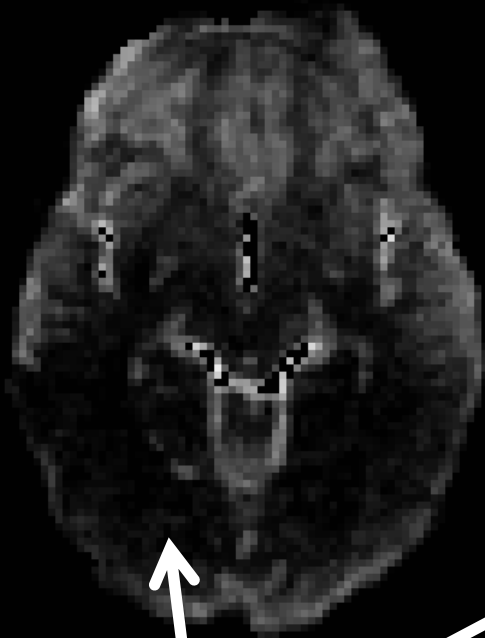
■ white matter skeleton voxels  
■ statistically significant voxels



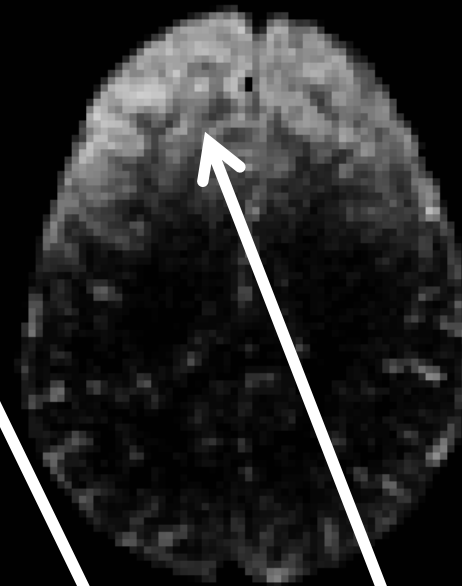
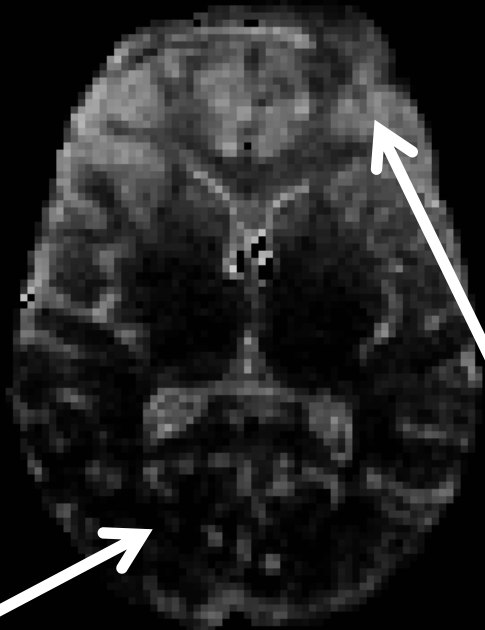
B) Clusters of significant differences in MD (AUT > TYP)



# Percentage of Outlier Data Points in a single subject example

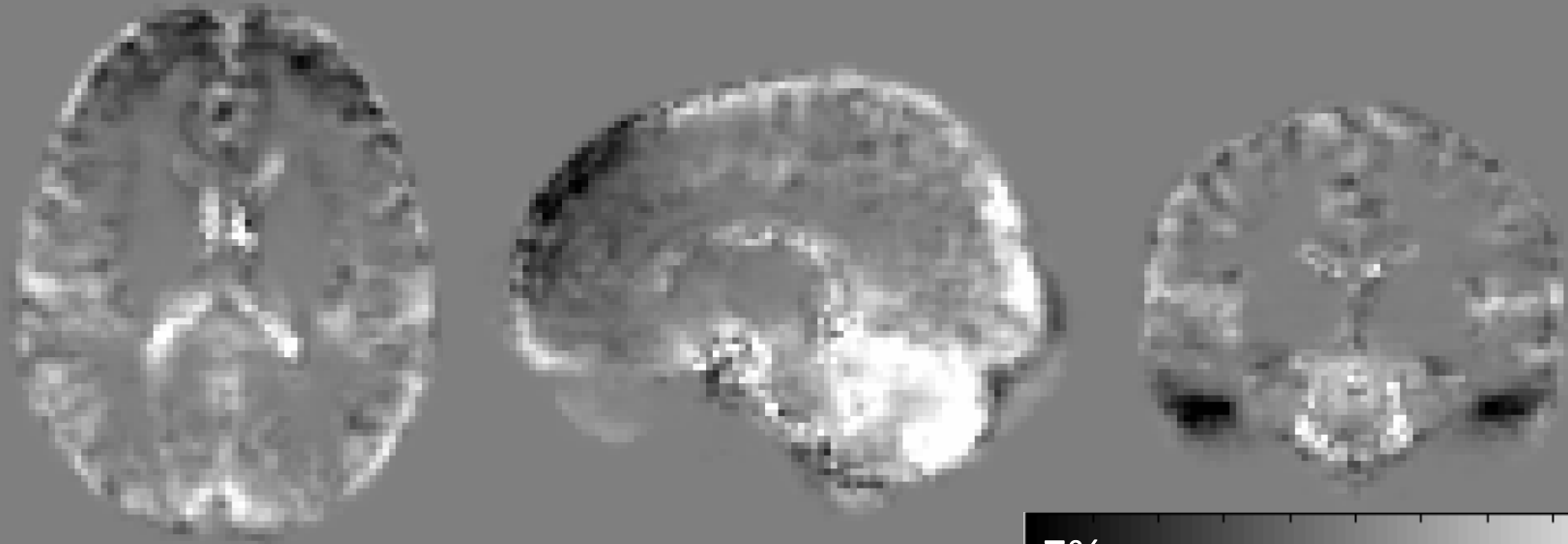


~3% outliers detected



up to 50% outliers detected

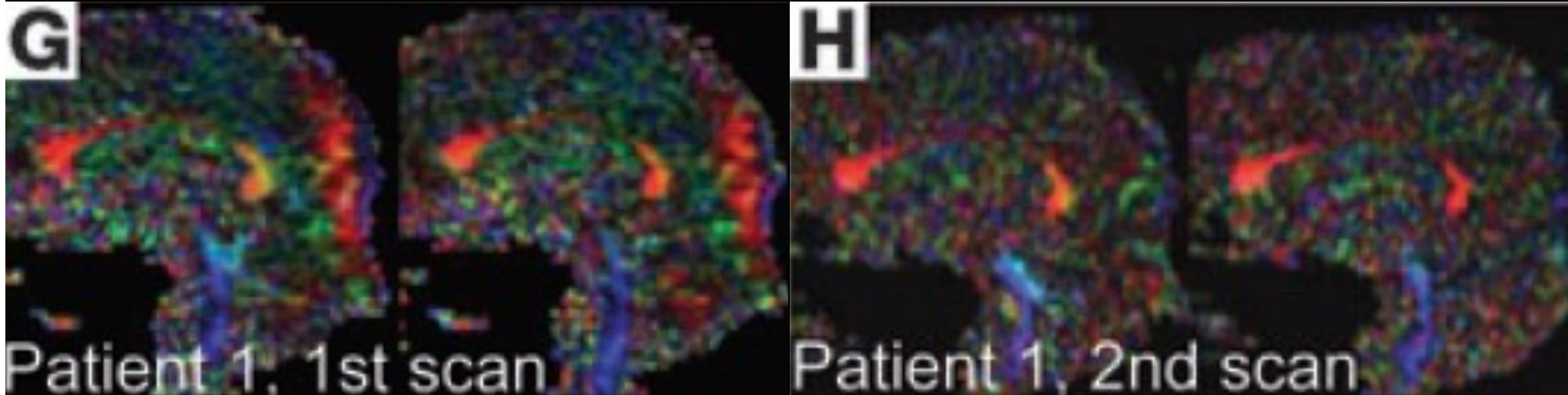
# Subtraction of Percentage of Outliers – AUT minus TYP



-7%

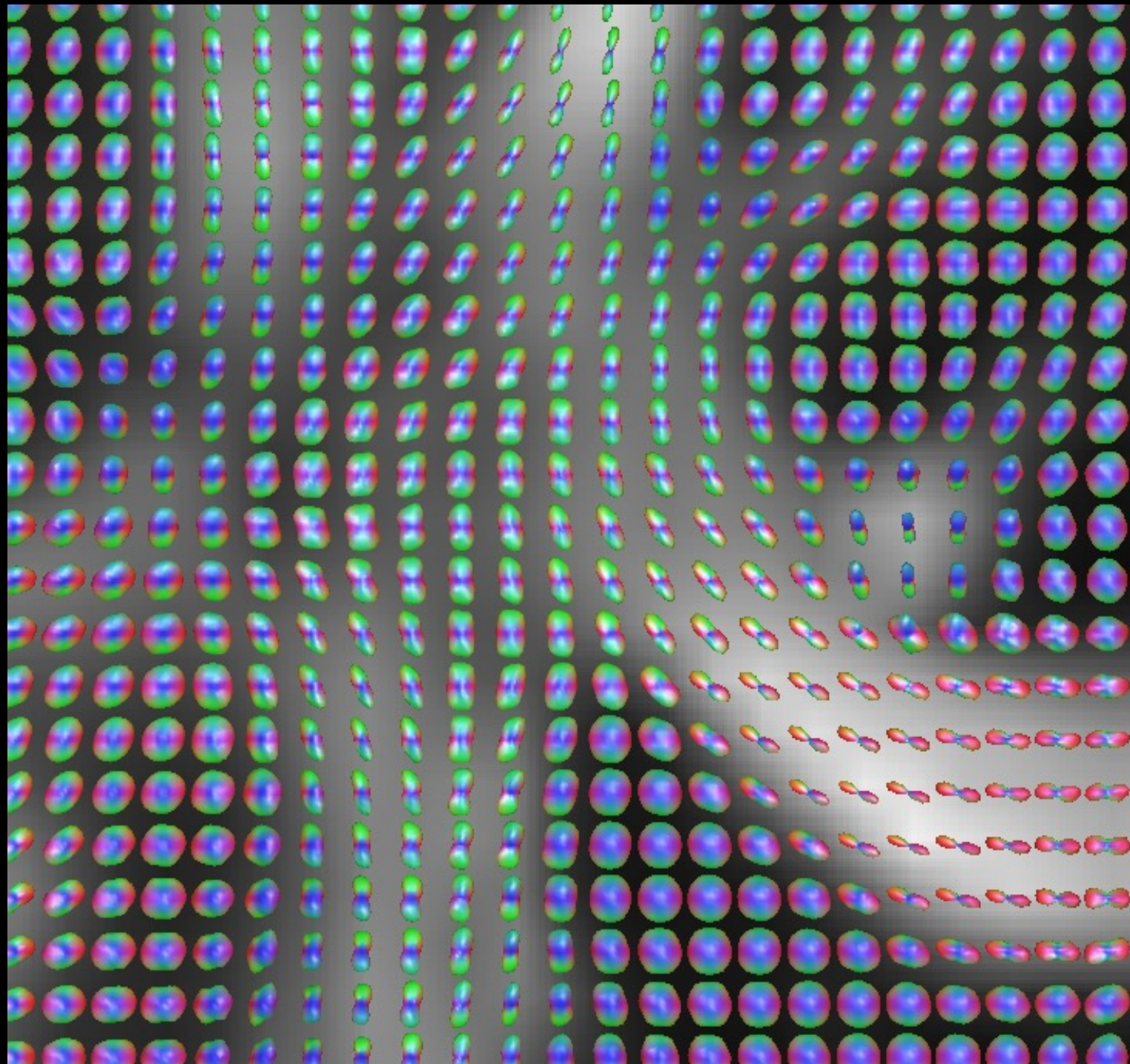
7%

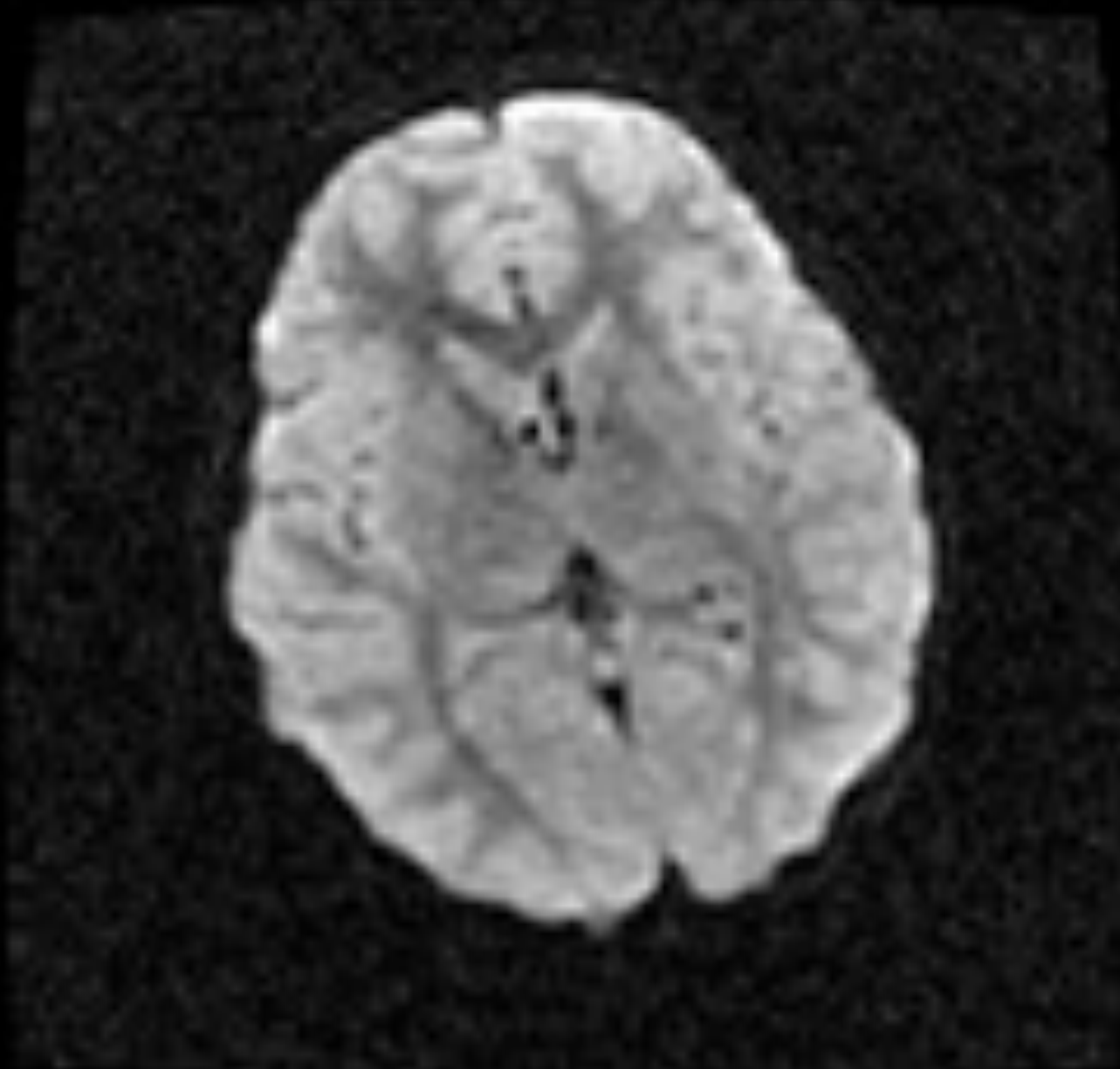
# “Interpretation” Artifacts

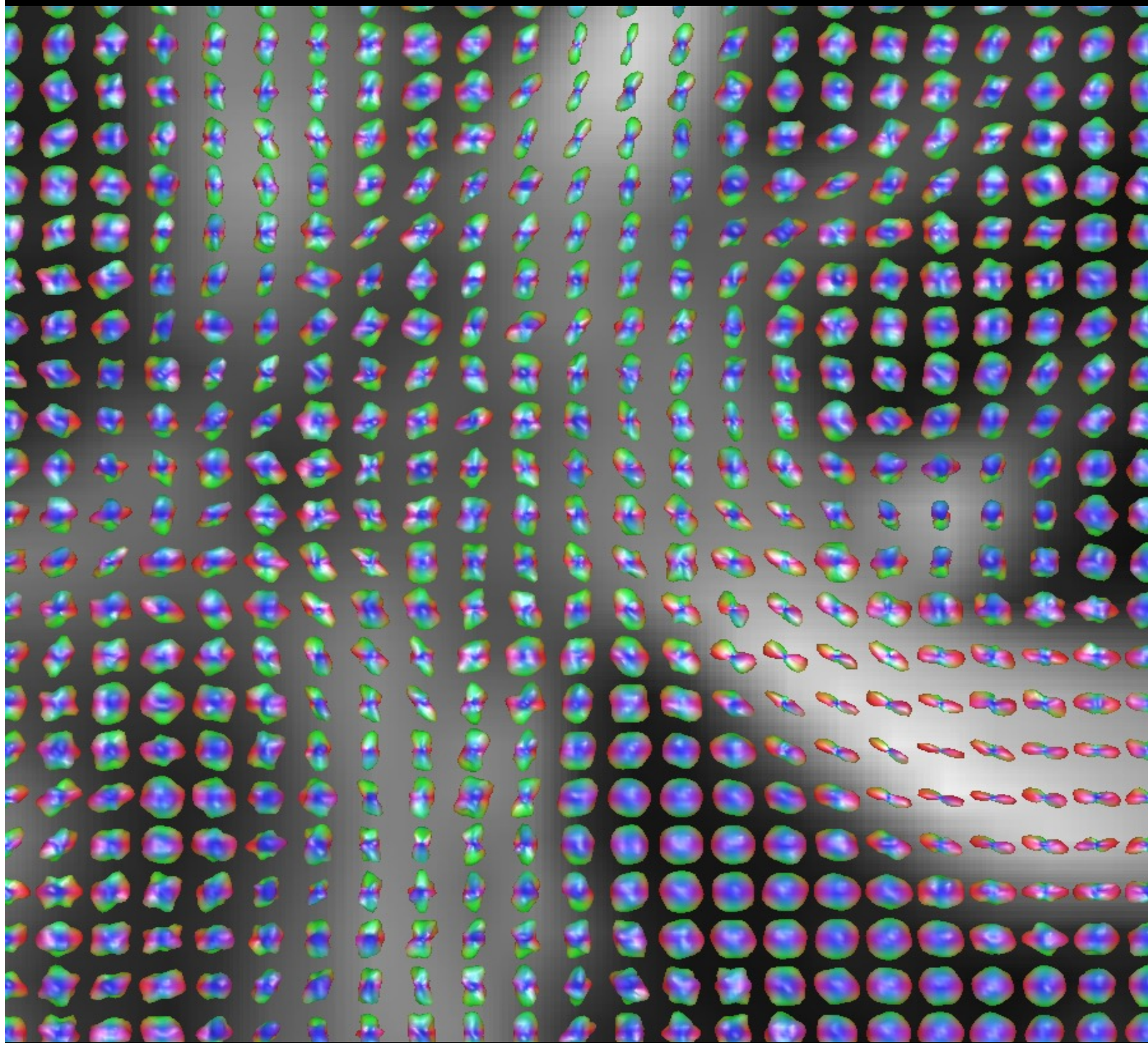


Possible axonal regrowth in late recovery from minimally conscious state  
Voss HU, et al. (2006) Journal of Clinical Investigation

One final consideration about  
HARDI data









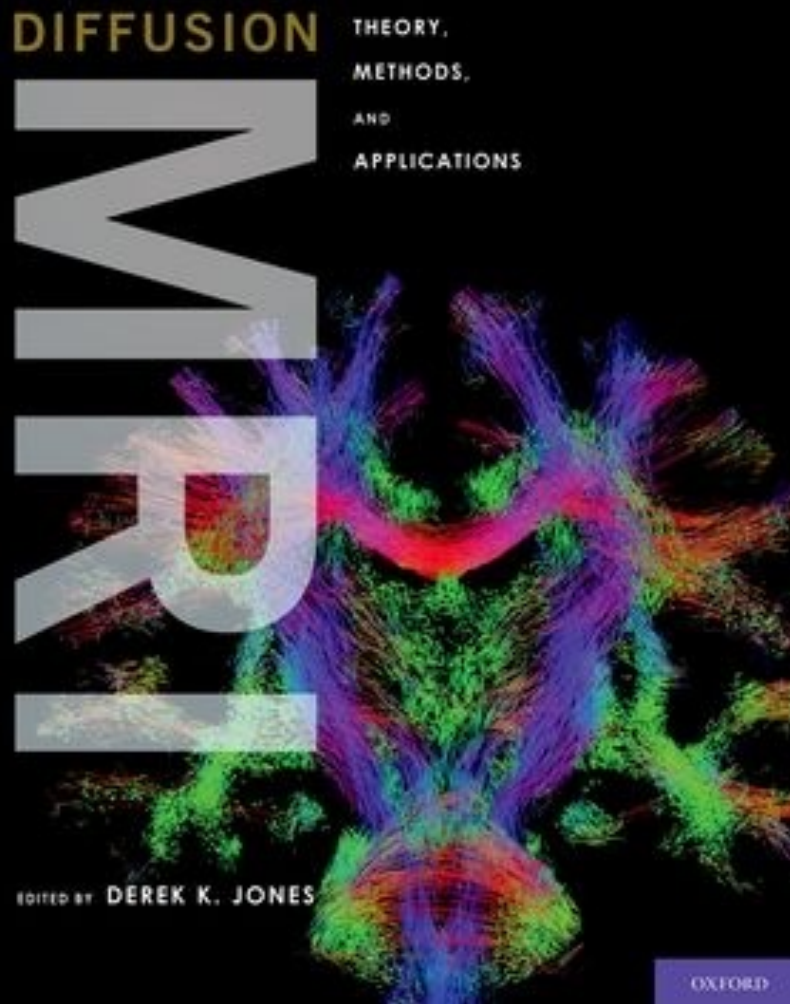
# Conclusions

Diffusion MRI provides unique information about tissue structure and architecture.

Clinical use of diffusion MRI requires the development of reliable (accurate and reproducible), specific, fast to acquire, and simple to interpret metrics.

HARDI acquisitions may help improving biological specificity, but are more prone to artifacts and lengthy than DTI.

Suggested reading:



**Diffusion MRI: Theory,  
Methods, and Applications**  
By Derek K. Jones - Oxford  
University Press (2010) - 624  
pages - ISBN 0195369777